Reduzierbarkeit von Fe(III) (Hydr)oxiden durch *Geobacter metallireducens* und *Clostridium butyricum*

von Diplom Agrarbiologe
Peter Dominik
aus Berlin

von der Fakultät VII – Architektur – Umwelt - Gesellschaft,
der Technischen Universität Berlin
zur Erlangung des akademischen Grades

Doktor der Naturwissenschaften
- Dr. rer. nat. -

genehmigte Dissertation

Promotionsauschuss:

Vorsitzender: Prof. Dr. Dr. B.-M. Wilke
Gutachter: Prof. Dr. M. Kaupenjohann
Gutachter: Prof. Dr. W.R. Fischer, Universität Hannover

Tag der wissenschaftlichen Aussprache: 20. Dezember 2002

Berlin 2003
D83

Inhaltsverzeichnis

Abbildungsverzeichnis

Tabellenverzeichnis

A. Problemstellung und Gliederung der Arbeit

Die Bedeutung der Fe(III)-Reduktion in anoxischen Systemen

Treten in einem Boden anoxische Verhältnisse (z.B. durch Wasserüberstau) auf, so erfolgt der Abbau der organischen Substanz nicht mehr mittels O_2-Atmung sondern über eine sequentielle Reduktion alternativer Elektronenakzeptoren: Nitrat (Denitrifikation) --> Mn(IV)/Fe(III) --> SO_4 --> CO_2 (Methanogenese) (*Patrick* und *Jugsujinda*, 1992; *Peters* und *Conrad*, 1996). Diese Reihenfolge folgt dem abnehmenden thermodynamischen Energiegewinn der jeweiligen Reaktion (*Zehnder*, 1988). In durchmischten Systemen (wie Boden- und Sedimentaufschlämmungen) laufen die Prozesse nacheinander ab und haben, wenn überhaupt, nur eine geringe zeitliche Überlappung (*Patrick* und *Jugsujinda*, 1992).

Böden enthalten häufig 2-5% Eisen und je nach Verwitterungsgrad liegt ein großer Anteil davon als Eisen(III)-(Hydr)Oxide (FHO) vor. Bei Abwesenheit von Sauerstoff stellen diese somit in der Regel den größten Vorrat der zur Verfügung stehenden Elektronenakzeptoren dar (*Thamdrup*, 2000). Daher hat das Ausmaß der Fe(III)-Reduktion entscheidenden Einfluß auf die Bildung von Methan und dessen Klimawirkung (*Lueders* und *Friedrich*, 2002).

Die Reaktivität von FHO

Im Unterschied zu vielen anderen Elektronenakzeptoren liegen die FHO nicht gelöst vor. Je nach Bildungsbedingungen während der Pedogenese entwickeln sich verschiedene Minerale, die stark in ihrer Kristallinität (Größe und Ordnungsgrad der Kristallite) sowie der isomorphen Substitution, insbesondere durch Al(III), variieren (*Schwertmann*, 1988, *Cornell* und *Schwertmann*, 1996).

Den Arbeiten von *Cornell* und *Schwertmann* (1996) bzw. *Fischer* (1987) kann entnommen werden, daß unterschiedlich kristalline Proben des selben Minerals sich auch im Löslichkeitsprodukt (K_{SO}) bzw. im Standardpotential unterscheiden. Das zeigt, daß solche Proben verschiedene Reaktivitäten aufweisen können (Als

Reaktivität eines FHO wird hier die Fähigkeit verstanden, reduziert zu werden; Stabilität und Reaktivität verhalten sich reziprok zueinander).

So können z.B. die K_{SO}-Werte von FHO in Böden eine Spannweite von mindestens 3-4 Größenordnungen haben (*Schwertmann*, 1991) und damit ein sehr großes Reaktivitätspektrum aufweisen. Durch diese Zusammenhänge wird verständlich, daß bei der anoxischen Inkubation von Böden und Sedimenten stets nur ein Teil der FHO reduziert wird. Unklar ist bis heute, welche FHO in natürlichen Sytemen reduziert werden, und wodurch diese Reduktion limitiert wird (*Thamdrup*, 2000).

FHO-reduzierende Mikroorganismen

Die bisher bekannten dissimilatorischen Fe(III)-reduzierenden Bakterien (DIRB), müssen in zwei physiologische Gruppen geteilt werden. Schon früh wurden fermentative Bakterien untersucht, die Fe(III) als einen zusätzlichen Elektronenakzeptor verwenden können (Übersichten bei *Lovley*, 1991 und *Ehrlich*, 1996). Der Anteil der Elektronen, die dabei auf Fe(III) übertragen werden ist mit höchstens 5% (meist jedoch viel weniger) gering.

In den vergangen 15 Jahren wurden jedoch respiratorische Bakterien isoliert (beziehungsweise bei schon bekannten Organismen dieser Stoffwechsel entdeckt), die nicht weiter vergärbare Substrate (also die Endprodukte von Gärungen: organische Säuren, Alkohole und H_2) meist vollständig zu oxidieren vermögen und dabei sämtliche Elektronen auf Fe(III) übertragen. Seit dem Erscheinen der neuesten Übersicht (*Lovley et al.*, 1997) wurden hauptsächlich Eisen(III)-Reduzierer extremer Standorte, nämlich thermophile (*Bridge* und *Johnson*, 1998; *Greene et al.*, 1997; *Kashefi* und *Lovley*, 2000; *Kieft et al.*, 1999; *Slobodkin et al.*, 1999; *Slobodkin* und *Wiegel*, 1997) und acidophile Organismen (*Cummings et al.*, 1999; *Küsel et al.*, 1999) beschrieben, und nur ein neuer Stamm, der Acetat unter mesophilen Bedingungen oxidiert (*Francis et al.*, 2000). Diejenigen Organismen, die Gärungsprodukte oxidieren, folgen in der anaeroben Nahrungskette nach den Gärern (*Zehnder*, 1988) und konkurrieren daher mit den Desulfurikanten und Methanogenen um dieselben Substrate.

Es scheint nun klar zu sein, daß den fermentativen Eisenreduzierern in Böden kaum eine quantitative Bedeutung bei der Fe(III)-Reduktion zukommt. Dies ist aus dem zeitlichen Verlauf von Substratkonzentrationen, Fe(III)-Reduktion und Methanbildung in vier Böden (*Peters* und *Conrad*, 1996) zu entnehmen.

Von den Desulfurikanten und Methanogenen ist schon länger bekannt, dass ihre Aktivität von der Thermodynamik begrenzt wird (*King*, 1984; *Ward* und *Winfrey*, 1985; *Winfrey* und *Zeikus*, 1977). Sie stellen ihre Aktivität ein, wenn die Elektronendonator-Konzentration unter einen Grenzwert (threshold) fällt, so dass die freie Reaktionsenthalpie (Gibbs free energy) unter ein Minimum zur Erhaltung ihres Stoffwechsels sinkt. Dies erklärt, warum die Verwertung alternativer Elektronen-Akzeptoren in der o.g. Reihenfolge abnehmenden Energiegewinns der Reaktion erfolgt, wenn ein Standort anoxisch wird.

Da respiratorische Fe(III)-Reduzierer die selben Substrate verwerten, aber ihre Reaktion einen größeren Energiebetrag liefert war es nur folgerichtig, dass *Lovley et al.*, 1994 sowie *Achtnich et al.*, 1995 zeigten, dass der threshold der Fe(III)-Reduzierer für H_2 niedriger liegt als für Sulfat-Reduzierer und Methanogene.

Hypothesen der Arbeit: Begrenzungen für die Reduktion von FHO durch DIRB

Da sich verschiedene FHO deutlich in ihrem Energiegehalt unterscheiden, wurde für die vorliegende Arbeit die Hypothese (1) aufgestellt, dass die Reduktion der FHO durch DIRB von der Thermodynamik der Reduktion nach Gleichung 1 oder 2 begrenzt wird. Wenn das der Fall ist, dann sollte ein DIRB verschieden stabile FHO mit unterschiedlichen Substratkonzentrationen jeweils soweit umsetzen, bis am Ende die freie Reaktionsenthalpie ΔG_r stets den selben Wert erreicht, nämlich den minimalen Energiebetrag, den der Organismus je umgesetztem Substrat benötigt, um seine Energieversorgung sicherzustellen.

$$8\ FeOOH + CH_3COO^- + 15\ H^+ \rightarrow 8\ Fe^{2+} + 2\ HCO_3^- + 12\ H_2O \qquad (1)$$

$$8\ Fe(OH)_3 + CH_3COO^- + 15\ H^+ \rightarrow 8\ Fe^{2+} + 2\ HCO_3^- + 20\ H_2O \qquad (2)$$

Da in Böden alle FHO außer Lepidokrokit, in Abhängigkeit vom Verwitterungsgrad der Böden, Al-Substitution aufweisen (*Cornell* und *Schwertmann*, 1996), stellte

sich eine weitere Frage für diese Arbeit. Was geschieht mit dem nicht reduzierbaren Al(III), dessen Löslichkeit nur wenig höher ist, als die des Fe(III), wenn es bei der Reduktion eines substituierten FHO aus dessen Kristallgitter freigesetzt wird? Es sollte die Hypothese (2) geprüft werden, dass dieses Aluminium auf der Oberfläche der FHO unlösliche Beläge bildet, die eine weitere Reduktion des FHO verhindern.

Gliederung der Arbeit

Um der Aufgabenstellung der vorliegenden Arbeit gerecht zu werden, waren folgende Arbeitsschritte nötig:

- **Synthese verschiedener FHO**, deren Stabiltät im Bereich von solchen liegt, wie sie an natürlichen Standorten vorkommen.
- **Charakterisierung** dieser FHO mittels:
    - üblicher Methoden, wie Bestimmung der spezifischen Oberfläche oder Bestimmung des mittleren Kristallitdurchmessers.
    - Bestimmung der thermodynamischen Stabilität, so dass die Standard freie Bildungsenthalpie $\Delta G_f°$ bestimmt werden kann, die benötigt wird um die freie Standard-Reaktionsenthaplie $\Delta G_r°$ der Reaktion nach Gleichung 1 oder 2 zu bestimmen. Nur wenn diese bekannt ist, kann bei Kenntnis der Aktivitäten der gelösten Reaktanden ΔG_r bestimmt werden. Zur Bestimmung des K_{SO} wurde hier eine neue Methode entwickelt, um nur gelöstes, aber kein kolloidales Fe zu messen (**Abschnitt B**).
    - Charakterisierung mittels Auflösungskinetik (**Abschnitt C und D**).
- **Bakterienversuche** mit unterschiedlich stabilen FHO und verschiedenen Substratkonzentrationen, um die Hypothese (1) zu überprüfen (**Abschnitt E**).
- **Bakterienversuche** mit FHO, die unterschiedlich stark mit Aluminium substituiert sind, um die Hypothese (2) zu überprüfen (**Abschnitt F**).

B. Simple spectrophotometric determination of Fe in oxalate and HCl soil extracts

Abstract

We describe a spectrophotometric method to determine the sum of Fe(II) plus Fe(III) in HCl and oxalate extracts. The principle of the method is to reduce Fe(III) by ascorbate in near neutral solution and to sequester the Fe(II) formed as a tri-ferrozine complex which is then determined photometrically at 562 nm. Because the complex is stable, the reaction is irreversible and complete. Fe(III) in HCl solution reacted very rapidly whereas oxalate decelerated the overall reaction so that pseudo first-order kinetics with respect to Fe(III) was detected. However, when extractions were conducted at the recommended soil:solution ratio, the absorption reached 98% of its final value within a few minutes.

To test the method, four soils differing considerably in texture, carbonate, organic matter, and Fe(III)(hydr)oxides contents were extracted with oxalate in the dark for amorphous (Fe_o), and with boiling oxalate for total Fe(III)(hydr)oxides (Fe_{bo}). This newly developed spectrophotometric method showed excellent correspondence with the conventional atomic absorption spectroscopy (AAS) method. The method presented here can therefore be used as an alternative method to determine the Fe content of oxalate and hydrochloric acid extracts if AAS is not available. Oxalate extracts low in Fe content, which cannot be diluted, are easier to determine by the photometric method than by AAS.

Introduction

The use of an oxalate buffer in the dark to extract amorphous or reactive Fe(III)(hydr)oxides from soil has long been established (*Schwertmann*, 1964; *Tamm*, 1922). The total amount, i.e. the sum of amorphous and crystalline Fe(III)(hydr)oxides is usually determined by extraction with citrate bicarbonate and dithionite (CBD) (*Mehra* and *Jackson*, 1960). This method is time consuming and produces toxic vapours. It can be replaced by extraction with boiling oxalate buffer (*Fischer* and *Fechter*, 1982), which may be supplemented with ascorbic acid (*Zeien* and *Brümmer*, 1989). These methods give essentialy the same results as the CBD method (*Schwertmann et al*., 1982a; *Schwertmann et al*., 1982b).

The extraction with boiling oxalate is based on the principle that heat (or ultraviolet radiation) induces a disintegration of oxalate in contact with Fe(III) to form CO_2 and Fe(II) (*Cornell* and *Schindler*, 1987). Fe(III) reduction is supported by ascorbic acid in the method of *Zeien* and *Brümmer* (1989). Fe^{2+} serves as a powerful catalyst in the dissolution of crystalline Fe(III)(hydr)oxides in an oxalate buffer (*Fischer*, 1973; *Suter et al*., 1988). Therefore, an extraction with oxalate buffer in the dark will overestimate the amorphous Fe(III)(hydr)oxide content in anoxic samples that contain Fe(II). Boiling oxalate extracts contain both Fe(III) and Fe(II), whereas extracts with oxalate in the dark contain only Fe(III). The total Fe content of such extracts is usually determined by AAS (*Schwertmann*, 1964; *Mehra* and *Jackson*, 1960; *Motomura* and *Yokoi*, 1969), while photometric methods generally detect only one of the two species (*Szilagyi*, 1971; *Rueda et al*., 1992).

Hydrochloric acid extractions are most commonly used to determine the amount of Fe(II) in soils or sediments (*Lovley* and *Phillips*, 1986; *Motomura* and *Yokoi*, 1969; *Schnell et al*., 1998). More concentrated HCl solutions are used for the dissolution kinetics of synthetic oxides as a matter of routine (*Ruan* and *Gilkes*, 1995; *Schwertmann*, 1991). In *Cornell et al*. (1974) 0.5 *M* HCl was used to determine the small amount of amorphous Fe(III)hydroxide that is always associated with synthetic crystalline oxides.

Here we present a simple and rapid method to determine the total Fe content of HCl and oxalate extracts by reducing Fe(III) and forming a coloured Fe(II)-ferrozine

complex in the same operation. Ferrozine is a highly sensitive reagent for the determination of Fe(II) (*Amonette et al.*, 1994; *Stookey*, 1970). The new photometric method can be applied if AAS technique is not available, if the sample number is small, or if Fe content of oxalate extracts is low.

A similar method was reported earlier (*Phillips* and *Lovley*, 1987; *Rasmussen* and *Nielsen*, 1996), but no data were presented to confirm the accuracy and precision of the method. That method used N-2-hydroxyethylpiperazine (HEPES) as a buffer and hydroxylamine as a reducing agent instead of acetate and ascorbate, respectively, and longer waiting periods were required than in our method.

Experimental

Standards:

As Fe(III) standard, a commercial standard solution for AAS ($Fe(NO_3)_3$ in 0.5 *M* HNO_3, Merck Art.Nr.1.19781) was used.

To obtain the Fe(II) standard, $(NH_4)_2Fe(SO_4)_2 * 6H_2O$ (Mohr's salt) was dissolved in diluted HCl.

Soils

Four soils were selected to represent a range in physical and chemical properties, i.e. in initial material and texture as well as in carbonate, organic matter, and iron oxide content (see Table B.1).

Methods

The photometric reagent consisted of 500 ppm ferrozine (Serva) buffered with 0.2 *M* ammonium acetate. If not stated otherwise (see below) 5 m*M* ascorbic acid were added to the reagent.

Test for completeness of reaction

1.0 mL of 0.5 *M* HCl or 0.2 *M* oxalate buffer according to Schwertmann (1964), containing either 0.5 m*M* Fe(II) or 0.5 m*M* Fe(III) standard, was mixed with 9.0 mL of photometric reagent either with or without ascorbic acid. All experiments were

performed in quadruplicate and the absorption was read after 30 min at 562 nm at a Zeiss PM2 DL spectrophotometer equipped with a 10 mm suck-off-cuvette. The theoretically expected absorbance was calculated according to the Lambert-Beer law ($A=\varepsilon dn/V$). Values for molar absorptivities were taken from *Amonette et al*. (1994).

Table B.1: Soil properties

Abbreviation	A	L	V	H
Soil-Classification according to FAO	Cambic Arenosol	Haplic Luvisol	Stagni-Eutric Vertisol	Terric Histosol
Soil-Horizon	mollic A	mollic A	mollic A	histic H
Sand [%]	86	3	9	
Silt [%]	9	79	51	
Clay [%]	4	18	40	
pH ($CaCl_2$)	7.1	6.6	6.6	7.5
$CaCO_3$ [%]	0.4	0	0	49.4
CEC* [$mmol_c\ kg^{-1}$]	92	170	216	993
$C_{organic}$ [%]	1.3	0.9	2.6	16.1
N_{total} [$g\ kg^{-1}$]	1.0	1.2	3.0	13.6
P_{CAL} # [$mg\ kg^{-1}$]	101	158	28	56
K_{CAL} # [$mg\ kg^{-1}$]	206	298	122	122
Fe_o † [$g\ kg^{-1}$]	1.1	3.2	10.9	3.0
Fe_d ‡ [$g\ kg^{-1}$]	2.2	11.2	24.3	3.8

*Cation Exchange Capacity, #Phosphorous or Potassium extracted by Calcium acetate lactate method, † amorphous iron oxides extracted by the oxalate method, ‡ sum of amorphous and crystalline iron oxides extracted by the CBD method.

This experiment was repeated using a reagent containig 500 ppm 2,2´bipyridyl instead of ferrozine. Because of the lower molar absorptivity, 8 mL of reagent were mixed with 2 mL of the “synthetic extracts”.

Because of good correspondence of standards and calculated absorbances (Table B.2) we used the latter for further data presentation.

Duration of color development

a) Influence of Fe(III) concentration

9.0 mL of reagent were mixed

1) with 1.0 mL of 0.2 *M* oxalic buffer containing either 0.05, 0.2 or 0.5 m*M* Fe(III) or

2) with 1.0 mL of 0.5 *M* HCl containing 0.5 m*M* Fe(III).

Aliquots of the four replicates were read at different times.

b) Influence of oxalate concentration

To 0.5 mL 1 mM Fe(III) in diluted HCl, increasing volumes of 0.2 *M* oxalic buffer (see Table B.3) were pipetted. 8 mL of reagent were added to start the reaction.

For both experiments, the expected absorbance was calculated according to the Lambert-Beer law. The remaining Fe(III) concentration at each time was calculated from the absorbance. The pseudo first-order rate constants of kinetics were determined by linear regression of logarithmically transformed data and expressed as the time necessary to attain 98% of the final absorbance.

c) Influence of elevated temperature

All above experiments were conducted at room temperature (RT, 22 ±2°C). In order to evaluate if elevated temperature would reduce the waiting time, the last experiment was repeated at 55 ±1°C: After mixing all reagents, the test tubes were placed in a waterbath. After transferring an aliquot from the waterbath into the cuvette, the absorbance increased very fast. Therefore, the aliquots were pipetted into the cuvette exactly 5 seconds prior to the respective reading-time. When this first reading (absorbance after 5 seconds) remained constant for succesive aliquots, the last aliquot remained whithin the cuvette and it’s absorbance was read over time until it remained constant again.

Iron content of soil extracts: Comparison of AAS and Photometry

Soil was extracted with oxalate buffer in the dark according to *Schwertmann* (1964) and with boiling oxalate according to *Zeien* and *Brümmer* (1989). The volume of the extracting agents was 50 mL. The soil mass added for soil A, L, V, and H amounted to 5, 2, 1 and 1.5 g for oxalate and 2, 0.5, 0.25 and 1.5 g for boiling oxalate. The extracts were centrifuged for 10 min at 1500 rcf (Haereus Megafuge 1.0) and filtered (blue ribbon, Schleicher&Schuell, Dassel, Germany).

In four parallel 1:10 dilutions of each extract, total Fe was analyzed both photometrically and by AAS (Perkin Elmer 3100, adjustment according to standard settings). Both methods were calibrated using the same Fe(III) standard.

The results were tested for significance of differences between the methods by means of a t-test.

Results and Discussion

Table B.2: Absorbance of either Fe(II) or Fe(III) dissolved either in different background solutions and different colour reagents. Total volume was 10 mL; SD means standard deviation of four replicates.

	Ferrozine at 562 nm with 0.5 µmoles Fe		bipyridyl at 522 nm with 1.0 µmoles Fe	
	Mean	SD	Mean	SD
Calculated from molar absorptivities (*Amonette et al*., 1994)	1.395		0.865	
Calibration with Fe(II)	1.382	0.005	0.866	0.001
Fe(III) in HCl, without ascorbate	0.112	0.002	nd	nd
Fe(III) in ox-b without ascorbate	0.022	0.001	0.043	0.003
Fe(III) in ox-b with ascorbate	1.382	0.002	0.856	0.002
Fe(III) in HCl with ascorbate	1.380	0.002	0.868	0.003

Test for completeness of reaction

Reading of the Fe(II) standard gave almost exactly the theoretically calculated absorbance (Table B.2). The Fe(III) standard, when dissolved in HCl, contained about 10% Fe(II), and when dissolved in oxalate only 3% Fe(II). This was shown using a reagent without ascorbic acid. However, ferrozine or 2,2´-bipyridyl (Table B.2, right) reagents containing ascorbic acid reduced all added Fe(III) and sequestered it as Fe(II)-ferrozine$_3$ or Fe(II)-bipyridyl$_3$ complex. This is demonstrated by good correspondence of the measured absorbance and the absorbance calculated from the molar absorptivities.

Duration of color development

When dissolved in HCl, Fe(III) was immediately converted into the Fe(II)-ferrozine$_3$ complex after mixing with the ascorbate containing reagent (Fig. B.1).

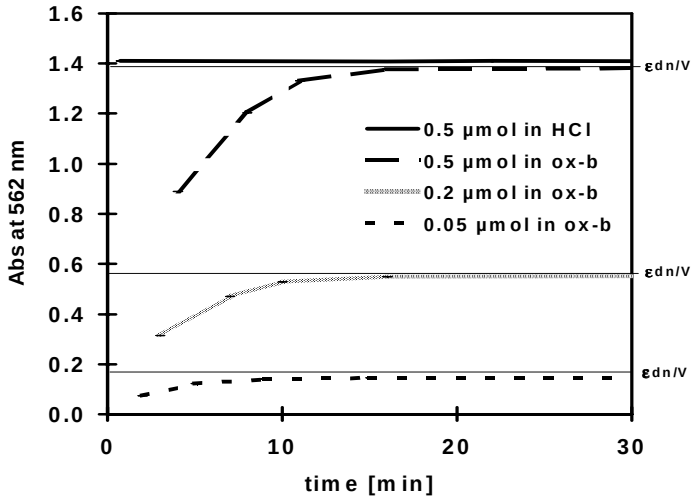

Figure B.1: Kinetics of Fe(II)-ferrozine$_3$ formation; different amounts of Fe(III) dissolved in 1.0 mL HCl or oxalic buffer; total volume was 10 mL; error bars (standard deviation of replicates) are not visible because of small error). The calculated absorbances are denoted by the Lamber-Beer law (A=εdn/V).

In the oxalate buffer, however, the color development took about 10 min, and with bipyridyl about 20 min (data not shown). Fig. B.1 shows that the absobance approached the expected value asymptotically. When the remaining Fe(III)

concentrations were calculated for the different points and plotted on a logarithmic scale, a straight line indicated pseudo first-order kinetics. Only the first point at t=0 did not fit very well in this kinetics, presumably because ferrozine-activity changed too much in this first period.

Linear regression of the logarithmic data indicated that it took about 13 minutes to obtain 98% of the final absorbance when 10 mL of the solution contained 200 µmol oxalate; thus, after 13 min the error was smaller than 2%. This waiting period was independent of the Fe concentration but increased sharply with the oxalate concentration. Waiting periods depending on the oxalate content are listed in Table B.3.

Table B.3: Waiting period to attain 98% of the final absorbance, depending on the amount of oxalate . The volume of the reagent was 8 mL.

0.2 M Oxalate [mL]	$T_{98\%}$ [min]	r^2
1.0	13	0.976
1.3	19	0.991
1.5	26	0.997
1.8	35	0.991
2.0	44	0.992
2.5	79	0.996

r is the regression coefficient of the logarithmic linearization of the first order kinetic curve

Fig. B.2 shows for the highest oxalate concentration that color development was much faster at 55°C than at RT, but absorbance did not nearly reach the calculated value. This calculated absorbance was reached only if the solution was allowed to cool down to RT.

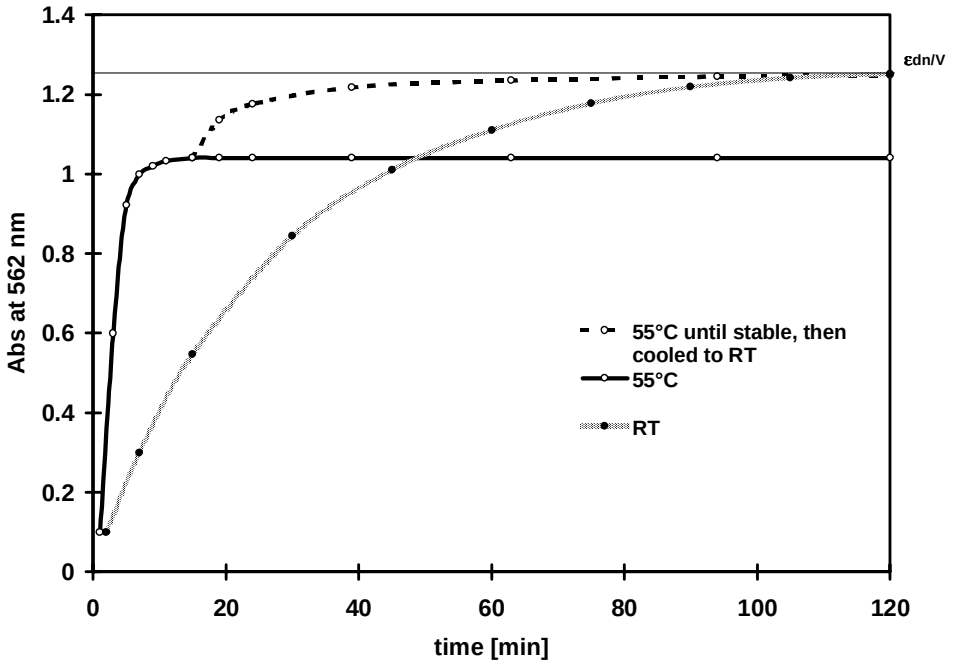

Figure B.2: Kinetics of Fe(II)-ferrozine$_3$ formation at different temperatures. The calculated absorbance is denoted by A=εdn/V.

The difference between the two constant values is explained only to a small extend by the volumetric expansion of water with temperature. The absobance reached its final value much slower than the temperature of solution inside the cuvette (25°C were reached whithin 2 minutes) as well. The data suggest that increasing temperatures shift the equilibrium of the over all reaction to the reactants, which is typically for exothermic reactions.

Fig. B.2 shows that a biphasic procedure (1. heating, 2. cooling to RT) could reduce the waiting time to attain 98% of calculated absorbance from 108 min to 92 min compared to the procedure at RT. However we believe that this gain in velocity does not warrant the extra work.

Larger aliquots of oxalate extracts than indicated in Table B.3 are not recommended because the absobance starts to decline slightly after about 2 hours. However, most soils contain so much Fe that the extracts must be diluted prior to determination (*Loeppert*, 1988).

Iron content of soil extracts: Comparison of AAS and Photometry

The developed method was tested on real soil extracts. Table B.4 shows that our method resulted in almost identical values for each soil extract to those of AAS.

Table B.4: Fe content [mg L^{-1}] of oxalate and boiling oxalate extracts of four soils; comparision of AAS and photometry; SD means standard deviation of four parallel dilutions.

Soil	Photometry		AAS	
	Mean	SD	Mean	SD
Oxalate extract				
A	107.0	0.50	109.3	2.53
L	130.5	0.46	128.9	1.17
V	216.4	3.15	218.1	4.50
H	87.8*	0.78	89.4	0.80
Boiling oxalate extract				
A	108.7*	0.71	113.0	2.77
L	175.1	1.54	175.8	2.01
V	172.5*	1.63	177.0	0.92
H	148.1*	1.64	143.8	0.80

* denotes significant differences between the two methods

Although differences between the methods were significant in four of eight cases, they were very small. We have no explanation for these small differences, because every value was confirmed using a calibration according to the standard addition method (data not shown).

Despite significant differences in some cases, the correspondence was always better than 96%, in most cases even better than 98%. Thus, none of the extremely variable soil properties critically affected the comparability of the two methods.

Besides complexing agents like oxalate, heavy metal cations may also interfere with the photometric determination of Fe(II) with ferrozine, leading to an overestimation. Stookey (*Stookey*, 1970) showed that Cu^{+} is the most effective cation by far. The molecular absorptivity of Cu-ferrozine, however, is only 1/30 of the Fe(II)-complex at 652 nm, indicating that an extract has to contain as least as much Cu as Fe to cause measurable error. Such an extreme content in available Cu is perhaps conceivable only in extremely contaminated samples, which would not support any life.

The photometric method developed here thus can be applied as an alternative to the usual AAS method in order to determine Fe in oxalate extracts. The experience in our laboratory even inicates, that oxalate extracts, which contain less than 20 mg L^{-1} Fe and therefore cannot be diluted to a great extent, are better to determine by the photometric method than by AAS. Instead of ferrozine, other substances forming a color complex selectively with Fe(II) also may be used (see Table B.1).

Recommended Procedure

The reagent contains 0.2 *M* ammonium acetate, 500 ppm ferrozine and 5 m*M* of ascorbic acid in aqueous solution. Once prepared the solution should be used only for a few days, because ascorbate will be oxidized by atmospheric oxygen at neutral pH (visible by intense yellow colouring). Without ascorbic acid, the reagent keeps for weeks. Therefore we recommend adding the ascorbic acid to the needed amount of reagent just prior to use.

For full colour development within 15 min, the measuring solution may contain up to 10 vol% of undiluted oxalate extract according to *Schwertmann* (1964), or up to 5 vol% of undiluted boiling-oxalate extract according to *Zeien* and *Brümmer* (1989). For larger aliqouts refer to Table B.3 for the appropriate waiting periods. When keeping the waiting period it is unnecessary to use oxalate for calibration in the standard preparation. To our experience, calibration always yields constant values.

The mixing ratio of HCl and reagent is limited only by the buffer capacity of acetate. The amount of HCl must not exceed 80% of the amount of acetate to keep the pH within the optimum range for color development (*Stookey*, 1970).

Acknowledgements

This study was financially supported by the Government of Baden-Württemberg, FRG and by the Deutsche Forschungsgemeinschaft. We thank Jürgen Rommel for selection and basic characterization of the soils.

C. Simple on-line determination of reductive dissolution kinetics of Fe(III) (hydr)oxides versus dissolution in oxalate

Abstract

Dissolution kinetics are a common tool to characterize the stability of Fe(III) (hydr)oxides. Although reduction at approximately neutral pH is probably the most frequent and effective process for dissolution of Fe(III) (hydr)oxides in natural environments, reductive dissolution kinetics are relatively seldom studied in laboratory experiments. This may be because reductive dissolution methods at near neutral pH have to be carried out under anoxic conditions in order to avoid oxidation by atmospheric oxygen. We have therefore developed a convenient method which allows reduction kinetics to be studied in a closed glass tube. A small quantity of ferric oxide, which does not cause visible turbidity, is reduced under sterile and anoxic conditions by means of ascorbate at pH 5.2. The Fe^{2+} formed, and thus the extent of the dissolution reaction, can be determined as a colored ferrozine complex at any time directly with a photometer equipped with a special tray for glass tubes.

The dissolution kinetics of eight synthetic Fe(III) (hydr)oxides (ferrihydrites, lepidocrocite, goethites and hematites) were determined both with the new method and compared to the dissolution kinetics in 0.2 M oxalate buffer, pH 3.0. The data were analyzed using the Kabai model as well as the initial dissolution rate. There was a strong correlation (r^2=0.92) between the logarithms of Kabai constant *k* of both methods. However, less stable oxides dissolved in oxalate buffers substantially faster than with the reductive method, while the most stable oxide dissolved in ascorbate approximately as fast as in oxalate. Linear regression of the log initial rate [µmol Fe h^{-1} m^{-2}] showed only minor shift from the 1:1 line but also showed a weaker correlation (r^2=0.79). In addition, the reactivity-sequence of iron oxides differed somewhat between the two dissolution methods. Thus, this study suggests a need to use a dissolution method whose reaction type fits the objective of the survey.

Introduction

In natural environments, Fe(III) (hydr)oxides not only play an important role for adsorption of organic and inorganic substances, but they are also the most important electron acceptors in periodically anoxic environments. Therefore, they can minimize the formation of CH_4, which is partly responsible for global climate change (*Lovley* and *Phillips*, 1987; *Roden* and *Wetzel*, 1996; *Frenzel et al.,* 1999; *Yao* and *Conrad*, 1999). As opposed to all other electron acceptors, however, the use of iron oxides requires a dissolution of the solid phase prior to or during reduction.

It is therefore of special interest to characterize the stability and especially the dissolution kinetics of different iron oxides.

Two distinct strategies are available to evaluate dissolution kinetics. One is to fit the parameters of a dissolution model to the data. Dissolution models describe the complete dissolution of a sample, irrespective of particle size or specific surface of a sample (for an overview see *Cornell* and *Schwertmann*, 1996). The other strategy is to normalize the dissolution rate – if it is initially linear – on the surface of the sample. This approach provides a more physical description of the kinetic stability of a surface, but is valid solely for the very first part of the dissolution reaction. Examples for this type of evaluation are given by *Dos Santos Afonso et al.* (1990), *Suter et al.* (1991) and *Deng* (1997).

There are three principal ways by which iron oxides may be dissolved: proton-promoted, ligand-promoted and reductive dissolution (*Stumm* and *Morgan*, 1981). Reductive dissolution at neutral pH may be the most frequent and effective process in natural environments (*Cornell* and *Schwertmann*, 1996).

However, determination of reactivity of Fe(III) (hydr)oxides in the laboratory via dissolution kinetics is rarely performed using only reduction, without complexing agents for Fe(III) and at approximately neutral pH (*Cornell* and *Schwertmann*, 1996). This may reflect the necessity of using strictly anoxic conditions to prevent decreasing concentrations of the reducing agent over time due to reaction with atmospheric oxygen (*Torrent et al.,* 1987; *Larsen* and *Postma*, 2001).

To date it remains unclear whether there is a difference in the relative stability of iron oxides determined by dissolution promoted by either protonation/complexation or by reduction. Recently, *Larsen* and *Postma* (2001) studied the dissolution of a set of Fe(III)hydroxides in ascorbic acid, but no attempt has been made to compare the dissolution kinetics of a set of iron oxides with different kinds of dissolving media. We therefore compared a reductive dissolution kinetics with a ligand-promoted dissolution for a set of Fe(III) (hydr)oxides.

In this study, we present a simple method for determining the reductive dissolution of Fe(III) (hydr)oxides; it allows the reaction process to be observed online in a closed glass tube, which maintains anoxic conditions throughout the experiment.

The objective was to test the applicability and precision of the new reductive method and to compare the dissolution kinetics (as a measure for the reactivity of the Fe(III) (hydr)oxide sample) with the kinetics of a ligand-promoted dissolution.

Materials and Methods

Fe(III) (hydr)oxides

A set of Fe(III) (hydr)oxides (Tab. C.1) was synthesized in order to achieve a broad range of stability, comparable to natural samples:

Table C.1: Examined Fe(III) (hydr)oxides

Abbr.	Mineral	SSA* [$m^2 * g^{-1}$]	MCD$^{\#}$ [nm] (hkl)
2LF	2-line ferrihydrite	280	1 (110)
6LF	6-line ferrihydrite	201	3 (110)
L	lepidocrocite	45	27 (020)
G 1	goethite	151	5 (110)
G 2	goethite	120	7 (110)
G 3	goethite	89	9 (110)
H 1	hematite	114	8 (104)
H 3	hematite	110	8 (104)

* specific surface area; $^{\#}$ mean crystal diameter

2-line ferrihydrite 2LF was synthesized according to *Schwertmann* and *Cornell* (1991), but NaOH was used instead of KOH and the centrifuged pellet of the washed product was shock-frozen by squeezing it undiluted through a syringe directly into liquid N_2 .

6-line ferrihydrite 6LF was synthesized according to *Schwertmann* and *Cornell* (1991), but the centrifuged pellet of the washed product was shock-frozen by squeezing it diluted (1+1) through a syringe directly into liquid N_2 .

Lepidocrocite L was synthesized according to *Schwertmann* and *Cornell* (1991).

Goethite G 1 was synthesized from a Fe(II) system according to *Schwertmann* and *Cornell* (1991), but with an increased oxidation rate. To achieve that, air was introduced directly above a quickly rotating stirrer-bar. This produced very small bubbles.

Goethite G 2 was synthesized from a Fe(II) system according to *Schwertmann* and *Cornell* (1991).

Goethite G 3 was synthesized from a Fe(III) system at 4°C according to *Schwertmann et al.* (1985), but NaOH was used instead of KOH.

Hematites H 1 and H 3 were synthesized by thermal dehydroxylation at 280°C for 90 min from goethites G 1 and G 3, respectively.

All samples were checked for mineralogical purity using a Siemens D 500 X-ray diffractometer. All goethites and the lepidocrocite were washed after synthesis for 1 h with 0.5 M HCl to remove amorphous impurities (*Cornell et al.,* 1974). The hematites were not washed again after thermal dehydroxylation.

Mean crystal diameter (MCD_{hkl}) was calculated from the half height broadness of the respective diffraction reflex using the Scherrer equation.

Because the samples were also used in bacterial incubation experiments and because it proved to be necessary to use sterilized oxides for reductive dissolution (see Results and Discussion), all samples were autoclaved for 10 min prior to both the dissolution experiments and the determination of specific surface.

Specific surface was determined using BET (3-point absorption of N_2, Quantachrom Nova 1200).

Dissolution kinetics in oxalate buffer

For the ligand-promoted dissolution, 40-60 mg of Fe(III) (hydr)oxide (three replicates) were continuously shaken in the dark with 150 ml of oxalate buffer according to *Schwertmann* (1964) in polyethylene bottles until dissolution was complete. The extent of dissolution was measured at 7-11 sampling dates: aliquots of 10 ml were taken while the suspension was stirred vigorously to maintain a constant solid:solution ratio. After centrifuging, 8 ml of the supernatant was acidified with 1 ml 2 M HCl to prevent precipitation of Fe(II)-oxalate. Finally, to determine the total amount of iron at 100 % dissolution, some solid ascorbic acid was added and the suspensions were heated in a water bath to 95°C following *Zeien* and *Brümmer* (1989). High concentrations were measured with atomic absorption spectroscopy (AAS), whereas low concentrations were measured spectrophotometrically according to *Dominik* and *Kaupenjohann* (2000).

To test the influence of autoclaving on the stability of a very temperature-sensitive Fe(III) hydroxide, the dissolution kinetic of a non-sterilized sample of 2LF was also read.

Reductive dissolution

The reductive dissolution medium consisted of 9.09 mM ascorbic acid, 90.9 mM sodium ascorbate and 1 mM ferrozine in a strictly anoxic glass tube. The reaction was started by adding 0.5 ml of iron-oxide-containing suspension.

Ascorbic acid was chosen as a well-studied reducing agent for Fe(III) (hydr)oxides (*Zinder et al.,* 1986; *Sulzberger et al.,* 1989; *Dos Santos Afonso et al*., 1990; *Suter et al*., 1991; *Deng*, 1997). To get a purely reductive dissolution mechanism, the pH should be approximately neutral. In order to avoid interferences between buffer substances and either Fe(III) (hydr)oxides or neoprene stoppers, ascorbic acid itself was used to buffer the pH. Because the pK_a of ascorbic acid is 4.20 (*Rilbe*, 1996), a pH of 5.2 was considered to be the maximum, which ensures a stable pH throughout the experiment.

Preparation of the reaction-solution-containing tubes.

To minimize oxidation of ascorbate we used the following procedure: Dissolve 9.688 g ascorbic acid and 0.271 g ferrozine in H_2O_{demin} to give a final volume of 500 ml. Fill portions of 10.0 ml from this solution into Duran® glass tubes (= reaction tubes), stopper them with neoprene stoppers (Aldrich), and degas them using a device for evacuation and gassing as described by *Widdel* and *Bak* (1995). To achieve sufficient degassing it is necessary to hit the tubes on the ball of the thumb while vacuum is applied. When bubble formation remains at a low level, fill the tubes with N_2, remove the stoppers and cautiously add 1.00 ml of degassed 1.00 M NaOH. Put the stoppers back on the tubes and degas and refill with N_2 several times as described above and leave a slightly excess pressure in the tubes.

Preparation of the oxide-containing tubes.

Weigh about 1 mg of each Fe(III) (hydr)oxide to be tested in other glass tubes and add 12 ml H_2O_{demin}, prepare another tube with 25 mM Na_2CO_3, and stopper and degas them all, as described above. All tubes are placed into a rack and the stoppers are fixed by means of two metal-plates and a screw clamp. All tubes are autoclaved for 10 min at 121°C.

A spectrophotometer with a special tray for glass tubes is used. Prepare a H_2O_{demin} -containing tube that is used throughout the experiment to adjust the absorption to zero. It is useful to mark the tubes horizontally to relocate the same position in the tray every time.

Immediately before starting the reaction: The surface of all stoppers was sterilized using 70% ethanol, and 0.5 ml of Na_2CO_3 solution was transferred to the oxide-containing tubes using a sterile and N_2-flushed syringe. The oxides were dispersed using an ultrasonic cleaner.

To start the reaction the surface of the stoppers was sterilized again and 0.5 ml of oxide suspension was transferred to each reaction tube. The absorption at the start of reaction was read immediately at 562 nm at the spectrophotometer.

The tubes were shaken on a horizontal shaker continuously at 23 ±1°C in the dark and the absorption was read from time to time. The useful reading interval

depended on the stability of the examined Fe(III) (hydr)oxide and the next determination was indicated when the intensity of the color had increased obviously. The dissolution was complete when the absorption remained constant.

To check the necessity of autoclaving the Fe(III) (hydr)oxides, the dissolution kinetic of a non-sterilized sample of G 1 was also measured.

Analysis of the dissolution data.

For reductive dissolution the initial absorption value as a blank was subtracted from all following absorption data. For both dissolution methods all values were calculated relative to the final ones. The parameters of the Kabai model (Eq. 1) were fitted to the data using SigmaPlot™.

$$\alpha = 1 - e^{-(k \times t)^a} \qquad (1)$$

α is the extent of the reaction as calculated above, k is the rate constant and a is a parameter which causes a sigmoidal (s-shaped) dissolution curve, if $a > 1$.

Initial dissolution rate was calculated from the linear regression of the first measurements, where the dissolution was quasi linear.

Influence of ferrozine on the dissolution.

In order to test if complexation of Fe^{3+} by ferrozine, followed by reduction of the dissolved and complexed Fe^{3+}, is a possible mechanism for the reaction, an autoclaveable dialysis tube (Visking type 27/32, MWCO = 14000) containing 6.1 mg of 2LF was placed in a 250 ml glass bottle, which contained 200 ml of 1 mM ferrozine solution (pH adjusted to 5.2 using NaOH). The bottle was autoclaved for 10 min at 121°C to prevent microbial reduction of the Fe(III)hydroxide and kept in the dark at 21°C. After 23 days the concentration of Fe outside the dialysis tube was determined using AAS (Varian SpectrAAA 200).

We also tested whether the presence of ferrozine enhances the dissolution kinetics in the new reductive method via enhanced detachment of Fe^{2+} from the surface of Fe(III) (hydr)oxides. A set of 36 reaction tubes were filled with 0.1 M ascorbic acid and 0.091 M NaOH (but without ferrozine), degassed and sterilized.

Suspensions of sterilized Lepidocrocite were added to all reaction tubes at t=0. After different times, three reaction tubes were opened and 14.8 mM ferrozine solution was added anaerobically to give a final concentration of 1 mM. The absorption at 562 nm was read against blank after a few minutes.

Analysis

Analysis of ascorbic acid.

To determine the ascorbic acid in the reaction medium the decolorization of 2,6-dichlorophenol-indophenol (DCIP) was measured photometrically. 8.5 ml of 50 mM acetate buffer, pH 4, were mixed with 0.5 ml of 4 mM DCIP (in 12% ethanol); then, 1 ml of 1:100 diluted reaction medium was added, mixed and absorption at 520 nm was read exactly after 2 min.

Analysis of dehydroascorbate.

Dehydroascorbate was determined using HPLC (Column: Prontosil 60-5-C18 (5µm, 125x4mm) Eluent: 0.25% tetrabutylammoniumhydrosulfate and 5.5 vol% methanol in H_2O_{deion}, UV-Detection at 254 nm).

Results and Discussion

Reductive dissolution kinetics

Accuracy and applicability of the Kabai model.

Figure C.1 shows the experimental data (absorptions) of the reductive dissolution kinetics of the goethite sample G 1. Some of the replicates yielded very different final values. Therefore, the reproducibility of the method is questionable. The absorption of tube no. 1 is higher by about the same value as the absorption of tube no. 2 is lower than the remaining tubes. The explanation could be the extremely small quantity (0.4-0.5 µmol) of iron oxide added to the tubes. Iron oxide was added as a suspension from a 1 ml syringe in volumes of 0.5 ml to two test tubes in succession. The observation from Fig. C.1 suggests that the suspension in the syringe had already settled before the addition to the first tube (no. 1), so that this tube received more iron oxide per volume of suspension than the next tube (no. 2).

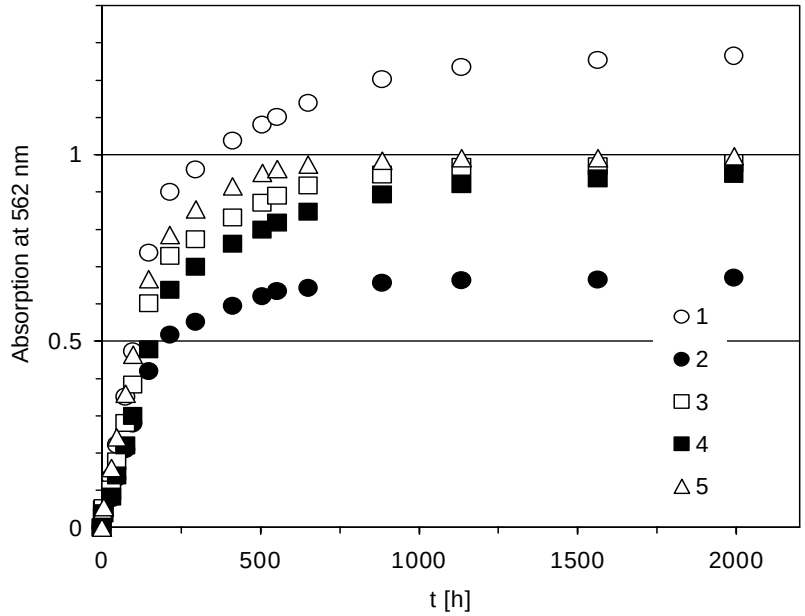

Figure C.1: Reductive method: time course of the absorptions of five parallel reaction tubes of goethite G 1.

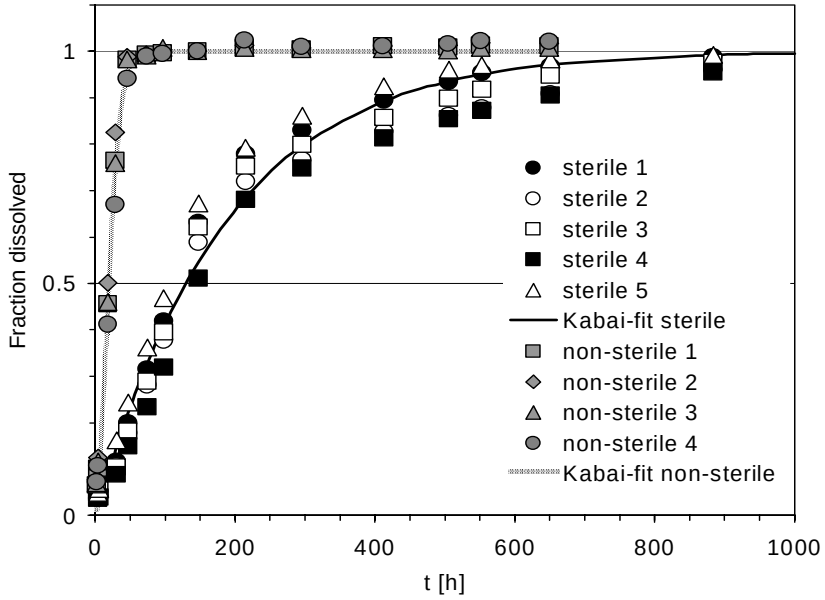

Figure C.2: Reductive method: dissolution kinetics of goethite G 1 at sterile and non-sterile conditions. Repetitions and Kabai fit.

Normalizing the absorptions to the respective final absorption - as a measure for the actual amount of iron oxide present in the tube - however, made the curves look much more similar in Fig. C.2, and the Kabai model could be fitted to all data.

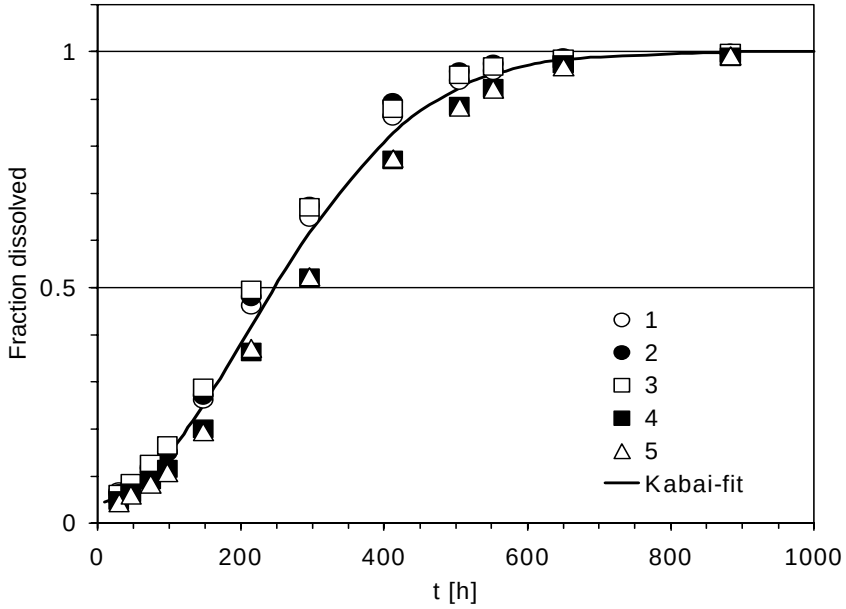

Figure C.3: Reductive method: dissolution kinetics of hematite H 1: Repetitions and Kabai fit.

In Fig. C.3 the relative dissolution of the hematite H 1 is plotted versus time. This sample clearly showed a distinct sigmoidal dissolution kinetic. *Schwertmann* (1984) attributed sigmoidal dissolution of goethites to multidomainic crystals, which disintegrate during dissolution and therefore show an increased specific surface in the meantime (*Schwertmann*, 1991). TEM images (not shown) revealed that, in H 1, new pores had developed along the needle axis during the dehydroxylation of G 1. The crystals of H 1 had probably also disintegrated along these pores during dissolution.

Fig. C.3 shows that the dissolution of H 1 started at a level clearly higher than zero. We therefore used an improved Kabai equation (2) to model the data in Fig. C.3:

$$\alpha = 1 - \left(e^{-(k \times t)^a}\right) \times (1 - b) \qquad (2)$$

In addition to the parameters *a* and *k,* a constant *b* is included in the Kabai equation; it allows the function to start at values different from zero.

The necessity of constant *b* indicates that the sample contained - beside the mineral proven by XRD - a second, easy-soluble (amorphous) phase, which is already completely dissolved at the first determination time. For H 1 this

amorphous phase amounted to approximately 4.5% of the total iron content of the sample in both the reductive dissolution kinetic and in the dissolution in oxalate. In addition to H 1, such impurities were also detected for H 3 and 6LF at 3.7 and about 6%, respectively (Table C.2). These results demonstrate the necessity of washing also the 6LF after the synthesis and the hematites again after the dehydroxylation with diluted HCl.

Table C.2: Comparison of Dissolution Parameters

	Reductive Dissolution				Dissolution in Oxalate			
Sample, remarks	Kabai k[1]	Kabai a	Kabai b	initial rate[2]	Kabai k[1]	Kabai a	Kabai b	initial rate[2]
L	$1.61 * 10^{-1}$	0.56	-	$5.44 * 10^{+1}$	$9.26 * 10^{-1}$	1.68	-	$1.34 * 10^{+2}$
L, without ferrozine	$1.76 * 10^{-1}$	0.9	-	$5.84 * 10^{+1}$	n.d.[3]	n.d.[3]	-	n.d.[3]
ss2LFH	$1.28 * 10^{-1}$	1.29	-	$3.30 * 10^{+0}$	$4.2 * 10^{0}$	1.8	-	$9.27 * 10^{+1}$
ss2LFH, non-sterile	n.d.[3]	n.d.[3]	-	n.d.[3]	$9.1 * 10^{0}$	2.28	-	$1.65 * 10^{+2}$
6LFH	$1.99 * 10^{-2}$	1.69	0.073	$6.05 * 10^{-1}$	$1.34 * 10^{-1}$	0.68	0.068	$1.19 * 10^{+1}$
G 2	$7.09 * 10^{-3}$	1.43	-	$2.77 * 10^{-1}$	$2.9 * 10^{-2}$	1.42	-	$1.23 * 10^{0}$
G 1	$5.37 * 10^{-3}$	1.01	-	$2.65 * 10^{-1}$	$6.27 * 10^{-2}$	0.95	-	$8.50 * 10^{0}$
G 1, non-sterile	$4.1 * 10^{-2}$	1.75	-	$9.40 * 10^{-1}$	n.d.[3]	n.d.[3]	-	n.d.[3]
H 3	$3.55 * 10^{-3}$	0.96	0.037	$2.94 * 10^{-1}$	$9.66 * 10^{-3}$	1.81	0.037	$1.02 * 10^{0}$
H 1	$3.22 * 10^{-3}$	1.9	0.043	$1.09 * 10^{-1}$	$1.07 * 10^{-2}$	1.88	0.047	$1.72 * 10^{0}$
G 3	$2.31 * 10^{-3}$	1.32	-	$6.59 * 10^{-2}$	$3.97 * 10^{-3}$	1.19	-	$3.22 * 10^{-1}$

[1] dimension of Kabai k is [h^{-1}] [2] dimension of initial rate is [µmol Fe h^{-1} m^{-2}] [3] not determined - not detected

Because the sample collective represented both sigmoidal and purely deceleratory dissolution kinetics, the Kabai model was the only one which allowed a mathematical description of all samples (*Cornell* and *Schwertmann*, 1996). Therefore, all dissolution data were fitted to the Kabai model. The Kabai parameters of all oxides are presented in Table C.2.

The oxide samples are arranged in decreasing value of Kabai constant *k* of the reductive kinetics. The exponent *a* varies from 0.59 to 1.9; values >1 indicate that the sample exhibits a sigmoidal dissolution kinetics. Although exponent *a* influences the shape of a Kabai curve in detail, the speed of the overall dissolution depends only on *k*. The Kabai constant *k* is therefore used as the measure for stability (*Schwertmann*, 1984; *Schwertmann et al.,* 1985; *Schwertmann et al*., 1987; *Schwertmann*, 1991; *Ruan* and *Gilkes*, 1995).

Rate constant *k* - *i.e.* the reactivity - varies over a range of two orders of magnitude between all iron oxides tested. Table C.2 also shows the initial dissolution rate expressed as µmol Fe m^{-2} h^{-1}. There is an excellent correlation between initial rate and Kabai constant *k*; moreover, the range and sequence of samples is largely the same, *i.e*. the differences in *k* cannot be reduced to differences in specific surface. Only lepidocrocite L, in which the Kabai constant is similar to 2LF, has an extremely high initial rate. This is because lepidocrocite is the most crystalline sample with the lowest specific surface.

Table C.2 shows that initial dissolution rates of samples of the same mineral can differ markedly, even if normalized to surface. However, the initial rates of G 1 and G 2 are almost identical, *i.e.* the stabilities of both samples are comparable; they differ in specific surface only.

Overall, the kinetics measured using this new method are rather slow compared to other laboratory methods for reductive dissolution of iron oxides (*Fischer*, 1987; *Torrent et al.,* 1987). The latter authors, however, worked under very strong reducing conditions, using H_2 or dithionite. On the other hand, the dissolution kinetics of our method are comparable to those of *Larsen* and *Postma* (2001), who used 10 mM ascorbic acid, pH 3. In addition, dissolution kinetics by microbial reduction in natural soil samples are much slower (*Peters* and *Conrad*, 1996).

Need for sterile conditions.

Fig. C.2 shows the dissolution of both a sterilized and non-sterilized sample of G 1: the non-sterile sample clearly dissolves much faster. The values of Kabai *k* differ by a factor 7.6 (see Tab. C.2). Hydrothermal treatment always increases

crystallinity (*Schwertmann* and *Fischer*, 1966; *Schwertmann et al.,* 1985). Therefore the question arises whether autoclaving at 121°C for 10 min (plus heating and cooling phase) could have caused this enormous decrease in dissolution kinetics on its own. *Schwertmann* and *Fischer* (1966) found that ferrihydrite gel converts into crystalline products with first-order kinetics when heated to 100°C. The solubility in oxalate (2 h) was reduced to 50% within 140 min. During the dissolution in oxalate, microbial growth can be neglected because of the low pH. We found, that autoclaving of 2LF decreased the Kabai constant for dissolution in oxalate by a factor 2 (Tab. C.2).

Schwertmann *et al.* (1985) treated an alkaline goethite with a specific surface of 153 m^2 g^{-1} hydrothermally (16 h, 125°C). This treatment reduced the Kabai constant *k* of the dissolution in 6 M HCl by a factor of 3.7. The decrease by a factor of 7.6 can therefore be attributed only minimally to modified crystallinity. Most of the difference has to be attributed to microorganisms, which can very rapidly reduce the tiny amount of ferric hydroxide in the tube. Exponent *a* in Tab. C.2 indicates that - in contrast to the sterile sample G 1 - the dissolution of the non-sterile sample exhibited remarkable sigmoidity. This also points to microbial growth (*Lovley* and *Phillips*, 1988; *Roden* and *Zachara*, 1996).

These considerations demonstrate that the analysis absolutely must be performed under sterile conditions to yield reproducible data. Moreover, non-sterile mode of operation can cloud the reaction medium by growth of microorganisms.

Stability of the final value.

The complete dissolution of the oxide sample is recognized by a stable absorption of each tube (see Material & Methods). Unfortunately, this is only approximately true. Tube no. 5 in Fig. C.1 reveals best that the absorption increased slowly, but continuously. Fig. C.4 shows the same effect for the blank values. Actually, the blank values gradually changed their color into pink. Our interpretation is that the neoprene stoppers released some iron. According to the manufacturer these stoppers should be metal-free, but after dry combustion and digestion with HCl we determined an iron content of 540 ppm. A screening of different stopper materials proved only the silicone stoppers of Verneret to be iron-free. However, when using

these silicone stoppers the reaction medium already changed its color after 32 days to an intense yellow, which increased the absorption even at 562 nm (see Fig. C.4).

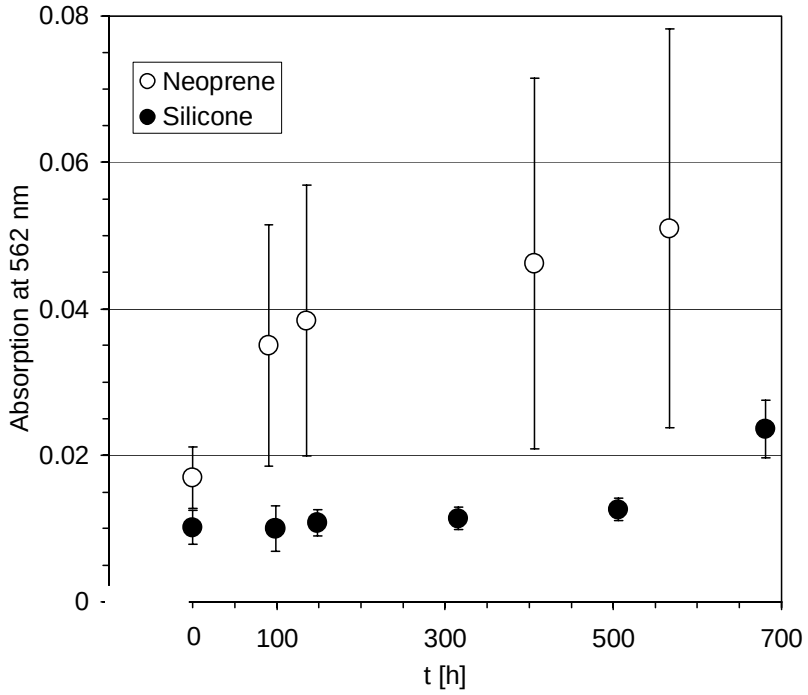

Figure C.4: Reductive method: Time course of blanks, reaction tubes closed either with silicone or neoprene stoppers. Whiskers indicate standard deviations.

This indicated oxidation of ascorbate (*Davies et al.,* 1991). Actually, only 82% of the initial ascorbate concentration (before sterilization) could be measured in the reaction medium at this time. The missing 18 % could not be detected as dehydroascorbate either. On the other hand, an 80-day-old blank tube with a neoprene stopper that had essentially no yellow but a pink tinge, still contained 94% of initial ascorbate and the remaining 6 % were found as dehydroascorbate. Presumably, a little ascorbate is oxidized by sterilization even under anoxic conditions. These data indicate that the oxygen permeability of silicone is clearly higher than that of neoprene. Based on these results, we recommend the use of silicone stoppers only for reactive oxides, which are dissolved quite rapidly, whereas neoprene stoppers should be used for more stable oxides. The end point

of dissolution is achieved when the increase of the mean of the repetitions no longer exceeds the increase of the blanks.

Influence of ferrozine on the dissolution.

The dissolution-mechanism of Fe(III) (hydr)oxides by ascorbate is well known (*Zinder et al.*, 1986; *Sulzberger et al.*, 1989; *Dos Santos Afonso et al.*, 1990; *Suter et al.*, 1991; *Deng*, 1997). It is generally accepted that the chemical mechanism involves at least three elementary steps:

1) Adsorption of ascorbate to form an inner-sphere ascorbato-Fe(III) complex.
2) Electron transfer within the complex and detachment of an ascorbate radical (which reduces another Fe(III) in a second reaction to form dehydroascorbate).
3) Detachment of Fe^{2+}

For a fixed pH, all authors found a linear relationship between dissolution rate and surface concentration of ascorbate. Because adsorption is fast compared to the onset of dissolution (*Suter et al.*, 1991; *Deng*, 1997), there is agreement that the detachment of Fe^{2+} is the slowest and therefore rate-determining step. For constant surface concentrations of ascorbate, *Dos Santos Afonso et al.* (1990) and *Suter et al.* (1991) found that the dissolution rate increased with decreasing pH. While the former authors concluded that adsorption to adequately protonated sites is a prerequisite for electron transfer, the latter authors concluded that the release of Fe^{2+} is accelerated by protonation of the surface sites. The question arises whether the presence of ferrozine in the method presented here will alter this known mechanism.

Phenanthroline forms a complex with Fe^{3+} that is even more stable than with Fe^{2+} (*Ueno et al.*, 1992). If this holds true for ferrozine too, the observed dissolution could be attributed to ligand-promoted dissolution of Fe(III) (hydr)oxides, followed by reduction of the ferrozine-complex rather than reduction of surface Fe(III). When we tried to dissolve 2LF in 1 mM ferrozine without ascorbate, the iron concentration remained below the detection limit of the AAS ($\leq$ 0.03 mg L^{-1}, α = 0.05, determined according to DIN 32645) after 23 days. This means that less than 0.2% of the ferrihydrite was dissolved after 23 days, whereas

it was completely dissolved in the reductive medium after 27 hours. The dialysis membrane might have reduced the diffusion, but from the determination of the solubility product we know that the diffusion-hindering effect of a dialysis membrane is minor: after 23 d of continuously shaking an iron oxide in diluted HNO_3, the concentration of dissolved Fe(III) was at the most 130% compared to the outside concentration, when the iron oxide was kept in a dialysis bag. If ferrozine forms a complex with Fe^{3+} at all, it is too weak or its kinetics of formation is very slow. Therefore we can conclude that complexation of Fe^{3+} by ferrozine is not involved in the mechanism of the method presented here.

In the reductive dissolution of lepidocrocite by ascorbate, pH 5.2, the Kabai constant k and the initial dissolution rate is identical in the absence and in the presence of ferrozine (Tab. C.2), *i.e*. ferrozine did not enhance the detachment of Fe^{2+}. *Suter et al.* (1991) showed that the dissolution rate of a hematite promoted by protons even at pH 3 was negligible compared to ascorbic acid concentrations as low as 10 µM. It is clear that at pH 5.2 there would be essentially no dissolution by protons alone. Therefore, the mechanism of the method presented here is a purely reductive dissolution attributed to ascorbate.

Although not tested, the pH and ascorbic acid concentration of the method presented here could no doubt be varied to some extent, if desirable. As the pK_a of ferrozine is 3.2 (*Amonette et al.*, 1994), it will react with Fe^{2+} even below pH 3. Since the reduction of approximately 40 µM iron oxide will produce about 80 µM OH^-, a stable pH throughout the reaction can be maintained with ascorbic acid concentrations even far below 100 mM. As an example, the excellent recent study of *Larsen* and *Postma* (2001) could presumably have been performed with less effort.

Comparison of kinetic parameters of the reductive dissolution and the dissolution in oxalate.

All Fe(III) (hydr)oxide samples whose reductive dissolution was examined with the new method were also dissolved in oxalate buffer according to *Schwertmann* (1964). In order to compare the kinetic parameters of both methods, the Kabai

model was fitted to the data and the initial dissolution rates, normalized to the surface, were calculated.

Table C.2 represents the best fit parameters for both dissolution kinetics. The oxide samples are arranged in decreasing value of the Kabai constant *k* of reductive kinetics. Figs. C.5 and C.6 compare, on a logarithmic scale, both dissolution methods for the Kabai constant and the initial dissolution rate. There is a good linear correlation of the Kabai constants in Fig. C.5, which can be written as:

$$\lg(k_{red}) = 0.66\lg(k_{ox}) - 1.14 \quad r^2 = 0.92 \quad (3)$$

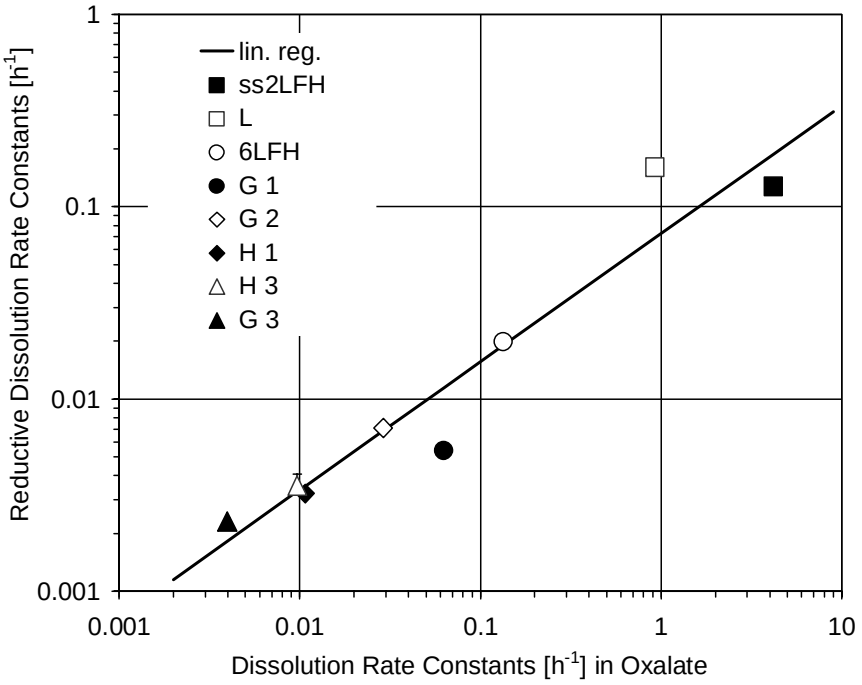

Figure C.5: Comparison of Kabai k: reductive method versus dissolution in oxalate.

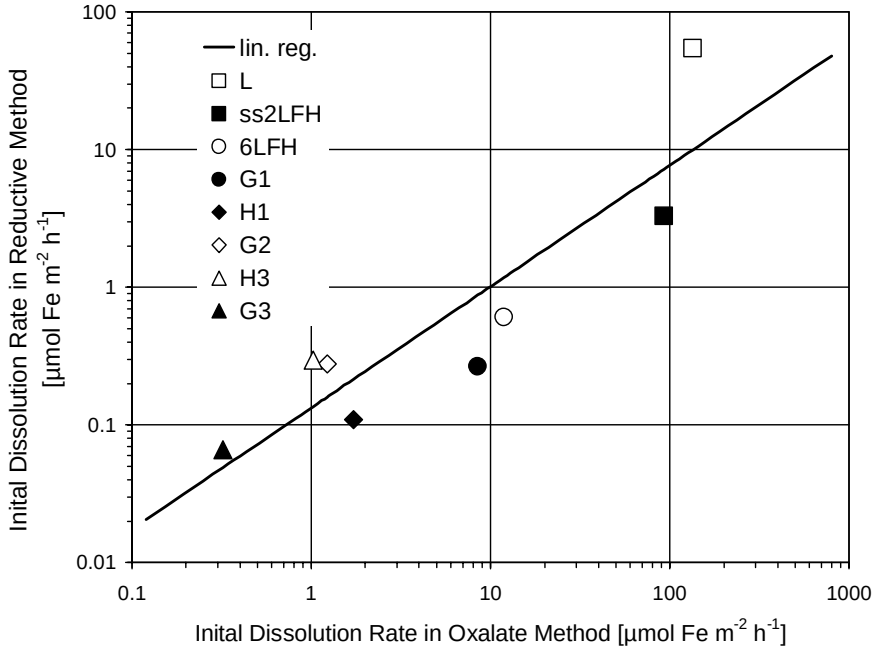

Figure C.6: Comparison of initial dissolution rates: reductive method versus dissolution in oxalate.

Fig. C.6 also demonstrates an acceptable correlation for the initial rates (Eq. 4) between both dissolution methods.

$$\lg(inir._{red}) = 0.88 \lg(inir._{ox}) - 0.87 \quad r^2 = 0.79 \qquad (4)$$

Thus, using one method would enable the results of the other method to be approximated. This is of special interest because there are also good correlations to other parameters of the iron oxides, including standard potential, solubility product and specific surface. These results are not presented here, because we had tried to use these correlations to determine - via dissolution kinetics - specific surfaces or standard potentials of iron oxides in complex mixtures of iron oxides, like in soil samples. These latter results will be published elsewhere.

In our opinion it is worth emphasizing that there is the good correlation between kinetic and thermodynamic data of iron oxides, which is not self evident. Further research is needed to confirm these correlations, but it may well be possible to

describe the kinetic as well the thermodynamic behavior of iron oxides using only one characterizing parameter. At any rate, the method presented here offers a low-cost opportunity to obtain kinetic dissolution data for Fe(III) (hydr)oxides.

Although the regressions are good, it is remarkable that both regression straight lines in Figs. C.5 and C.6 are shifted not parallel to the 1:1 line; the slope in eq. 3 and 4 is below 1. This means that the parameter values of the different dissolution methods become more similar with increased crystallinity of the Fe(III) (hydr)oxides. For example, the ratio of Kabai constants of the two methods are 33 and 1.7 for 2LF and G 3, respectively. The respective ratios of the initial dissolution rates are 29 and 4.9.

Why the kinetics of both methods approach each other with increasing stability remains unclear. Thermodynamic data (MinQuery) indicate that the oxalate method is far from equilibrium with the solubility product of even a goethite of reasonable crystallinity (*Schwertmann*, 1991). The reductive method is also far from equilibrium: The measured redox potential of the reduction medium (below 0 mV at pH 5.2) is low enough to yield an Fe^{2+} activity of 10^{-4} M in equilibrium with a reasonably crystalline goethite (*Brookins*, 1988), but ferrozine maintains the Fe^{2+} activity below 2×10^{-11} M (*Amonette et al*., 1994).

Beyond the good correlations, problems arise if the Kabai constant or initial dissolution rates are taken as a measure for reactivity of the iron oxide samples and if one compares the two dissolution methods. For Kabai constants the sample collective spans a range of over almost two orders of magnitude in the reductive dissolution, whereas for the dissolution in oxalate this range is three orders of magnitude. Thus, in the reductive dissolution, 2LF is about 55 times more reactive than the most stable sample, G 3. In the dissolution in oxalate, however, this factor is 1060. The stability of the oxides relative to each other therefore greatly depends on the dissolution method used.

As opposed to the Kabai constants, the initial dissolution rates for the sample collective span a range of almost 3 orders of magnitude for both dissolution methods (see Fig. C.6). This difference is caused by lepidocrocite, which has a much lower specific surface than 2LF and dissolves in oxalic buffer much slower

than 2LF, whereas these two samples behave the opposite in reductive dissolution.

Beyond the variable differences of the Kabai constants of two compared iron oxide samples in the two dissolution methods, another problem arises if dissolution kinetic parameters are used as a measure of stability. Figs. C.5 and C.6 show that the sequence of iron oxide stability is partly different for both dissolution methods. This is true for Kabai constants as well as for initial rates. Therefore, the relative stability of two iron oxides may depend on which dissolution method is used. The data presented here do not clarify whether these discrepancies depend on the dissolution mechanism (reduction versus ligand-promoted dissolution) or on specific influences of the chemicals used.

Our results might be eminently relevant for studies that use dissolution kinetic parameters to describe iron oxide stability. Specifically, the dissolution method should be tailored to the objective of the study.

Conclusions

The new method for reductive dissolution kinetics presented here is simple and convenient, even though more stable oxides take time to be dissolved.

The data obtained with the new method could be described very well by the Kabai model. The Kabai constant *k* or the initial dissolution rate obtained from this dissolution method can be used as a measure for the reactivity of the Fe(III) (hydr)oxide sample.

There are good correlations between the Kabai constant k or initial dissolution rate and other characterizing parameters of Fe(III) (hydr)oxides, such as specific surface or solubility product. It may be possible to describe the thermodynamic and kinetic reactivity of Fe(III) (hydr)oxides using only one parameter.

The relative stability of iron oxides may differ depending on whether they are determined via reductive dissolution kinetics or via dissolution in oxalate, or may even depend on whether the Kabai model constant or initial dissolution rate is used as the measure for stability.

D. Identification of stability fractions of Fe(III) (hydr)oxides in soil using kinetic experiments

Abstract

This study examines whether the dissolution kinetics of soil Fe(III) (hydr)oxides (FHOs) can be reduced to fractions that dissolve simultaneously according to pseudo-first-order kinetics, each fraction *i* having a homogeneous rate constant (k_i). This would potentially allow the assignment of physicochemical parameters like specific surface area, solubility product, and standard potential to each fraction, because these parameters were found to be highly correlated to k_i for synthetic FHOs. A new efficient and precise method was used to measure the dissolution kinetic in an anoxic glass tube filled with 100 mM ascorbate, 1 mM citrate and 1 mM ferrozine, pH 5.2. The extent of the dissolution reaction (as absorption of Fe(II)(ferrozine)$_3$ complex) could be read at any time directly in the glass tube using a photometer with a special tray for glass tubes.

Using both linearization and fitting, the measured kinetic of soil FHOs could be very well described by 4 fractions (k_i of 10^{-3}-10^{1} and fraction sizes u_i of 0.05-0,49 relative to Fe_d). The mean difference between both data analysis methods was 0.042 for u_i, and a factor of 1.56 for k_i for every fraction. The u_i of synthetic FHOs, which were added to soils whose own FHOs had been removed using boiling oxalate, were recovered quite precisely, but the k_i of crystalline FHOs increased by a factor of 2-8. The reasons for this remain unclear. It was possibly an artefact due to the boiling oxalate treatment, because using the correlation between *k* of dissolution of synthetic FHOs in ascorbate/citrate versus oxalate we were able to predict the amount of Fe_o. In the future we therefore hope to be able to assign the above-mentioned physicochemical parameters to the fractions.

1 Introduction

Fe(III) (hydr)oxides (FHOs) play an eminent role in the ecological functioning of soils. They are responsible for the adsorption of anions, contribute substantially to the adsorption of hydrophilic organic substances and heavy metals, and provide the predominant amount of electron acceptors in periodically anoxic soils. Because FHOs appear as different minerals which exhibit variable crystal perfection, size and degree of isomorphous substitution, they exhibit a broad range of physicochemical characteristics. *Schwertmann* (1988) determined ranges of mean crystal diameter (MCD) for goethites, hematites and lepidocrocites to be 8-660, 11-690, and 13-1000 nm, respectively. Minerals and MCD can be determined by XRD. However, properties such as specific surface area, solubility product or standard potential – and not so much mineral forms – account for ecological behavior (*Jones*, 1981). These properties are easy to determine for synthetic samples (*Schwertmann* and *Cornell*, 2000), but difficult for FHOs in soils.

Determination of MCD from XRD line broadening of XRD works only on the assumption that no strain causes additional line broadening (*Schwertmann*, 1988). The determination of surface area of FHOs in soils using EGME-adsorption or the BET-technique in soils is a difference method (before and after extracting FHOs) which assumes that FHOs do not share surfaces with other soil components; this is doubtful (*Schwertmann*, 1988). The combined use of XRD and Mössbauer-spectroscopy is presumably the only possibility to determine true mean crystal sizes of iron oxides in soils (*Murad*, 1990). Nonetheless, this yields only a mean diameter for every mineral and these methods are expensive and time consuming.

It is not possible to determine the solubility product K_{SO} or the standard potential Eh° of FHOs in soils because the fraction with the lowest stability will govern the solution. Based on mineralogy and particle size, it is assumed that the range of K_{SO} in soils is at least 3-4 orders of magnitude (*Schwertmann*, 1991).

Chemical extraction procedures were developed to fractionate FHOs. A standard method is to extract amorphous Fe(III) hydroxides in soils with oxalic acid buffer (Fe_o), according to *Schwertmann* (1964). However, all FHOs of a soil sample dissolve simultaneously in this buffer, although with different kinetics

depending on their stability (*Schwertmann et al.,* 1982). The duration of extraction was therefore limited to 2 h, when ferrihydrites are completely dissolved, whereas more crystalline fractions are dissolved to a minor extent only. This example demonstrates the principally impossibility of capturing exactly a single stability fraction using an extraction.

At the same time, it could be possible to calculate different fractions of FHOs in soil from an overall dissolution kinetic. *Kaupenjohann* (1989), *Süsser* and *Schwertmann* (1991), and *Van de Sand* (1997) reduced the proton buffering kinetics of soils to 2 or 3 fractions, which reacted simultaneously according a pseudo-first-order kinetic.

“Multicomponent differential kinetic methods“ gain increasing interest in analytical chemistry (*Perez-Bendito* and *Silva*, 1996). In these methods more than one analyte from a single sample reacts simultaneously, but with different kinetics to produce a sum-signal (mostly recorded by spectrophotometry). Computer models are used to calculate the concentrations from the time course of the signal. In most, but not all cases, the rate constants of all analytes are known.

The idea of this paper is to record the sum dissolution kinetic of the FHOs of a soil sample and to try to calculate of which single dissolution kinetics it is composed. The dissolution kinetics of FHOs depends on the solution as well as on many factors of the FHO such as specific surface area, reactivity, shape and irregularities of the crystal (*Cornell* and *Schwertmann*, 1996). Although the dissolution is a surface controlled process, if the parameters of the solution do not change considerably during the reaction, the complete dissolution kinetic of FHOs can be described satisfactorily by dissolution models. These models account for shrinking surface area during dissolution. For an overview on dissolution models see chapter 12.3 in *Cornell* and *Schwertmann* (1996). If the differently reactive FHOs of soil dissolve according to a pseudo-first-order kinetic, it should be possible to reduce the overall dissolution kinetic to unnamed “fractions” of FHOs which are characterized by a homogeneous dissolution rate constant. This idea is encouraged by the finding that the stability parameters mentioned above are highly correlated to the dissolution rate constant of synthetic FHOs (*Dominik* et al., submitted). If this is also true for soil FHOs, such a differential dissolution kinetic

method would enable us to assign approximated values of specific surface area, K_{SO} and Eh° to these “fractions”, and therefore to predict functioning of soil FHOs like adsorption or redox phenomena.

The objective of this work was to test if “stability fractions”, delimited from each other by a homogeneous rate constant, could be identified from the dissolution kinetics of soil FHOs and to check the accuracy of the results.

2 Materials and methods

Recently, we developed a convenient method which allows reduction kinetics of synthetic FHOs to be studied in a closed glass tube (*Dominik et al.,* submitted). A small quantity of ferric oxide, which does not cause visible turbidity, is reduced under sterile and anoxic conditions by means of ascorbate at pH 5.2. The Fe^{2+} formed, and thus the extent of the dissolution reaction, can be determined as a colored ferrozine complex at any time directly with a photometer equipped with a special tray for glass tubes. Before this method could be applied to soil samples, a few questions had to be answered:

1) The FHO content of soil samples seldom exceeds a few percent. The mass of soil which has to be introduced into the glass tubes in order to add sufficient FHOs will cause turbidity. This requires centrifuging the glass tubes prior to determining absorption.

2) Contrary to the samples we had studied using this method until now, most FHOs in soil are Al-substituted (*Schwertmann* and *Taylor*, 1989). *Bousserrhine et al.* (1998) found that Al-substituted goethites were only incompletely dissolved by dithionite in the absence of a complexing agent like citrate. It must therefore be tested whether ascorbate pH 5.2 also needs some citrate to completely dissolve Al-substituted goethites.

3) It proved to be necessary to use sterile conditions for synthetic FHOs in order to yield reproducible kinetics. Complete sterilization of soil samples, however, is difficult to achieve and may alter soil properties (*Wolf et al.,* 1989). Most laboratories are equipped with an autoclave, but thermal treatment changes

FHO reactivity (*Schwertmann et al.,* 1985). It was therefore desirable to compare threefold-repeated autoclaving and γ-ray treatment.

2.1 Determination of dissolution kinetics

The dissolution medium contained 9.09 mM ascorbic acid, 90.9 mM sodium ascorbate (yielding pH 5.2), 1 mM sodium citrate, and 1 mM ferrozine in a strictly anoxic glass tube. The reaction was started by adding 0.3 ml of iron-oxide-containing suspension. The extent of reaction could be determined as a colored Fe(II)(ferrozine)$_3$ complex directly in the glass tube after centrifugation.

2.1.1 Preparation of the reaction-solution-containing tubes

Reaction-solution-containing tubes lacking citrate were prepared according to *Dominik et al.* (submitted).

The corresponding tubes with citrate were prepared in a similar manner: 6.35 ml of a solution containing 19.636 g l^{-1} ascorbic acid, 0.543 g l^{-1} ferrozine and 0.232 g l^{-1} citric acid monohydrate was filled in Duran® glass tubes (16x100mm) and degassed using a device as described by *Widdel* and *Bak* (1995). After cautiously adding 0.65 ml of degassed 1M NaOH, each tube was sealed using neoprene stoppers (Aldrich), degassed and refilled with N_2 (for detailed description of degassing, see *Dominik et al.* (submitted)). Finally, the tubes were autoclaved for 10 min at 121°C. To keep the stoppers in place, the tubes were placed in a rack and the stoppers were fixed by means of two metal-plates and a screw clamp.

2.1.2 Dissolution of Al-substituted goethite

An Al-substituted goethite was synthesized according to the method 5.5.1.1 in *Schwertmann* and *Cornell* (2000). After dissolution in boiling oxalic buffer according to *Zeien* and *Brümmer* (1989), the degree of substitution was determined using AAS (Varian SpectrAAA 200) to be 7.2 mol%. This goethite was dissolved in a reductive medium consisting of 100 mM ascorbic acid, 1 mM ferrozine, pH 5.2 (*Dominik et al.,* submitted). Two variants, with and without 1 mM sodium citrate, were run.

2.1.3 Dissolution kinetics of synthetic FHOs

Because a new dissolution medium was used, it was necessary to check the correlation between the first-order rate constant *k* of the dissolution kinetics and the characterizing parameters of the oxides, i.e. specific surface, solubility product K_{SO}, and standard potential $E_h°$. The same samples and the method reported earlier (*Dominik* et al., submitted) was used to determine the dissolution kinetics, but the citrate-containing reaction medium was used.

2.1.4 Dissolution kinetics of soil FHOs

Table D.1. Soil properties

Abbreviation	H	L	V
Soil-Classification according to FAO	Terric Histosol	Haplic Luvisol	Stagni-Eutric Vertisol
Soil-Horizon	histic H	mollic A	mollic A
Sand [%]		3	9
Silt [%]		79	51
Clay [%]		18	40
pH ($CaCl_2$)	7.5	6.6	6.6
$CaCO_3$ [%]	49.4	0	0
CEC* [$mmol_c\ kg^{-1}$]	993	170	216
$C_{organic}$ [%]	16.1	0.9	2.6
N_{total} [$g\ kg^{-1}$]	13.6	1.2	3.0
P_{CAL}# [$mg\ kg^{-1}$]	56	158	28
K_{CAL}# [$mg\ kg^{-1}$]	122	298	122
Fe_o† [$g\ kg^{-1}$]	3.0	3.2	10.9
Fe_d‡ [$g\ kg^{-1}$]	3.8	11.2	24.3

*Cation Exchange Capacity, #phosphorus or potassium extracted by calcium acetate lactate method, † amorphous iron oxides extracted by the oxalate method, ‡ sum of amorphous and crystalline iron oxides extracted by the CBD method.

To represent a wide range of soil characteristics, three soil samples differing in main properties (Tab. D.1) were selected: The air-dried topsoils of a Terric Histosol "H", a Haplic Luvisol "L" and a Stagni-Eutric Vertisol "V" were carefully ground separately in a mortar to disintegrate aggregates and shells and were suspended in 100 ml of 5 mM NaCl to give a final concentration of 1.07 mM Fe_d (iron oxides). The Erlenmeyer flasks were closed with butyl stoppers and the latter

were fixed using a stainless steel wire. Two different methods were used to sterilize these "starter-suspensions". One set was autoclaved at 121°C for 20 min on three days in succession (variants "3a"). The other set was exposed to > 29.4 kGy in a ^{60}Co γ-radiation treatment plant (Fa. Rüsch, 71394 Kernen-Rommelshausen, Germany) (variants "γ").

To start the reaction, the surface of the stoppers of all vessels was sterilized using 70% ethanol, and 0.3 ml of soil-containing suspension was transferred to each reaction tube by means of a N_2-flushed syringe. One blank omitting ferrozine (humus blank) was started with one soil-suspension in each of the two sets. Five blanks containing normal reaction solution but no soil were also included (stopper blank). All tubes were shaken on a horizontal shaker (90 rpm) continuously in the dark at 23±1°C. The absorption of all tubes at 562 nm was read 22-24 times using a Zeiss PM2 DL spectrophotometer equipped with a special tray for glass tubes. Prior to reading, the tubes were centrifuged at 1500 g for 5 min.

2.1.5 Recovery of synthetic FHOs added to iron-oxide free soil (control experiment)

In order to examine the influence of soil components on the dissolution kinetics of known FHOs, the dissolution kinetics of synthetic FHOs were examined in the presence of soil samples whose own FHOs had been extracted.

The same soil samples as used above were therefore extracted two times with boiling oxalate buffer according to *Zeien* and *Brümmer* (1989), fraction 6 and centrifuged. To desorb excess oxalate, the pellet was resuspended in H_2O_{deion}, adjusted to pH 7.5, shaken overnight in 0.2 M Na_2SO_4 and washed with H_2O_{deion} until electric conductivity was below 0.5 mS cm^{-1}.

From these "soil samples" the same mass as in 2.1.4 was weighed in 100 ml Erlenmeyer flasks. To every flask, 36 µmol of lepidocrocite L, 6-line-ferrihydrite 6LF, and goethite G 3 was added. The suspensions were made up to a final volume of 100 ml and to a final NaCl-concentration of 5 mM. The flasks were stoppered and sterilized as in 2.1.4 to yield two sterilization-variants of each soil sample ("γ-boe" and "3a-boe"). Determination of dissolution kinetics was carried out as described in 2.1.4.

2.2 Data treatment

From the absorption data in 2.1.3, the stopper blank was subtracted, and from the absorption data in 2.1.4 and 2.1.5, both the stopper blank and the humus blank were subtracted. Dissolution was complete when this value showed no further increase. All values were normalized to this final value. The parameters of the first-order model as well as the Kabai model were fitted to the data using SigmaPlot™.

To reduce the measured sum dissolution kinetics from 2.1.4 and 2.1.5 to the dissolution kinetics of fractions showing a uniform rate constant, it was assumed that each fraction dissolves according to the first-order model (Eq.1).

$$\alpha = 1 - e^{-k \cdot t} \qquad (1)$$

where α is the already dissolved portion (ranging from 0 to 1) at time t, and k [h^{-1}] is the rate constant. If several fractions dissolve simultaneously the equation for each phase becomes:

$$\alpha_i = u_i - u_i \cdot e^{-k_i \cdot t} \qquad (2)$$

where α_i is the amount of fraction i, normalized to the total amount of iron oxides dissolved at time t, u_i is the size which has fraction i relative to the total (molar) amount of FHOs, and k_i is the rate constant of the fraction i.

The sum kinetic of all fractions is then described by Eq. 3 (first-order sum model)

$$\alpha_{tot} = \sum_{i=1}^{n} (u_i - u_i \cdot e^{-k_i \cdot t}) \qquad (3)$$

where α_{tot} is the portion of the total amount of FHOs dissolved at time t. Clearly, it is necessary to determine two parameters to describe every fraction (u_i and k_i).

As an example, the sum kinetic composed of three fractions differing in rate constant and fraction size is shown in Fig. D.1a.

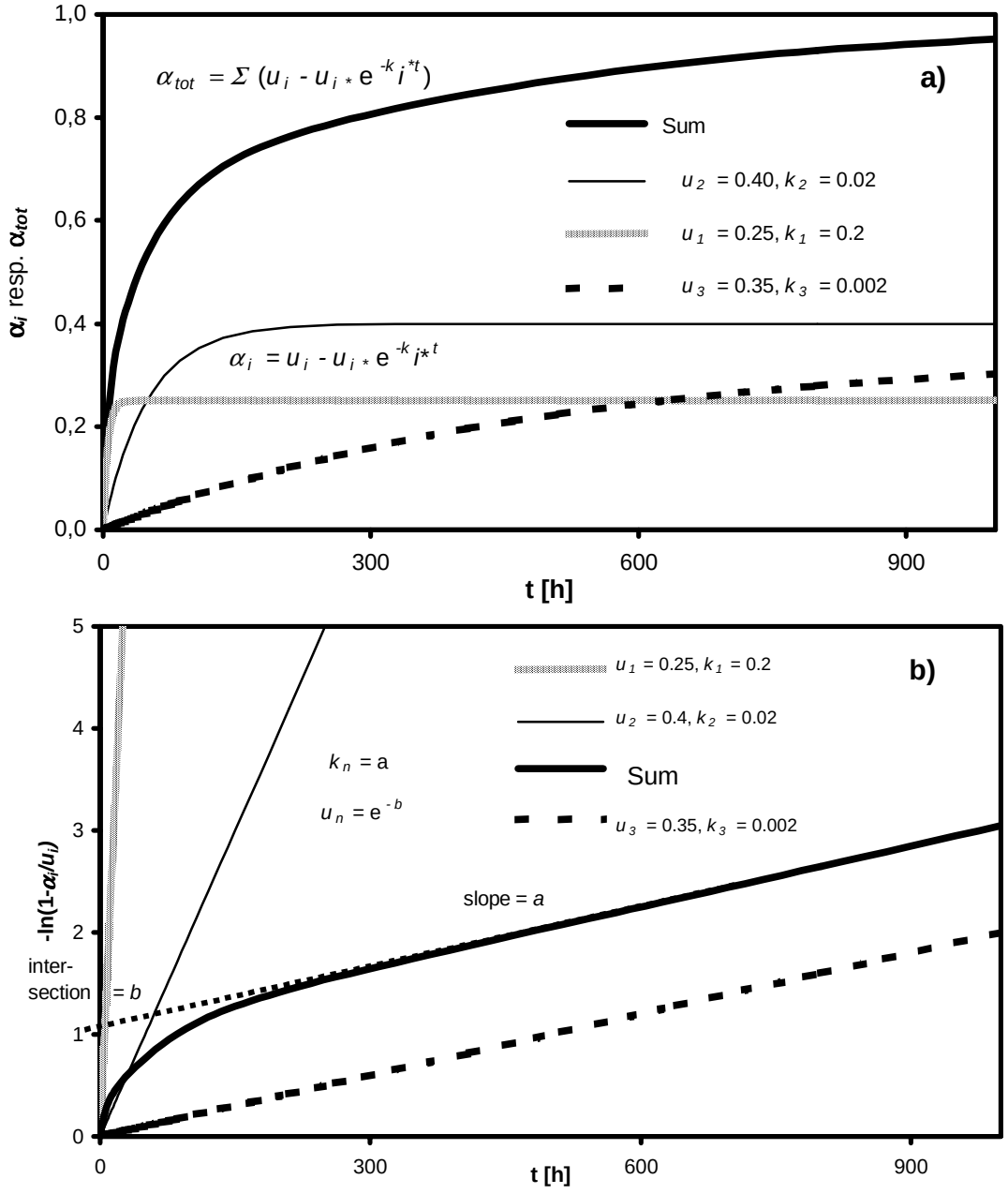

Figure D.1: Schematic representation of the first-order sum model (Eq. 3). a) Normal plot of three fractions, differing in rate constant k_i and in fraction size u_i relative to the total amount of FHOs, as well as the sum of these fractions to yield a sum kinetic, with α_{tot} ranging from 0-1. b) Linearization of the curves from Fig. D.1a, representing the relationships between parameters of the straight line at the end of the sum curve and the parameters k_n and u_n determine the most stable fraction.

The reduction to the sum of the kinetics of individual fractions was carried out both using data fitting (SigmaPlot™) and a graphical method. In the graphical method the linearization (plotting –ln (1-α) versus t (*Cornell* and *Schwertmann*, 1996) chapter 12.3) was used. Fig. D.1b shows the linearization of the dissolution kinetics from Fig D.1a. The individual fractions exhibit a straight line, intersecting the origin, whereas the sum kinetic is straight only in the far end, where the most stable fraction (lowest k_i) is dissolving alone, because all other fractions have already dissolved completely (see Fig. D.1a). This straight line is described by the slope a and the intersection b. The parameters of the most stable fraction can be determined from these parameters of the straight line.

$$k_n = a \qquad (4)$$

$$u_n = e^{-b} \qquad (5)$$

Using these parameters, α_i of the most stable fraction can be calculated at every measuring time. Subtraction of these values from the original dissolution data leads to the dissolution data with one phase less. After normalization of these data to the new total amount (division by (1-u_n)) these data were linearized again, and so on. This ultimately leads to a linearization which intersects the origin. This indicates that this fraction makes up 100% of the remaining amount of FHOs and that this fraction is the most reactive one in the sample. The measured sum kinetic can then be described by Eq. 3 using all determined u_i and k_i.

In addition, the sum kinetic (Eq. 3) with varying numbers of fractions was fitted to the measured kinetics of soil samples using SigmaPlot™. Precision of the respective first-order sum model was expressed by ø |Δ|, which is the mean deviation of the model from the measured data.

In contrast to fitting the sum of an unknown number of fractions, the graphical method has the advantage that there is no need to decide on a number of fractions in advance.

3 Results and discussion

3.1 Dissolution kinetics of synthetic FHOs

In contrast to the complete dissolution in the reaction medium containing citrate, only 5.6% of the Al-substituted goethite dissolved in the medium lacking citrate. In order to achieve complete dissolution of substituted FHOs in soil samples, all subsequent experiments were therefore conducted using the citrate-containing medium.

Table D.2: Properties of synthetic Fe(III) (hydr)oxides

Abbr.	Mineral	Specific Surface [$m^2 \cdot g^{-1}$]	MCD* (hkl) [nm]	Dissolution in asc/citr 3a first-order rate constant *k* [h^{-1}]
2LF	2-line ferrihydrite	280	1 (110)	$2.18 \cdot 10^{-1}$
6LF	6-line ferrihydrite	201	3 (110)	$2.51 \cdot 10^{-2}$
Lep	lepidocrocite	45	27 (020)	$1.73 \cdot 10^{-1}$
G 1	goethite	151	5 (110)	$1.47 \cdot 10^{-2}$
G 2	goethite	120	7 (110)	$1.30 \cdot 10^{-2}$
G 3	goethite	89	9 (110)	$4.50 \cdot 10^{-3}$
H 3	hematite	110	8 (104)	$4.81 \cdot 10^{-3}$

* Mean Crystal Diameter

As established for the citrate-lacking medium, the lg of the pseudo-first-order rate constant of dissolution in this medium also showed good correlations to lg K_{SO} , *Eh*°, and specific surface of the samples (Tab. D.3). The specific surface area of Lep did not correlate with lg *k* (therefore it was omitted in this linear regression) because Lep generally had the highest rate constant but low specific surface.

Table D.3: Linear regressions between lg *k* (=*x*) and oxide parameters

y	slope	intersection	r^2
log K_{SO}	1.376	-38.58	0.93
E_h° [V]	0.0781	0.976	0.98
Specific Surface Area [$m^2\ g^{-1}$]	111.9	357.2	0.94
log *k*, dissolution in oxalate	2.169	2.550	0.92

3.2 Dissolution kinetics of soil FHOs

The modified method allowed the dissolution kinetics of soil FHOs to be determined very efficiently: The reading of the complete dissolution kinetic (22-24 time steps) of 12 soil samples (each with 5 replicates and a blank) took only 12 hours. Preparation of glass tubes and starting the dissolution consumed an additional 12 hours. Furthermore, the data showed good precision: The mean standard deviation of α_{tot} was 0.012.

The results of reducing the sum dissolution of soil FHOs to fractions, dissolving according to Eq. 3, are presented in Tab. D.4. Because the graphical method yielded 4 fractions in all cases, only the best SigmaPlot™ fits of a model including n = 4 fractions are shown in Tab. D.4. In two cases (3a-L and γ-boe-L) SigmaPlot™ assigned two fractions an identical k_i, i.e. detected only 3 fractions. It is apparent that ø $|\Delta|$ of the fitted model was always below ø s of the measured data, and that ø $|\Delta|$ of the graphical method was in most cases below these values. Thus, the model represented the data well.

There were only minor differences between the two sterilization methods. The dissolution rate constants k_i of the respective fractions detected tended to be lower for autoclaving than for γ-ray treatment, which is known for hydrothermal treatment (*Schwertmann* et al., 1985; *Schwertmann* and *Fischer*, 1966).

There was good correspondence between the results of both data analysis methods. Rate constants k_i determined by linearization of fitting differed in the mean by a factor of 1.56; this is minor because the values ranged over 4 orders of magnitude. The graphical method worked best for soil H. In every linearization step a clearly linear end could be distinguished from a curved beginning of the curve (not shown). Also in the linearizations of soil V the differentiation of fractions was mostly unambiguous and the results of fitting were very similar.

Soil L showed the largest differences in k_i and u_i from the sample collective, probably because a problem had occurred in the second linearization. It exhibited a long, upwardly curved end of the data. It was necessary to calculate the linear regression over this entire region of the data in order to yield results in the subsequent linearizations.

Table D.4: Fractions of soil Fe(III) (hydr)oxides detected, either graphically or fitted, from sum dissolution kinetic.

		H				L				V			
		graphically		fitted		graphically		fitted		graphically		fitted	
		k_i	u_i	k_i	u_i	k_i	u_i	k_i	u_i	k_i	u_i	k_i	u_i
γ	*i*=4	$2.90\cdot10^{-3}$	0.136	$2.78\cdot10^{-3}$	0.134	$1.22\cdot10^{-3}$	0.415	$9.55\cdot10^{-4}$	0.299	$2.42\cdot10^{-3}$	0.196	$2.48\cdot10^{-3}$	0.196
	i=3	$4.79\cdot10^{-2}$	0.248	$5.18\cdot10^{-2}$	0.275	$1.02\cdot10^{-2}$	0.396	$6.30\cdot10^{-3}$	0.470	$1.40\cdot10^{-2}$	0.424	$1.33\cdot10^{-2}$	0.407
	i=2	$2.32\cdot10^{-1}$	0.316	$2.90\cdot10^{-1}$	0.334	$1.35\cdot10^{0}$	0.136	$3.34\cdot10^{-1}$	0.103	$2.56\cdot10^{-1}$	0.278	$1.99\cdot10^{-1}$	0.262
	i=1	$2.25\cdot10^{0}$	0.301	$3.72\cdot10^{0}$	0.257	$>5\cdot10^{0}$	0.053	$4.38\cdot10^{0}$	0.128	>2.5	0.101	$2.85\cdot10^{0}$	0.136
	ø |Δ|	$5.50\cdot10^{-3}$		$4.90\cdot10^{-3}$		$1.14\cdot10^{-2}$		$4.17\cdot10^{-3}$		$3.70\cdot10^{-3}$		$2.54\cdot10^{-3}$	
	ø s	$1.09\cdot10^{-2}$				$1.05\cdot10^{-2}$				$1.06\cdot10^{-2}$			
3a	*i*=4	$1.81\cdot10^{-3}$	0.112	$2.44\cdot10^{-3}$	0.131	$1.45\cdot10^{-3}$	0.495	$1.15\cdot10^{-3}$	0.083	$2.20\cdot10^{-3}$	0.208	$2.13\cdot10^{-3}$	0.179
	i=3	$2.50\cdot10^{-2}$	0.198	$4.06\cdot10^{-2}$	0.264	$1.07\cdot10^{-2}$	0.335	$1.15\cdot10^{-3}$	0.258	$1.19\cdot10^{-2}$	0.361	$9.79\cdot10^{-3}$	0.356
	i=2	$1.88\cdot10^{-1}$	0.428	$2.84\cdot10^{-1}$	0.420	$8.37\cdot10^{-1}$	0.126	$5.68\cdot10^{-3}$	0.443	$2.05\cdot10^{-1}$	0.353	$1.20\cdot10^{-1}$	0.293
	i=1	$2.28\cdot10^{0}$	0.261	$7.11\cdot10^{0}$	0.185	$>2.0\cdot10^{1}$	0.044	$5.50\cdot10^{-1}$	0.212	$>2.0\cdot10^{0}$	0.077	$1.02\cdot10^{0}$	0.170
	ø |Δ|	$5.63\cdot10^{-3}$		$5.13\cdot10^{-3}$		$1.30\cdot10^{-2}$		$5.42\cdot10^{-3}$		$5.16\cdot10^{-3}$		$2.79\cdot10^{-3}$	
	ø s	$1.53\cdot10^{-2}$				$1.04\cdot10^{-2}$				$1.57\cdot10^{-2}$			

k_i homogeneous rate constant of a fraction i; u_i size of the respective fraction relative to Fe_d =1; ø |Δ| mean deviation of model data from measured data; ø s mean standard deviation of measured data.

Table D.5: Fractions of Fe(III) (hydr)oxides detected from a mixture of synthetic FHO (G 3, 6LF, and Lep) in soils whose own FHO had been extracted usiig boiling oxalate.

				H				L				V			
		expected		graphically		fitted		graphically		fitted		graphically		fitted	
		k_i	u_i	k_i	u_i	k_i	u_i	k_i	u_i	k_i	u_i	k_i	u_i	k_i	u_i
γ-boe						$1.0 \cdot 10^{-15}$	0.003	$2.40 \cdot 10^{-3}$	0.061	$2.06 \cdot 10^{-3}$	0.062	$3.40 \cdot 10^{-3}$	0.053	$2.32 \cdot 10^{-3}$	0.040
	G 3	$5.60 \cdot 10^{-3}$	0.333	$1.22 \cdot 10^{-2}$	0.181	$5.59 \cdot 10^{-4}$	0.006	$3.11 \cdot 10^{-2}$	0.256	$3.10 \cdot 10^{-2}$	0.244	$2.78 \cdot 10^{-2}$	0.287	$3.49 \cdot 10^{-2}$	0.229
	6LF	$3.03 \cdot 10^{-2}$	0.333	$3.26 \cdot 10^{-2}$	0.529	$2.50 \cdot 10^{-2}$	0.685	$3.63 \cdot 10^{-2}$	0.438	$3.10 \cdot 10^{-2}$	0.421	$4.16 \cdot 10^{-2}$	0.412	$3.49 \cdot 10^{-2}$	0.455
	Lep	$2.58 \cdot 10^{-1}$	0.333	$9.53 \cdot 10^{-1}$	0.290	$9.98 \cdot 10^{-1}$	0.306	$2.15 \cdot 10^{0}$	0.244	$1.59 \cdot 10^{0}$	0.275	$1.98 \cdot 10^{0}$	0.247	$1.64 \cdot 10^{0}$	0.277
	ø |Δ|			$7.50 \cdot 10^{-3}$		$5.97 \cdot 10^{-3}$		$9.76 \cdot 10^{-3}$		$6.91 \cdot 10^{-3}$		$5.32 \cdot 10^{-3}$		$3.90 \cdot 10^{-3}$	
	ø s			$6.14 \cdot 10^{-3}$				$3.86 \cdot 10^{-2}$				$9.20 \cdot 10^{-3}$			
3a-boeE						$1.56 \cdot 10^{-2}$	0.001			$4.90 \cdot 10^{-4}$	0.018			$4.60 \cdot 10^{-14}$	0.001
	G 3	$4.50 \cdot 10^{-3}$	0.333	$1.35 \cdot 10^{-2}$	0.338	$1.56 \cdot 10^{-2}$	0.111	$2.94 \cdot 10^{-3}$	0.094	$1.33 \cdot 10^{-2}$	0.392	$8.61 \cdot 10^{-3}$	0.229	$1.38 \cdot 10^{-2}$	0.094
	6LF	$2.51 \cdot 10^{-2}$	0.333	$1.70 \cdot 10^{-2}$	0.338	$1.56 \cdot 10^{-2}$	0.559	$1.94 \cdot 10^{-2}$	0.740	$1.33 \cdot 10^{-2}$	0.290	$1.93 \cdot 10^{-2}$	0.534	$1.38 \cdot 10^{-2}$	0.613
	Lep	$1.73 \cdot 10^{-1}$	0.333	$6.33 \cdot 10^{-1}$	0.324	$5.64 \cdot 10^{-1}$	0.328	$6.66 \cdot 10^{-1}$	0.166	$3.48 \cdot 10^{-1}$	0.300	$3.99 \cdot 10^{-1}$	0.237	$3.27 \cdot 10^{-1}$	0.291
	ø |Δ|			$1.22 \cdot 10^{-2}$		$1.15 \cdot 10^{-2}$		$2.23 \cdot 10^{-2}$		$1.43 \cdot 10^{-2}$		$9.23 \cdot 10^{-3}$		$4.78 \cdot 10^{-3}$	
	ø s			$1.30 \cdot 10^{-2}$				$6.94 \cdot 10^{-3}$				$3.29 \cdot 10^{-2}$			

k_i homogeneous rate constant of a fraction i; u_i size of the respective fraction relative to Fe_d =1; expected k_i from separate dissolution; expected u_i from mixing ratio 1:1:1; ø |Δ| mean deviation of model data from measured data; ø s mean standard deviation of measured data.

Table D.6: Approximation of Fe_o in fractions of soil FHO via correlation of synthetic FHO rate constants.

	H (Fe_O = 78.9% of Fe_d)				**L (Fe_O = 28.6 % of Fe_d)**				**V (Fe_O = 44.9% of Fe_d)**			
	k_i (asc/citr)	u_i	k_i (ox, non-ster)	% diss. 2 h	k_i (asc/citr)	u_i	k_i (ox, non-ster)	% diss. 2 h	k_i (asc/citr)	u_i	k_i (ox, non-ster)	% diss. 2 h
γ	$2.78 \cdot 10^{-3}$	0.134	$1.01 \cdot 10^{-3}$	0.2	$9.55 \cdot 10^{-4}$	0.299	$9.98 \cdot 10^{-5}$	0.0	$2.48 \cdot 10^{-3}$	0.196	$7.91 \cdot 10^{-4}$	0.2
	$5.18 \cdot 10^{-2}$	0.275	$5.77 \cdot 10^{-1}$	68.4	$6.30 \cdot 10^{-3}$	0.47	$5.97 \cdot 10^{-3}$	1.2	$1.33 \cdot 10^{-2}$	0.407	$3.02 \cdot 10^{-2}$	5.9
	$2.90 \cdot 10^{-1}$	0.334	$2.42 \cdot 10^{1}$	100.0	$3.34 \cdot 10^{-1}$	0.103	$3.28 \cdot 10^{1}$	100.0	$1.99 \cdot 10^{-1}$	0.262	$1.07 \cdot 10^{1}$	100.0
	$3.72 \cdot 10^{0}$	0.257	$6.12 \cdot 10^{3}$	100.0	$4.38 \cdot 10^{0}$	0.128	$8.72 \cdot 10^{3}$	100.0	$2.85 \cdot 10^{0}$	0.136	$3.43 \cdot 10^{3}$	100.0
	sum of fractions (% of Fe_d)			77.9				23.7				42.2
3a	$2.44 \cdot 10^{-3}$	0.131	$1.17 \cdot 10^{-3}$	0.2	$1.15 \cdot 10^{-3}$	0.083	$2.61 \cdot 10^{-4}$	0.1	$2.13 \cdot 10^{-3}$	0.179	$8.93 \cdot 10^{-4}$	0.2
	$4.06 \cdot 10^{-2}$	0.264	$3.19 \cdot 10^{-1}$	47.2	$1.15 \cdot 10^{-3}$	0.258	$2.61 \cdot 10^{-4}$	0.1	$9.79 \cdot 10^{-3}$	0.356	$1.87 \cdot 10^{-2}$	3.7
	$2.84 \cdot 10^{-1}$	0.420	$1.55 \cdot 10^{1}$	100.0	$5.86 \cdot 10^{-3}$	0.443	$6.72 \cdot 10^{-3}$	1.3	$1.20 \cdot 10^{-1}$	0.293	$2.77 \cdot 10^{0}$	99.6
	$7.11 \cdot 10^{0}$	0.185	$9.53 \cdot 10^{3}$	100.0	$5.50 \cdot 10^{-1}$	0.212	$5.78 \cdot 10^{1}$	100.0	$1.02 \cdot 10^{0}$	0.17	$1.98 \cdot 10^{2}$	100.0
	sum of fractions (% of Fe_d)			73.0				21.8				47.5

A possible reason for this behavior could have been FHOs showing sigmoidal (s-shaped) dissolution kinetics. Sigmoidal dissolution was attributed to multidomainic crystals: they disintegrate during dissolution and therefore show an increased specific surface in the interim (*Schwertmann*, 1991), which is well described by the Kabai model (*Cornell* and *Schwertmann*, 1996, chapter 12.3). When a Kabai-sum-model (Eq. 6) whose most stable fraction has an $a_i > 1$ is linearized according to first-order kinetics, the phenomenon described above occurs.

$$\alpha_{tot} = \sum_{i=1}^{n} \left(u_i - u_i \cdot e^{-\left(k_i \cdot t\right)^{a_i}}\right) \qquad (6)$$

The higher the values a_i and k_{i+1}/k_i are, the more pronounced is this phenomenon. As the Kabai-model had described the dissolution of most synthetic FHOs better than the first-order-model (*Dominik* et al., submitted), it would to be logical to analyze the dissolution of soil FHO according to a Kabai-sum-model (Eq. 6) as well. A linearization for a single Kabai-function also exists (*Cornell* and *Schwertmann*, 1996, chapter 12.3), but it is not possible to derive 3 parameters (a_i, k_i, and u_i,) from a straight line. In addition, fitting of a Kabai-sum-model to the soil dissolution data yielded arbitrary values for the parameters, indicating that the dissolution kinetics of soil FHOs can be described very well by different Kabai-sum-functions. We therefore continued working with the first-order approach. From ø $|\Delta|$ it is clear that, for L, the fitted parameters describe the dissolution better than the graphically derived ones.

We were able to reduce the dissolution kinetics of all soils to 4 fractions each, which dissolve simultaneously according to first-order-kinetics. *Postma* (1993) measured the dissolution kinetics of synthetic FHOs as well as of sediment samples in 10 mM anoxic ascorbic acid, pH 3.0. He found the kinetics to be described well by a modified model of *Christoffersen* and *Christoffersen* (1976), which had been proposed for polydisperse samples. Thus, *Postma* (1993) plotted log of the rate of dissolution J, normalized to m_0, versus –log m/m_0, in which m is

the amount which is not yet dissolved and m_0 is the initial amount of FHOs. In this plot the data of every sediment sample exhibited a straight line described by two parameters: the initial dissolution rate J/m_0 and a constant, which represents the logarithm of the factor by which the rate is decreased while the degree of dissolution increases from 0 to 90%. Because this constant clearly exceeded values from polydisperse yet mineralogically homogeneous samples like ferrihydrite, he conclude the presence of a continuum of reactivity of FHOs in the samples.

When we used the same plot for our data, however, soil H yielded data scattered around a straight line with an r^2 of 0.93, whereas soil V and L yielded a scattered plot with 2 or even 3 clearly distinct linear parts. Thus, the sample which our analysis definitely showed to be composed of fractions with distinct dissolution rate constants, would have been described in *Postma*'s (1993) approach to have a continuum of reactivity. We have no explanation for this contradiction, but we consider it advantageous to assign definite quantities and a distinct rate constant. On the other hand this finding opens up the possibility to also detect distinct stability fractions in *Postma*'s data using the data analysis proposed here.

The method presented here allows a more precise definition of soil FHO reactivity than existing methods. Tab. D.4 clearly reveals that in soil H most FHOs show relatively high k_i, whereas especially in soil L most FHOs have rather low k_i.

3.3 Recovery of synthetic FHOs added to iron-oxide free soil (control experiment)

In Fig. D.2 the control experiment of the dissolution kinetics of 3a-boe-H as well as the expected time course, calculated from the rate constants of the FHOs in separate dissolution are shown. These two time courses clearly differed. The measured dissolution kinetic is faster than the calculated one in the first and in the last part. In contrast, both curves come quite close together in the middle part at $\alpha \sim 0.6$. This behavior indicates that the lepdocrocite (Lep) and the goethite (G 3), which are the FHOs with the highest and the lowest rate constant here, dissolved much faster in the presence of soil components than in separate dissolution. This

effect seems to be less pronounced for the 6-line-ferrihydrite (6LF), whose rate constant is in the middle.

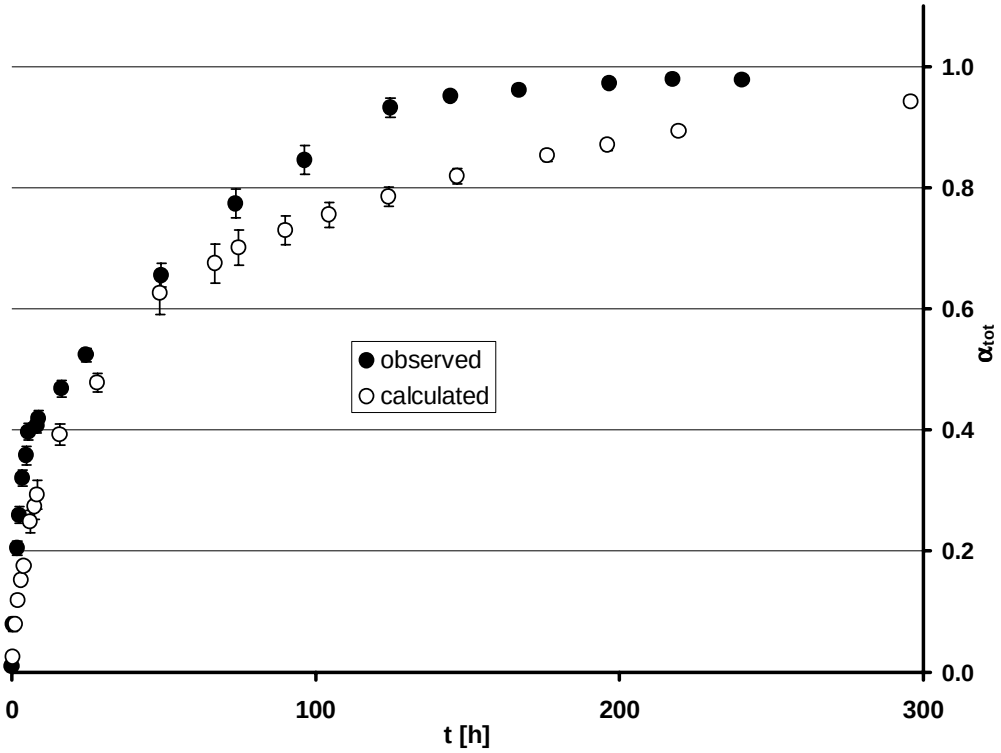

Figure D.2: Measured time course of the dissolution of an equimolar mixture of three synthetic FHOs (lepidocrocite, 6-line-ferrihydrite, and goethite G 3) in the presence of an iron-oxide free soil sample (3a-boe-H). In addition, the theoretical dissolution kinetic, calculated from the rate constants of the FHOs in separate dissolution and using an equimolar mixing ratio, is shown.

This behavior was detected in all variants of the control experiment. The results are shown in Tab. D.5. The first column shows the rate constants derived from separate dissolution of the synthetic FHOs. They are lower for the 3a samples than for γ-ray sterilized samples, probably due to increased crystallinity caused by thermal treatment.

The expected fraction size u_i was 0.333 for every fraction because the 3 synthetic FHOs had been added in equal (molar) amounts to the soil samples.

The changed dissolution rate constants k made it difficult to reduce the dissolution kinetics to fractions in both the graphical and fitting method. Because k_i

of G 3 had increased by a factor of 2.2-6.6, it approached the mainly unchanged k_i of 6LF and both minerals were difficult to distinguish graphically. In fact, the fitting program never differentiated between these two fractions, but detected one fraction with a big size u_i and homogeneous k_i. Nonetheless, the size of this united fraction was determined as expected to be 0.665-0.707, i.e. close to 2 x 0.333 = 0.666. Because the rate constant k of Lep also increased by a factor of 2.2-8.3, it was easy to distinguish from 6LF, and u_i was estimated as expected between 0.275 and 0.328. In addition to the three added FHOs, a fourth fraction with a rate constant of about $2.5 \cdot 10^{-3}$ h^{-1} and a u_i up to 0.06 was detected in γ-boe-L and γ-boe-V. Based on the rate constants (compare Tab. D.4), these fractions are probably remains of incompletely dissolved crystalline FHOs of the soils, even after two extractions with boiling oxalate.

It can be inferred from both soil experiments that the difference in k_i of two fractions must be at least a factor of about 5 in order to distinguish clearly between both fractions. *Quencer* and *Crouch* (1994) stated, for multicomponent kinetic determination in analytic chemistry, that rate constants needed to be differ by a factor 2.5-3 in order to achieve acceptable results. A reason for this lower value could be the use of a Kalman-filter; this statistical approach different from least squares is increasingly being used in differential kinetic methods (*Perez-Bendito* and *Silva*, 1996). On the other hand analytical chemistry deals with defined dissolved species, which certainly react more precisely according to a first-order kinetic than polydisperse soil FHOs do. In addition, sampling of solids clearly introduces higher error than sampling of solutions.

The increased rate constants of Lep and G 3 in contact with soil components indicate a catalytically enhanced dissolution. But the rate constant of 6LF was only increased minimally. A possible reason could be the fine-structure of these minerals. While the former samples exhibited an outer-surface in the main, the latter formed relatively large aggregates during freezing, even when shock-frozen. Most of the 6-line-ferrihydrite particles had a diameter of 10-30 µm and were isodiametric, i.e. the outer-surface (even when taking into account a marked surface roughness as determined by SEM) did not exceed 1% of the specific surface as measured using N_2 adsorption. The entire remaining surface is

accessible solely through narrow pores. One could therefore also conclude that the enhanced dissolution is due to a catalytic activity bound to particle surfaces. This catalytic activity can act at outer-surfaces only, whereas dissolved ascorbate also can act at inner-surfaces. Examples for abiotic, particle-bound catalytic activity in soils have been reported recently (Griessbach and *Lehmann*, 1999; *Petigara* et al., 2002).

Whatever the reason for this enhanced dissolution is, it clearly demonstrates that caution must be exercised in assigning characteristics to the found fractions via correlation to the rate constant.

Finally, this enhancement may merely represent an artefact (perhaps due to the pretreatment of soils with boiling oxalate) because we found a meaningful transferability of dissolution rate constants in another context: As previously reported, we detected – for synthetic FHOs – a good linear correlation between logarithms of rate constants of dissolution in 0.1 M ascorbate pH 5.2 and 0.2 M oxalate pH 3.0 (*Dominik* et al., submitted). There, we found a relatively preferred dissolution of reactive FHOs by oxalate, i.e. a 2LF dissolved in oxalate 33-times faster than in ascorbate, whereas the most stable FHO in the sample collective G 3 dissolved in oxalate only 1.7-times faster than in ascorbate.

In a next step, we calculated a correlation using the dissolution rate constants of non-sterile synthetic FHOs (because non-sterilized soil samples are used for the Fe_o extraction according to Schwertmann (1964)) in oxalate and the rate constants of dissolution of sterilized (γ or 3a) samples in the ascorbate/citrate medium (Table D.3). This enabled transformation of the rate constants in Table D.4 to theoretical rate constants of the same fractions in non-sterile oxalate extraction. The results are shown in Table D.6. Clearly, the range of rate constants in oxalate is stretched compared with ascorbate/citrate. The last column of every soil presents the percentage to which the fraction will be dissolved after 2 h (i.e. the duration of Fe_o extraction in *Schwertmann* (1964)). The last row of every sterilization type in Tab. D.6 represents the sum of the products of these percentages and their respective fraction sizes u_i. While this may be a bold calculation, the values show a remarkable agreement with the measured Fe_O values of the respective soil! So,

in contrast to the control experiment, rate constants derived from the dissolution of synthetic FHOs have been successfully applied in this case.

Although it was stated before that a single extraction will also dissolve remarkable amounts of more stable fractions (see Introduction), the Fe_O extraction divided the 2nd fraction of soil H through the middle only. In the other soils the Fe_O extraction captured fractions quite precisely because the rate constants were stretched. This finding of unexpected selectivity may underline the unique significance of this simple method.

The correspondence to the Fe_O values increases the plausibility of the FHO fractions detected by the method presented here. Further research is needed – not only on the results of the control experiment – but there is reason to believe that correlations between rate constants and FHO properties can be applied to this method in the future.

Finally, we can give an initial evaluation on the meaning of k_i as determined by the new method. From the comparison with Fe_O, we can approximate that values below $3 \cdot 10^{-2}$ will represent FHOs which show only minor or negligible oxalate solubility. The lower a rate constant, the higher the crystallinity of that fraction. It is possible that the highest rate constants determined here represent organically bound iron.

4 Conclusions

- The slightly adapted method allows a convenient and very precise determination of the overall dissolution kinetic of soil FHOs.
- The overall dissolution kinetic of soil can be described by a first-order sum kinetic model very well.
- In most cases there is good correspondence of the data analysis between the graphical method and fitting of Eq. 3 to the data.
- The difference in results between sterilization of soil using γ-ray or autoclaving is almost negligible.
- The recovery of the amount of synthetic FHOs added to soils is good.

- The recovery of the rate constants of synthetic FHOs added to soils is unacceptable, but this may merely reflect the pretreatment of the soil with boiling oxalate.
- Currently, correlations found for synthetic FHOs between rate constant and characteristics such as specific surface, K_{SO}, and Eh° cannot be applied to the fractions detected in soils.
- Further experiments are needed to examine the meaning of the dissolution rate constants derived by this method. Excellent prediction of Fe_O in the soils using correlations of dissolution rate constants of synthetic FHOs is promising for the applicability of the correlations in the future.

Acknowledgement

We would like to thank the DFG for the financial support of this work. We would also like to thank Dr. Jürgen Rommel for selection and basic characterization of the soils.

E. Thermodynamics of reduction of Fe(III) (hydr)oxides by *Geobacter metallireducens*

Abstract

Sulfate-reducing bacteria and methanogenic archaea become inactive when the concentration of the electron donors drops below a threshold determined by the minimum Gibbs free energy required for the bacterial metabolism to be maintained. Thus, their activity is thermodynamically controlled. The energy content of different Fe(III) (hydr)oxides (FHOs) varies significantly. It was therefore tested in this paper if the activity of dissimilatory Fe(III) reducing bacteria is also limited by the thermodynamics of the reaction. We synthesized five FHOs of moderate stability (all samples were freeze-dried) and determined the solubility product (log K_{SO} (-39.1)-(-41.8)), in order to calculate their standard free energy of formation. HCO_3^- and PIPES-buffered mediua, containing 45 mM of one of these FHOs and either 1, 10, or 100 mM acetate were inoculated with *Geobacter metallireducens*. When the bacterial activity had ceased (no longer increase of HCl-soluble Fe(II)), acetate, pH, HCO_3^- and dissolved Fe(II) were measured and the free energy was calculated. The Gibbs free energy of the reaction showed significant differences between the different FHOs, sometimes even between different acetate concentrations. The termination of the bacterial activity was consequently not triggered thermodynamically. However, the non-dissolved Fe(II) showed an excellent correlation with the surface of the FHOs (15 µmol m^{-2}). It is therefore likely that the termination of the reaction was caused by blocking of the FHO surface with insoluble Fe(II). The ecological significance of either a thermodynamic limitation or a surface availability limitation is discussed for FHOs of different K_{SO} at locations with approximately neutral pH.

Introduction

Fe(III) (hydr)oxides (FHOs) amount in soils and sediments to 0.2-20% (*Scheffer* and *Schachtschabel*, 1998) and represent therefore - besides CO_2 - the quantitatively most important electron acceptor in anoxic environments. Until 1980, only fermentative bacteria were known to reduce iron dissimilatorily. They can use ferric iron as an additional electron acceptor, and generally transfer only a small percentage of electrons on FHO (*Lovley*, 1991; *Ehrlich* 1996). In the following years, however, numerous bacteria were detected, which use non-fermentable electron donors (i.e. fermentation products like H_2, acetate, propionate, lactate, alcohols or aromatics). The physiology and phylogenesis of these organisms was reviewed by *Lovley et al.* (1997). The electron donors are oxidized completely to H_2O and CO_2 in most cases, and all electrons transferred are used to reduce Fe(III), which means that these organisms exhibit a respiratory metabolism. These organisms have been isolated from several habitats (*Lovley et al.* 1997), and the stoichiometry of electron donators and acceptors in soil slurries (Peters and *Conrad*, 1996) indicates that this respirative group is responsible for iron reduction in natural habitats rather than the fermentative group.

In the anaerobic food chain this iron-respiring group follows on fermentative organisms and therefore competes with sulfate reducers and methanogens for identical electron donors. For the latter groups *Winfrey* and Zeikus (1977) established the hypothesis of competition for electron donors, which means that the process with higher energy yield is still feasible at lower concentration of electron donor. This hypothesis was later validated for various anoxic environments (*King*, 1984; *Ward* and *Winfrey*, 1985) and is now generally accepted (*Conrad*, 1996). *Lovley et al.* (1994) and *Achtnich et al.* (1995) extended this hypothesis to iron reducing bacteria and presented evidence that the threshold of H_2, which is the minimal needed concentration for the ferric iron reduction, sulfate reduction and methanogenesis, respectively, increased in the same sequence.

Contrasting to all other electron acceptors mentioned, FHOs are insoluble and the rate of reduction therefore depends on their specific surface. Furthermore

FHOs in soils exhibit a broad range of stability, due to different minerals, imperfection and sizes of crystals as well as degree of isomorphous substitution. *Schwertmann* (1991) assumed that the range of solubility product (K_{SO}) of FHOs in soils is at least 3-4 orders of magnitude. As FHOs are differing in K_{SO}, the energy yield of their reduction will depend on their stability also. If this holds true, it would be necessary to extend the hypothesis of competition for electron donors to FHOs with different thermodynamic stability. Thus, for the reduction of FHOs with high stability up to a certain equilibrium concentration of ferrous iron, a higher concentration of electron donors should be needed than for the reduction of less stable FHOs.

Using e.g. an acetate oxidizing iron reducer like *Geobacter metallireducens* (*Lovley et al.*, 1993) the extent of the reduction according to Eq. 1 or 2

$$8\ FeOOH + CH_3COO^- + 15\ H^+ \rightarrow 8\ Fe^{2+} + 2\ HCO_3^- + 12\ H_2O \qquad (1)$$

$$8\ Fe(OH)_3 + CH_3COO^- + 15\ H^+ \rightarrow 8\ Fe^{2+} + 2\ HCO_3^- + 20\ H_2O \qquad (2)$$

should be governed by the energy yield which is necessary to maintain the metabolism of the organism. The objective of the present work was to test this hypothesis, which is the thermodynamic control of bacterial reduction of FHOs.

Materials and methods

Bacteria and media

For handling bacteria, strict anaerobic techniques as described by *Widdel* and *Bak* (1995) were used throughout. We used the type strain of *Geobacter metallireducens* (DSM 7210) (*Lovley et al.*, 1993) which was purchased from the German Collection of Microorganisms and Cell Cultures (DSMZ), Braunschweig, Germany. The bacteria were routinely cultured in the FWA-Fe(III) medium as described by *Lovley* and *Phillips* (1988), however, the $NaCH_3COO$ concentration was 11 instead of 30 mM. The trace element solution used was essentially the one described in *Balch et al.* (1979), but NTA was replaced by 0.1 M HCl to avoid enhanced dissolution of Fe(III) (hydr)oxides due to complexation. Because anionic

trace elements exhibit a low solubility at low pH, these were dissolved separately in an alkaline solution. 3 mg Na_2SeO_3 $5H_20$ and 4 mg Na_2WO_4 $2H_2O$ were dissolved in a liter of 12.5 mM NaOH, and added at 0.1 vol% to the final medium after autoclaving. The vitamin solution of *Widdel* and *Bak* (1995) was used, however phosphate buffer was omitted and 30 mg mg l^{-1} folic acid (neutralized stoichiometrically with 2 NaOH), and 50 mg l^{-1} DL-α-lipoic acid were added. In addition 50 mg l^{-1} riboflavine was dissolved in 0.7 mM HCl and 50 mg l^{-1} cyanocobalamine was dissolved in H_2O_{deion}, and both were autoclaved for 10 min at 121°C. All three vitamin solutions were added at 0.1 vol% to the medium after autoclaving.

In the experiment to test the hypothesis of thermodynamic control of bacterial reduction of FHOs, a medium was used, which contained 45 mM of the desired FHO. 14.4 ml of the medium was filled into 21 ml test tubes. Its composition was calculated to be essentially the FWA-medium (*Lovley* and *Phillips*, 1988) after inoculation, but it contained 20 instead of 25 mM of $NaHCO_3$ and 1, 10, or 100 mM of $NaCH_3COO$. In order to avoid a strong increase in pH during Fe(III) reduction (Eq. 1 or 2), and to maintain identical Na^+ activities in all acetate variants, 132.4, 124.4 or 44.4 mM PIPES pH 6.4 was added, respectively. All media contained 0.5 mM $FeCl_2$ as a reducing agent. Prior to filling into the test tubes the pH of the medium was adjusted to 6.4, the gas phase was N_2:CO_2 (50:50). The tubes were sealed using black rubber stoppers of Aldrich.

For each variant 3 replicates were inoculated with 1.6 ml of *G. metallireducens* culture in FWA-medium, by means of a sterile anaerobically flushed (N_2:CO_2 = 50:50) syringe.

The cultures were incubated horizontally at 30±1°C in the dark on a 10° wave shaker (Heidolph, Polymax 2040), which was controlled by a timer. In order to resuspend the sediment, but to avoid unnecessary agitation, the tubes were moved every 8 hours for 15 min at 10 rpm.

Fe(III) (hydr)oxides (FHOs)

The FHOs were synthesized as previously described (*Dominik et al.*, submitted). The minerals were autoclaved prior to the determination of their characteristics also.

Specific surface area (SSA) of the FHOs was determined using BET (3-point absorption of N_2, Quantachrom Nova 1200).

Table E.1: Examined Fe(III) (hydr)oxides

Abbr.	Mineral	Specific Surface [$m^2 * g^{-1}$]	MCD [nm] (hkl)	lg K_{SO} † (25°C)	at % Dissolution	$\Delta G_f°$ ‡ (25°C) [kJ mol^{-1}]
2LF	2-line ferrihydrite	280	1 (110)	-39.08	51.4	-699.58
6LF	6-line ferrihydrite	201	3 (110)	-40.41	23.9	-707.18
L	lepidocrocite	45	27 (020)	-39.90	30.9	-467.11
G 2	goethite	120	7 (110)	-41.38	3.6	-475.56
G 3	goethite	89	9 (110)	-41.77	1.7	-477.79

* Mean Crystal Diameter; ††lg solubility product $\{Fe^{3+}\}\{OH^-\}^3$; ‡ standard free energy of formation

For determination of the thermodynamic stability of the Fe(III) (hydr)oxides, the solubility product K_{SO} was determined: 12-25 mg of sample were weighed into 12 ml test tubes and shaken aerobically at 23 ±1°C in the dark (in sum over 10 month) within 7 ml of 32 mM HNO_3, in order to minimize complexing effects. At selected timepoints the tubes were centrifuged at 1300 g for 10 min and the dissolved iron was determined according to *Dominik* and *Kaupenjohann* (2000). When the concentration of dissolved iron showed no further increase, the pH was determined. To do so precisely, the electrode was calibrated in the mV mode using 6 pH-buffer solutions (in the range of pH 1.2-3.2) prepared from mixtures of glycine and HCl-solutions according to *Anonymous* (1999). Synthetic crystalline FHOs are known sometimes to contain some surface bound ferrihydrite-like amorphous material (Cornell *et al.,* 1974) or the initial solubility may be enhanced due to irregularities of the original surface (*Cornell* and *Schwertmann* 1996). In

order to determine the true K_{SO} of the sample the FHOs had been washed with 0.5 M HCl after synthesis (*Dominik et al*., submittted) and the K_{SO} was determined two times in succession (final degree of dissolution see Table E.1). Both determinations showed good correspondence. The K_{SO} was calculated using the activity coefficient of *Davies* (1962), and hydrolysis constants for Fe^{3+} from *Lindsay* (1979).

The values were transformed to the K_{SO} values at 25°C, using the Van't Hoff equation and tabulated values of the standard enthalpies of formation (*Weast*, 1985). From these K_{SO} values at 25°C the standard Gibbs free energies of formation ($\Delta G_f°$) of the respective Fe(III) (hydr)oxides were calculated using $\Delta G_f°$ values for H_2O, H^+, OH^-, and Fe^{3+} from *Sigg* and *Stumm* (1994). The resulting $\Delta G_r°$ for Eq. 1 and 2 (25°C) were transformed to 30°C, using the Van't Hoff equation.

Analyses

The progress in bacterial Fe(III) reduction was determined as HCl soluble Fe(II). An aliquot of the suspension was shaken for 24 h in 0.5 M HCl and determined photometrically with 1 mM ferrozine in 0.2 M ammonium acetate (*Dominik* and *Kaupenjohann*, 2000). As HCl-extactable Fe(II) showed no further increase after 30 days of incubation, it was assumed, that bacterial reduction had ceased. The sealed tubes were centrifuged for 10 min at 1350 g, opened anaerobically and the following parameters were determined:

An aliquot was pipetted into ferrozine in acetate buffer to determine the dissolved concentration of ferrous iron. The amount of iron, which was reduced during the bacterial experiment was calculated as HCl-soluble Fe(II) minus Fe(II), which was added to the medium as a reducing agent as well as Fe(II), which was introduced with the inoculum.

The pH was measured using a Schott combination electrode, whose diameter was close to the inner diameter of the test tubes. It was put carefully into the tube as deep as possible, to minimize oxygen contact. The concentration of HCO_3^- was calculated from a titration of an aliquot of the solution to pH 4.4 using 0.1 M HCl,

assuming that CH_3COO^-, PIPES, HCO_3^-, and $FeOH^+$ were the only buffering substances in this pH range.

Acetate was analyzed using the enzymatic test no. 148261 from Boehringer, Mannheim.

Results and Discussion

Extent of reduction

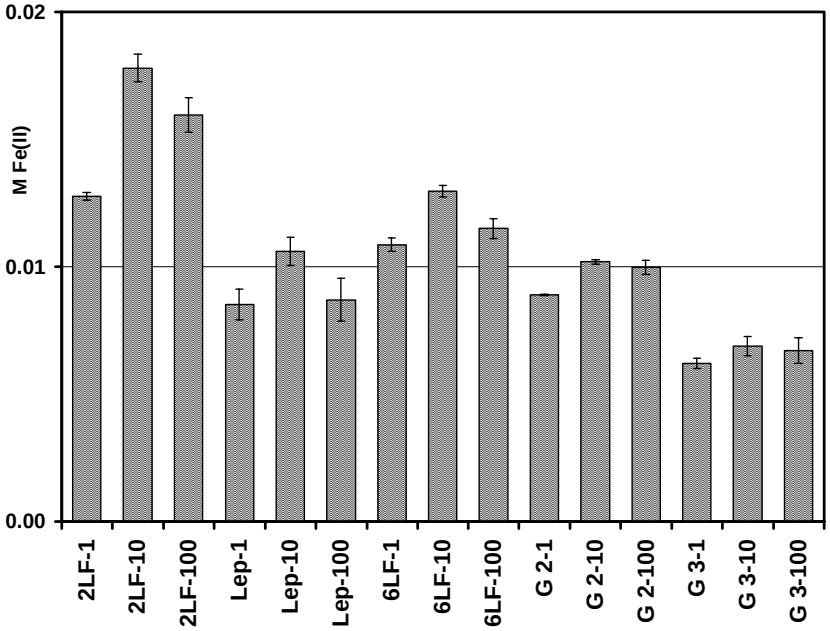

Figure E.1: Reduced amounts of iron at the end of reduction of FHOs *by G. metallireducens* with 3 different acetate concentrations. Whiskers indicate standard deviation of 3 replicates.

It is obvious, that the reduced amount decreased in the order 2LF > 6LF > Lep = G2 > G3 (Fig. E.1). This means, that the amorphous Fe(III) (hydr)oxides (FHOs) were reduced to a higher extent, than crystalline ones. However, according to the hypothesis of thermodynamic control of bacterial reduction of FHOs, it was expected, that Lep, which shows a minor stability than 6LF, would be reduced to a higher extend than the latter one.

If the reduced amount is normalized to the initial content of FHO (45 mM), it may be compared to results of other studies. In summary the percentage to which the FHOs were reduced in our study are comparable or even higher than those of

Table E.2: Solution parameters at the end of bacterial reduction.

Fe(III) (hydr)oxide	Acetate-variant	dissolved Fe(II) [M]		pH		CH_3COO^- [M]		HCO_3^- [M]		S.I.* Siderite	
		avg	SD	avg	SD	avg	SD	avg	SD	avg	SD
2LF	1	$6.5\cdot10^{-3}$	$3.4\cdot10^{-5}$	6.39	0.03	$5.7\cdot10^{-5}$	$6.1\cdot10^{-5}$	$3.1\cdot10^{-2}$	$2.3\cdot10^{-3}$	1.77	0.01
	10	$3.1\cdot10^{-3}$	$6.7\cdot10^{-4}$	6.35	0.05	$7.7\cdot10^{-3}$	$4.1\cdot10^{-4}$	$2.5\cdot10^{-2}$	$1.1\cdot10^{-3}$	1.31	0.14
	100	$2.2\cdot10^{-3}$	$3.1\cdot10^{-4}$	6.42	0.03	$9.5\cdot10^{-2}$	$2.0\cdot10^{-4}$	$2.2\cdot10^{-2}$	$6.8\cdot10^{-4}$	1.17	0.08
Lep	1	$7.9\cdot10^{-3}$	$1.9\cdot10^{-4}$	6.45	0.49	$3.1\cdot10^{-4}$	$1.1\cdot10^{-4}$	$2.9\cdot10^{-2}$	$2.8\cdot10^{-2}$	1.70	0.18
	10	$8.3\cdot10^{-3}$	$3.7\cdot10^{-4}$	6.15	0.49	$8.6\cdot10^{-3}$	$2.1\cdot10^{-4}$	$4.4\cdot10^{-2}$	$2.0\cdot10^{-2}$	1.80	0.20
	100	$4.9\cdot10^{-3}$	$6.6\cdot10^{-4}$	6.39	0.09	$9.5\cdot10^{-2}$	$1.5\cdot10^{-3}$	$2.7\cdot10^{-2}$	$3.0\cdot10^{-3}$	1.60	0.08
6LF	1	$6.7\cdot10^{-3}$	$2.5\cdot10^{-4}$	6.35	0.15	$4.8\cdot10^{-4}$	$2.6\cdot10^{-4}$	$3.3\cdot10^{-2}$	$8.4\cdot10^{-3}$	1.77	0.04
	10	$5.4\cdot10^{-3}$	$5.5\cdot10^{-4}$	6.37	0.06	$8.2\cdot10^{-3}$	$9.9\cdot10^{-5}$	$3.1\cdot10^{-2}$	$2.7\cdot10^{-3}$	1.67	0.05
	100	$2.8\cdot10^{-3}$	$3.6\cdot10^{-4}$	6.61	0.16	$9.4\cdot10^{-2}$	$4.0\cdot10^{-4}$	$1.8\cdot10^{-2}$	$4.2\cdot10^{-3}$	1.31	0.05
G 2	1	$6.3\cdot10^{-3}$	$1.3\cdot10^{-4}$	6.28	0.15	$5.0\cdot10^{-4}$	$1.6\cdot10^{-5}$	$3.8\cdot10^{-2}$	$6.9\cdot10^{-3}$	1.75	0.05
	10	$7.0\cdot10^{-3}$	$1.3\cdot10^{-4}$	6.39	0.03	$8.8\cdot10^{-3}$	$3.0\cdot10^{-4}$	$3.4\cdot10^{-2}$	$1.6\cdot10^{-3}$	1.84	0.01
	100	$5.9\cdot10^{-3}$	$1.1\cdot10^{-4}$	6.35	0.05	$9.1\cdot10^{-2}$	$2.2\cdot10^{-3}$	$3.0\cdot10^{-2}$	$2.2\cdot10^{-3}$	1.69	0.01
G 3	1	$6.0\cdot10^{-3}$	$1.2\cdot10^{-4}$	6.22	0.19	$9.8\cdot10^{-4}$	$6.3\cdot10^{-5}$	nd	nd	nd	nd
	10	$6.4\cdot10^{-3}$	$1.8\cdot10^{-5}$	6.43	0.22	$9.6\cdot10^{-3}$	$2.9\cdot10^{-4}$	nd	nd	nd	nd
	100	$5.8\cdot10^{-3}$	$1.3\cdot10^{-4}$	6.43	0.21	$9.5\cdot10^{-2}$	$3.6\cdot10^{-3}$	nd	nd	nd	nd

* Solubility index = log (IAP/K_{SO}), IAP = ion activity product, K_{SO} = solubility product, nd = not determined

similar minerals with comparable specific surface area (SSA) in *Lovley* and *Phillips* (1986b) and *Roden* and *Zachara* (1996). The higher extent to which 2LF was reduced herein, compared to *Roden* and *Zachara* (1996) is presumably explained by smaller size of the aggregates in our experiments, which was achieved by shock-freezing (*Dominik et al.*, submitted).

Test of the hypothesis of thermodynamic control of bacterial reduction of FHOs:

The parameters of the solution at the end of bacterial reaction are shown in Tab. E.2. The dissolved concentrations of Fe(II) are relatively high, compared to the results of *Fredrickson et al.* (1998). Contrasting to the latter we used centrifugation instead of membrane filtering to separate solids from solution. However, we do not believe that we included some colloidal Fe(II) particles in the determination, because the color of the Fe(II)(ferrozine)$_3$ complex had developed almost immediately (*Dominik et al.*, submitted; *Dominik* and *Kaupenjohann*, 2000). It is more likely that the lower pH in our experiments prevented a higher Fe^{2+} activity from precipitation in the form of siderite than in the experiments of *Fredrickson et al.* (1998) (see below).

In spite of all assumptions made, the HCO_3^- determination yielded plausible data. The medium contained 20 mM, additional HCO_3^- came from the inoculum and from the bacterial respiration of acetate. In fact the bacteria consumed more acetate than stoichiometrically needed for the reduction of iron, especially in the 100 mM variant, a phenomenon, which was also detected by *Fredrickson et al.* (1998). Finally the headspace of the test tube contained 50 vol% CO_2, which obviously had dissolved in part in the solution, as the pH at the end of the experiment was below the initial pH in some cases.

The Gibbs free energies of the reactions (ΔG_r) according to Eq. 1 or 2 (Fig. E.2) are much lower (i.e. the reactions are much more exergonic), than reported for methanogenic bacteria (*Yao* and *Conrad*, 1999). ΔG_r differed for the different Fe(III) (hydr)oxides, significantly in most cases. The lower the standard free

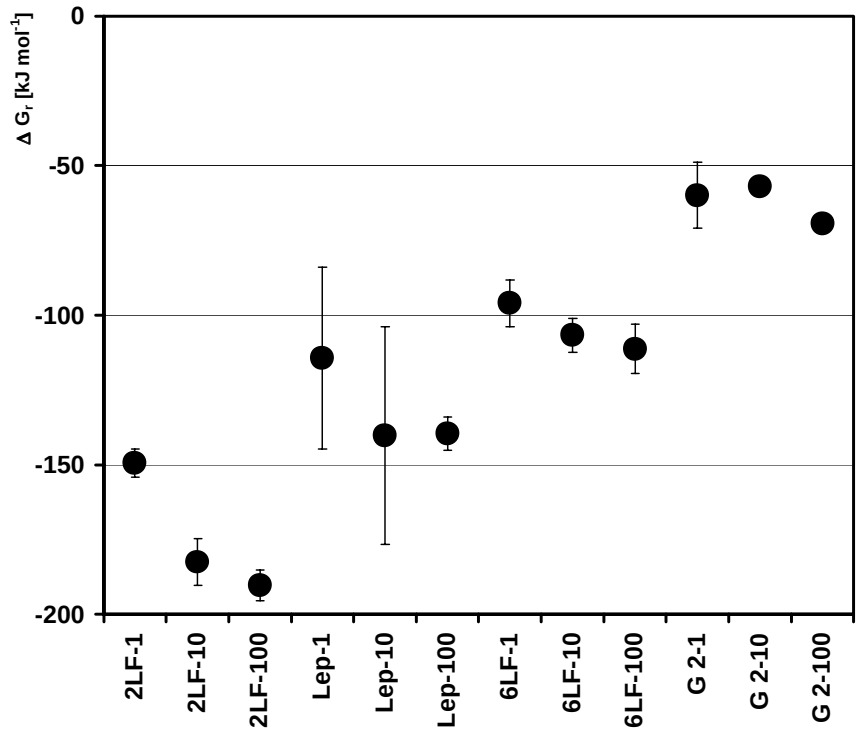

Figure E.2: Gibbs free energies at the end of reduction of FHOs by *G. metallireducens* with 3 different acetate concentrations. Whiskers indicate standard deviation of 3 replicates.

energy of formation of a FHO, the higher was the free energy at the end of the bacterial reduction. This becomes also apparent from the data of dissolution (Table E.2), because dissolved Fe(II) as well as pH, which both strongly effect the calculation of ΔG_r (Eq. 1 or 2), show no opposing tendency, and the effect of acetate is not strong enough to offset the $\Delta G_f°$ of the FHOs. We could not calculate ΔG_r for goethite G 3, because data of HCO_3^- concentrations were lacking, but if we use the average concentration of the other variants, ΔG_r reaches values between – 28 and –47 kJ mol^{-1}. These values would perfectly extend the "staircase" in Fig. E.2. Even for different acetate variants within one FHO, the ΔG_r differed statistically significant in some cases. These data clearly indicate, that the end of bacterial reduction of the FHOs in our experiment was not determined by the thermodynamics of the reactions according to Eq. 1 or 2. Thus, we have to reject the hypothesis of thermodynamic control of bacterial reduction of FHOs under the experimental conditions, choosen here.

Fig. E.1 shows for all FHOs, that Fe(III) was reduced at the most within the 10 mM acetate variants. Because the ionic strength was the same in all variants, acetate may have been limiting in the 1 mM variant and, presumably, 100 mM acetate impeded the activity of *G. metallireducens*.

Limitations to the reduction of FHOs by G. metallireducens:

As the bacterial reduction was not limited by the thermodynamics of Eq. 1 or 2, the question arises, what else restricted the reduction of the FHOs in our experiments.

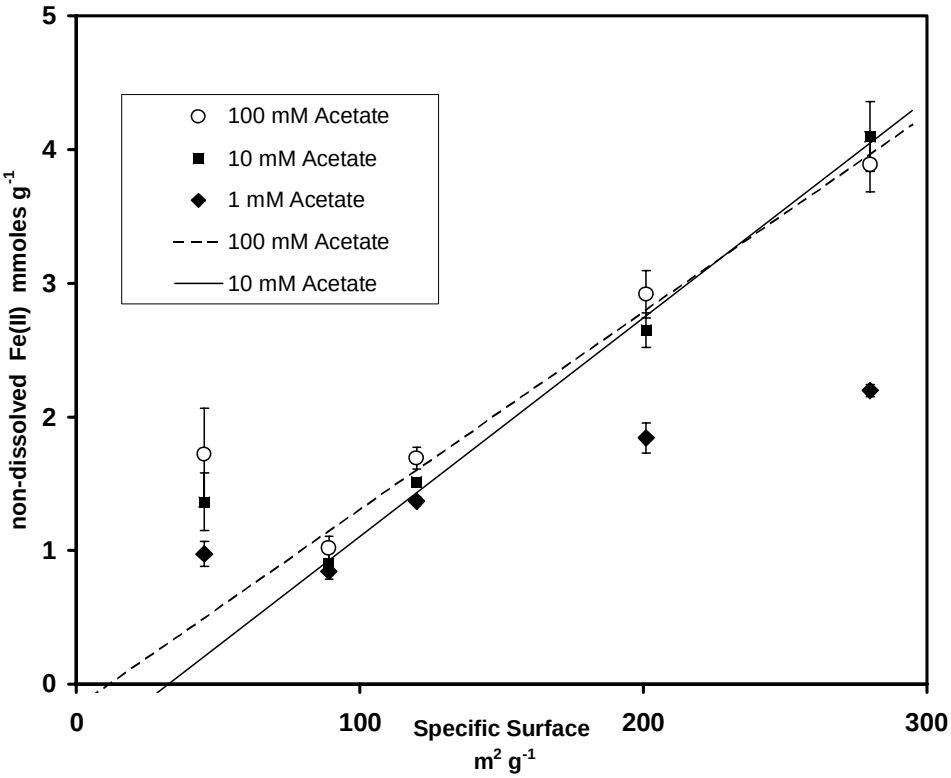

Figure E.3: Non-dissolved amounts of Fe(II) at the end of reduction by *G. metallireducens* with 3 different acetate concentrations versus specific surface of FHOs. Whiskers indicate standard deviation of 3 replicates. Lep, 2LF-1, and 6LF-1 were excluded from linear regressions.

In Fig. E.3 the reduced, but non-dissolved Fe(II) is plotted against SSA of the samples. Most data are arranged along a straight line whose intersection is close to the origin. Thus, the non-dissolved Fe(II) exhibits a proportionality to the surface of the FHOs. The slope of the regressions is about 15 µmol Fe(II) per m^2 of surface. *Roden* and *Zachara* (1996), using *Shewanella alga*, strain BrY, found a

similar correlation and concluded that the reduction was restricted by occupation of the surface of the FHOs. The slope of their regression was about 7.5 µmol m^{-2}, only. However, in *Urrutia et al.* (1998) a goethite (SSA = 153 m^2 g^{-1}) was reduced up to 30%, thus the reduced Fe(III) was about 20 µmol Fe per m^2 of surface in their experiments. *Urrutia et al.* (1998) determined in a chemical adsorption isotherme, that the capacity of adsorption of a goethite at pH 6.9 in bacterial medium or PIPES buffer is about 3.6 µmol Fe^{2+} per m^2 of goethite, which was reached at an equilibrium concentration of 1-2 mM Fe^{2+}. Both values, the adsorbed amount and the equilibrium concentration are clearly exceeded herein, which gives rise to suspect surface precipitation.

After the reduction of a ferrihydrite gel by *Shewanella putrefaciens*, *Fredrickson et al.* (1998) detected siderite as well as vivianite in HCO_3^- buffered media, which contained phosphate. In PIPES buffered media they found mainly magnetite of low crystallinity. We used a medium, which was buffered by both HCO_3^-, and PIPES. Magnetite formation is thermodynamically favored only at pH values higher than those reached here (*Kostka* and *Nealson*, 1995). In fact the color of our incubations, which had changed towards a dark grey due to the magnetite containing inoculum, did not change visible during bacterial reduction.

We did not measure the concentration of dissolved phosphate at the end of the incubation, but it can be assumed from the final Fe^{2+} activities and pH, that phosphate was precipitated as vivianite, almost completely. This could account for up to 6.5 mM of precipitated Fe(II), which was exceeded in most cases. The solubility index (S.I.),

$$S.I. = \log (IAP/K_{SO}) \qquad (3)$$

in which IAP is the ion activity product and K_{SO} is the solubility product, indicates a thermodynamic tendency to precipitation if S.I. > 0. The S.I. for siderite of all variants (Table E.2) was in the range of 1.2-1.8 (i.e. a super saturation by a factor of 15-69), which is very similar to the data given by *Fredrickson et al.* (1998). The authors proved the precipitation of siderite using XRD. It is therefore likely, that

reasonable parts of the non-dissolved Fe(II) in Fig. E.3 were precipitated as siderite.

All variants of Lep, as well as the 1 mM acetate variants of 2LF and 6LF did not fit into the linear regressions in Fig. E.3. For the ferrihydrites it is likely, that acetate limited the production of sufficient ferrous iron to occupy the surface to the same extent as in the other variants, because the final acetate concentrations are (together with 1m M variant of Lep) the lowest of all experiments (Table E.2). It has to be emphasized, that even for this 1 mM variants of the ferrihydrites, whose surface coverage was lower than for all other variants, our hypothesis of thermodynamic control of bacterial reduction of FHOs has to be rejected (Fig. E.2).

The concentrations of non-dissolved Fe(II) on the surface of all Lep variants exceeded the one of all other FHOs. The most plausible explanation would be reaction kinetics. *Fredrickson et al.* (1998) reported an overshoot of the dissolved Fe(II) in the reduction kinetic of a ferrihydrite gel *by S. putrefaciens*, i.e. the precipitation of Fe(II) minerals was slower, than the production of Fe^{2+}. Unfortunately we do not have kinetic data for the bacterial reduction of FHOs. The reduction of *G. metallireducens* in the experiments, reported here, was much faster, than in preliminary incubations, presumably due to the intermitting mode instead of continuos of agitation. The reduction was therefore completed already, when we determined its extent for the first time. But in a chemical reductive dissolution of the FHOs used here, we found for Lep by far the highest initial dissolution rate compared to all other FHOs, when normalized to the surface area of the sample (*Dominik et al.*, submitted). A fast reduction of Lep by *G. metallireducens* could have produced more dissolved ferrous iron, than has been necessary to cover the surface in form of precipitated ferrous iron minerals, and at the end of the experiment most of this ferrous iron had been precipitated.

We can conclude, that the reduction of FHOs in our experiments was presumably restricted by the occupation of their surface by precipitated Fe(II) minerals. Likely this precipitation hindered the bacteria to further reduce Fe(III) until the energy yield of the reactions according to Eq. 1 or 2 reached a threshold to support their metabolism. Limited bacterial reduction of FHOs, due to blocking their surface by non-reducible coatings has also been reported for example by

Roden and *Zachara* (1996), *Urrutia et al.* (1998), *Bousserrhine et al.* (1999), *Roden et al.* (2000), and *Dominik et al.* (2002). To account for that, it would be necessary to enlarge the thermodynamic description of the reaction by a factor, which describes the occupation of the surface of the FHOs, as *Roden* and *Urrutia* (1999) did for the description of the reduction kinetics of a FHO by *Shewanella alga*.

In order to further test the hypothesis of thermodynamic control of bacterial reduction of FHOs, Fe^{2+} precipitation must be avoided. If FHOs with higher stability and lower acetate concentrations are used than used herein, Fe^{2+} activities at the end of bacterial reduction might stay below saturation of precipitates like siderite or vivianite and therefore the bacterial activity could be restricted by the energy yield of the reaction according to E. 1 or 2. However, FHOs of low stability are reduced preferentially (*Ponnamperuma et al.* 1967, *Lovley* and *Phillips*, 1986a) in natural soils and sediments. In addition, activities of Fe^{2+} and HCO_3^- which are assumed for anoxic environments in average (*Lindsay*, 1979; *van Capellen et al.* 1996) exceed the solubility product of siderite by far. It is therefore likely that in natural environments reduction of FHOs is limited by precipitated siderite, too.

In addition, natural environments are open systems and reduced Fe^{2+} may be dislocated from the place of reduction by convection or diffusion, processes which are important in classification of redoximorphic soils (*Scheffer* and *Schachtschabel*, 1998). *Roden et al.* (2000) demonstrated, that a goethite could be reduced almost completely by *S. putrefaciens*, if the Fe^{2+} formed was removed in continuous-flow reactors. Thus, in addition to precipitation, dislocation of reaction products could be another process to impede the achievement of a thermodynamic equilibrium in bacterial iron-reduction in natural environments.

Acknowledgement

We would like to thank the DFG for financial support of this work.

F. Limitations to the reductive dissolution of Al- substituted goethites by *Clostridium butyricum*

Abstract

The effect of increasing Al substitution of synthetic goethites on chemical reductive dissolution is well known. But little is known about the bacterial reductive dissolution of Al- substituted goethites, although Fe(III) oxides are Al substituted in most natural sites. Batch cultures of the fermentative Fe(III) reducer *Clostridium butyricum* were used to reduce goethites with 1.4 (AL1), 5.2 (AL5), 8.1 (AL8), and 32 (AL32) mol% Al for Fe substitution. As known for chemical reductive dissolution experiments, maximum bacterial dissolution rates (normalized to initial specific surfaces) were negatively linear correlated with the degree of Al-substitution. Although there was no deficiency of carbon substrate, the iron oxides were not dissolved completely and the final degree of dissolution decreased with increasing Al-substitution. Because the medium lacked an effective complexing agent, Fe and Al dissolved incongruently: Only 11-55% of the Al released during reduction of Fe(III) was found in solution at the end of incubation. It was calculated that the remaining Al was mainly associated (80-93%) with the goethites but only to a minor extent with the bacteria. Therefore, one possible reason for the total inhibition of dissolution of goethites is that with increasing Al-substitution a minor degree of dissolution is sufficient to cover the goethite surface with undissolved, non-reducible Al. In fact, it was calculated, that 1.1-1.4 µmol Al m^{-2} of initial surface were associated with the goethites. Other possible reasons for inhibition of dissolution include direct inhibition of the microbial activity. Due to the slower reduction of the higher Al-substituted goethites the pH decreased to lower values and even less glucose was fermented. Toxic effects on bacteria could result from a) the acidity itself or its influence on b) Al solubility and shifting speciation of Al towards toxic Al^{3+} and c) on the speciation of butyric acid. As indicated in the literature, all these factors are within the bounds to inhibit activity of *C. butyricum*.

On the basis of our data it is not possible to decide whether one factor was of major importance or all acted together.

Introduction

Microbial reductive dissolution of Fe(III) oxides is one of the most important biochemical processes in anoxic soils and sediments. In anaerobic environments Fe(III) oxides may serve as an electron acceptor for microbial metabolism when energetically more favorable alternatives are not available (*Munch* and *Ottow*, 1977, 1983*; Berthelin,* 1982*; Lovley* and *Phillips,* 1986, 1989). Under these conditions, a variety of microorganisms are able to decompose a large number of organic substances, including aromatic compounds, using Fe(III) oxides as final electron acceptor in fermentation and respiration (*Lovley* and *Phillips,* 1988; *Lovley et al.,* 1989*; Lovley,* 1991). Consequently, microbial reductive dissolution of Fe(III) oxides allows mineralisation of organic matter in oxygen-deficient environments (*Lovley*, 1991).

The extent of microbial reductive dissolution of Fe(III) oxides not only depends on the capability of bacteria to use Fe(III) as electron acceptor. The quality of the organic substrate as well as of the Fe(III) oxide itself have their particular influences (*Munch* and *Ottow,* 1980, 1983*; Lovley* and *Phillips,* 1986*; Bousserrhine et al.,* 1998, *Bousserrhine et al.,* 1999).

Rajot (1992) pointed out the predominant role of Al substitution as the crystallographic factor influencing the bacterial reductive dissolution of natural Fe(III) oxides. He observed both an inhibition of reduction activity before all Fe(III) oxide was dissolved, and the non-congruent dissolution of Al and Fe, i.e. a lower percentage of Al than of Fe was released into the solution during reduction.

In contrast, it is well known that the chemical reductive dithionite citrate bicarbonate-method dissolves Fe(III) oxides congruently and completely irrespective of isomorphous substitution. This is likely due to the complexation of Al by citrate and therefore keeping Al in solution (*Torrent et al.,* 1987*; Jeanroy et al.,* 1991*; Schwertmann,* 1991).

Because the bacterial medium did not contain any effective complexing agent, *Rajot* (1992) concluded that the Al, which was not found in solution, accumulated at the surface of Fe(III) oxides and inhibited further reductive dissolution of Fe by bacterial - or chemical - activity (*Segal* and *Sellers*, 1984; *Borggaard,* 1990).

Bousserrhine et al. (1998) were the first to study the effect of an increasing Al substitution on the bacterial reductive dissolution of well defined synthetic goethites. Their incubations confirmed the non-congruent dissolution of Al and Fe. Further, with increasing Al substitution, the rate of dissolution and the degree of dissolution of the goethites by the end of the experiment decreased. *Bousserrhine et al*. (1998) therefore supported the hypothesis of *Rajot* (1992) that coatings of non-reducible Al inhibited further reduction of the goethites. Nevertheless, both studies were not able to prove that precipitated Al-coatings were the reason for the observed inhibition.

The objective of this study was to examine the effects of differing amounts of Al-substitution on the reductive dissolution of goethites by *Clostridium butyricum* and on its metabolism. The main focus was to test the hypothesis, that coatings of non reducible Al are responsible for limitation of dissolution.

To do this we monitored the kinetics of reductive dissolution of goethites - differing in the amount of Al substitution - including the kinetics of carbon source and products. Subsequent it was determined whether the Al released during dissolution but not found in solution was localized on the goethites or in the bacterial cells. In addition we looked into the changes of the goethites due to bacterial dissolution using TEM.

Material and methods

Fe(III) oxides

Goethites with an Al mole fraction <10 % (Al1, Al5, and Al8) were synthesized from a Fe(III) system (*Schwertmann* and *Cornell,* 1991, p.71), high Al substituted goethite (Al32) was obtained from a Fe(II) system (*Schwertmann* and *Cornell*, 1991, p.79).

Total metal ratios of the goethites were determined after a wet chemical dissolution in 15 M nitric acid using a microwave oven for 30 min. The metal

concentrations were determined by inductively coupled plasma atomic emission spectroscopy (ICP-AES, Jobin Yvon 238 Ultrace). The principle of this method is to bring the elements in the solution into a plasma so that element-specific photons are emitted. Due to the high temperature a lot of known interference among elements occur, which have to be eliminated by the software.

Surface area was calculated from N_2 adsorption measurements (*Brunauer et al.,* 1938*; Boer et al.,* 1965). Nitrogen adsorption was measured by six to eight different nitrogen pressures in a range from 0 to 0.3 (relative to ambient pressure).

The aluminum-substitution of the goethites were 1.4 mole-% (AL1), 5.15 mole-% (AL5), 8.14 mole-% (AL8) and 32 mole-% (AL32) and the specific surfaces amounted to 56.8 , 46.5, 45.5, and 157.8 m^2g^{-1}, respectively.

Bacterial dissolution experiments

Bacterial dissolution experiments were carried out using the bacterial strain 66/4-8 G isolated from a tropical soil rich in Al and Fe oxides (oxisol). The strain was identified as *Clostridium butyricum* and characterized and studied for its physiology and fermentatory metabolism by *N. Bousserrhine* (1995).

A modified medium A (*Bromfield,* 1954) was used for isolation and maintenance of the bacterium. In 1000 ml, the medium contained 150 mg yeast extract, 0.5 g KH_2PO_4, 0.5 g $MgSO_4x7H_2O$, 1 g $(NH_4)_2SO_4$, 10 g glucose and 14 g agar (Difco).

For reductive dissolution of Fe(III), the bacteria were grown in four replicates in the same medium, but agar was omitted. To do this 150 ml of medium and 80 mg goethite were placed into a 250 ml serum glass bottle, mixed and then autoclaved for 30 min at 110 °C. The suspensions were flushed with N_2 to remove O_2. The inoculum of bacteria was prepared by culturing on the solid medium A. After anoxic incubation at 28 °C, bacterial colonies were suspended in sterile physiological solution, washed twice, centrifuged at 13500 x g for 20 min and then resuspended. Bottles were inoculated with 10^7 bacteria per bottle and incubated at 28 °C for 164 h.

In a first incubation experiment Fe and Al release were monitored 10 times over 164 h by sampling 3 ml of the suspension with a syringe. Suspensions were

centrifuged at 13500 g for 20 min and the supernatant analyzed for total Fe and Al, aliphatic acids, alcohols and glucose. Total Fe and Al were measured at ICP-AES. Aliphatic acids, alcohols and glucose were analyzed by HPLC using a Gold Beckman instrument equipped with an UV detector at 195 nm (Animex column HPX-87H).

The initial rate of dissolution b was determined by linear regression of dissolved Fe versus time in the interval of 5-43.5 h.

Analysis of the solid phase after bacterial incubation

In order to determine whether the Al which was released during reduction but not found in the solution, was associated with the bacteria or with the goethite a second identical incubation experiment was run. The final concentrations of dissolved Fe and Al were very similar to the first run. The pellet after centrifugation exhibited a distinct gradient. The bacteria were mainly on the top whereas the goethites were mainly on the bottom. The pellet was frozen at –48°C and fractionated into upper and lower parts. To determine the localization of the undissolved Al we made the following assumptions for the pellet:

a) the amount of solution and its components in the pellet can be neglected, therefore Fe exists only in the undissolved lattice of goethite and N only in the bacterial cells.

b) both, Al adsorbed to the bacteria (Al_b) relative to the mass of bacteria as well as Al adsorbed to the goethites (Al_g) relative to the mass of goethites are the same in both parts of the pellet.

Using subsamples the total amount of elements in each sample was determined. Iron (Fe_t) and aluminum (Al_t) were analyzed after dissolution in 15 M nitric acid using the microwave oven followed by ICP-OES, and nitrogen (N_t) using dry combustion (CHNS+O EA 1108 Elemental Analyzer, Carlo Erba Instruments).

Total Al (Al_t) in each sample can be described as:

$$Al_t = Al_l + Al_g + Al_b \qquad [\mu mol] \qquad (1)$$

where Al_l is the residual amount of structural Al within the undissolved lattice of goethite which can be calculated from the degree of substitution:

$$Al_l = Fe_t * (mol\%Al) / (100 - mol\%\ Al) \quad [\mu mol] \quad (2)$$

according to assumption b) Al_g and Al_b can be written as

$$Al_g = m * Fe_t \quad [\mu mol] \quad (3)$$

and

$$Al_b = n * N_t \quad [\mu mol] \quad (4)$$

m and *n* can be read as accumulation factors of Al on goethite-Fe or bacteria-N, respectively. Therefore equation 1 can be written as

$$Al_t = Al_l + m*Fe_t + n*N_t \quad [\mu mol] \quad (5)$$

in which every term can be measured or easily calculated (eq. 2) except *m* and *n*. But because *m* and *n* are identical in both parts of the pellet (assumption b) we got an equation system with two equations and two unknowns, which can be easily resolved. Using equation 3+4 the Al dissolved during reduction but not found in the solution could be attributed to goethite and bacteria, respectively.

Chemical dissolution kinetics

The chemical dissolution kinetics of the goethites was measured using the dithionite citrate bicarbonate method of *Mehra* and *Jackson* (1960).

Transmission electron microscopy

The carbon grids were prepared according to *Schwertmann* and *Cornell* (1991*).* With the transmission electron microscope (TEM; Phillips CM 20, 120 kV), proportions of elements were determined by energy-dispersive X-ray analysis (EDX), and amorphous phases were distinguished from crystalline phases by electron diffraction.

Statistics

Significance of differences of the data was tested with the Scheffé test, using SPSS™.

Results

Dissolution kinetics of Fe and Al

The dissolution kinetics for Fe were curvilinear and almost stable at the end of the experiment for all goethite samples (Fig. F.1), i.e. dissolution was complete after

164 h. The percentage of goethite which had dissolved - determined as percentage of dissolved Fe - decreased dramatically with increasing Al substitution. Whereas almost 62% of Al1 had dissolved at the end of the experiment, only 28, 13 and 7% of Al5, Al, and Al32 were dissolved, respectively. For all samples the relationship of degree of dissolution at the end of experiment relative to the ratio of mole% Al-substitution to specific surface could be described both by a linear and an exponential equation. (Fig. F.2).

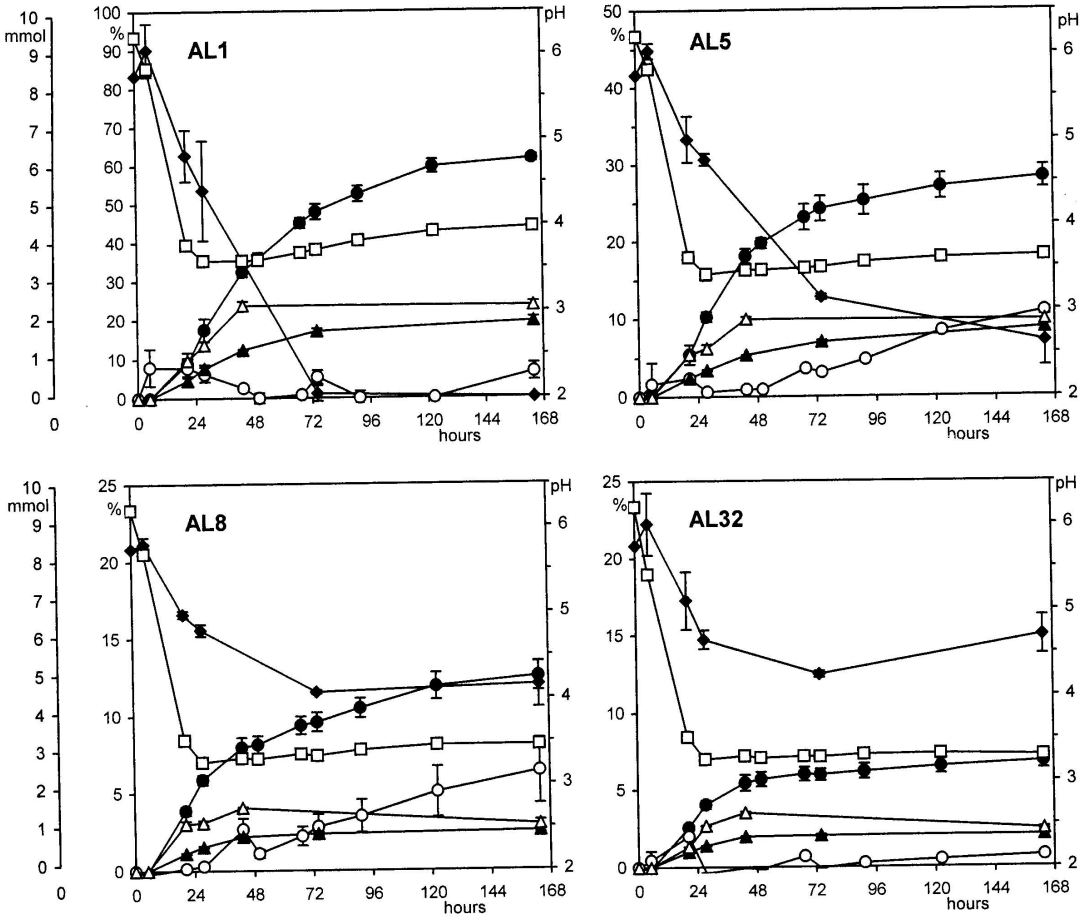

Figure F.1: Dissolution kinetics of Al-substituted goethites and metabolic parameters of *Clostridium butyricum*. Percentages of Fe and Al are related to the initial content of each element in the sample. Substrate and metabolites are expressed as amounts in mmol per experiment. ● dissolved Fe (%); ❍ dissolved Al (%); ◆ glucose; ▲ acetic acid; Δ butyric acid; □ pH. Whiskers indicate standard deviation of four replicates.

The ratio b-to-s (initial rate of Fe reduction normalized to the initial surface) was negatively correlated to the degree of Al substitution. There was a linear correlation for Al1, Al5, and Al8 (Fig. F.3), but Al32, which derives from another synthesis series, did not fit into this linear relationship.

The dissolution of Al was not congruent with the dissolution of Fe. Since both, the dissolution of Al and Fe are shown as the percentage of total content in Fig. F.1, both curves must be identical in the case of congruent dissolution. Aluminum was released to solution to a much lower extent than Fe. There was no significant trend in Al release of Al1 and Al32. This is mainly due to the low concentrations of Al which were often close to the detection limit of ICP-AES.

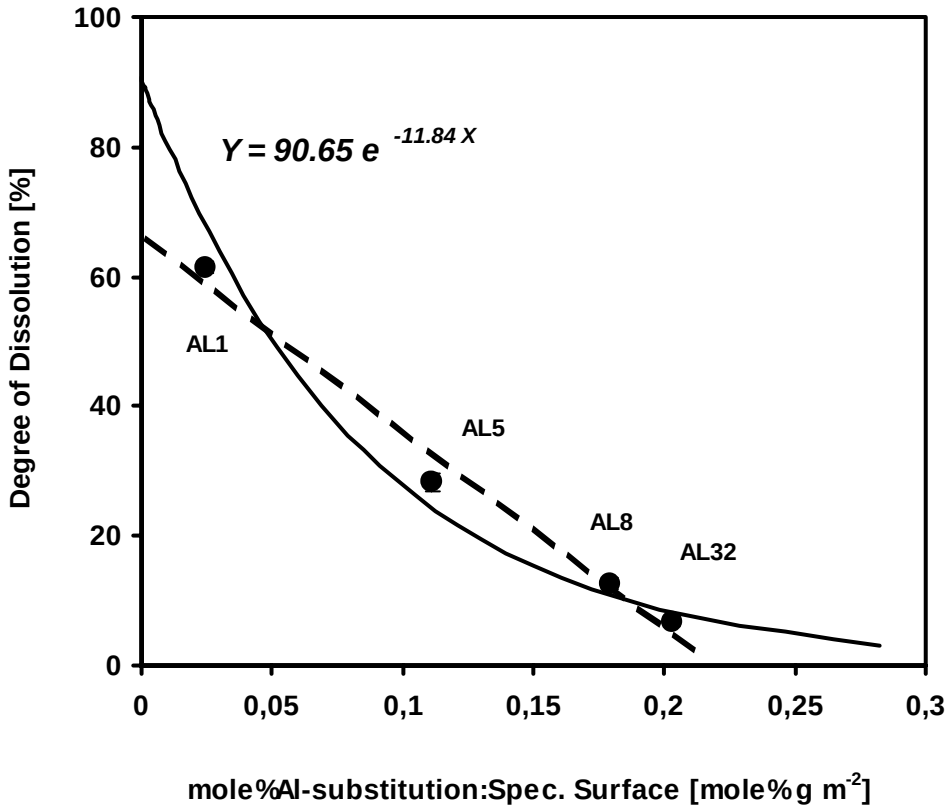

Figure F.2: Degree of dissolution of Al-substituted goethites at the end of experiment versus the ratio of Al substitution to specific surface of the oxide samples Lines show the linear and exponential regression of the data. Whiskers indicate standard deviation of four replicates.

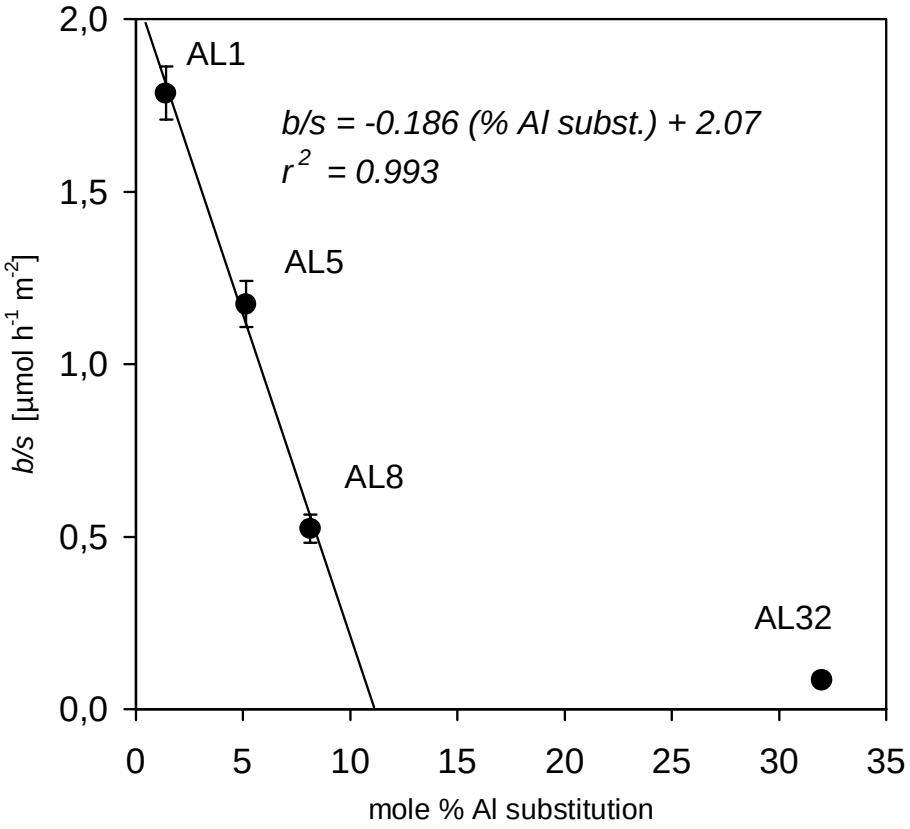

Figure F.3: Slope of the dissolution kinetics in the exponential phase b (µmol h^{-1} in the interval 5-43.5 h) normalized to the initial surface (b-to-s) in dependence to the degree of Al substitution and their linear regression. In respect to the different way of synthesis, AL32 was not considered for the regression. Whiskers indicate standard deviation of four replicates.

Bacterial metabolism

The initial amount of glucose was 8.3 mmoles in every experiment. The rate of glucose consumption (slope of glucose in Fig. F.1) reached its maximum in the period between 5 and 74 h of incubation and decreased with increasing Al substitution. Only in the case of Al1 was glucose consumed completely. Parallel to the highest consumption rate of glucose the formation rate of organic acids reached its maximum. The concentrations of butyric acid as well as undissociated butyric acid at the end of incubation are shown in Table F.1.

Table F.1: Concentrations of undissociated butyric acid in the medium after 43.5 h of incubation (pK_a=4.82). Different letters indicate significant differences according to Scheffé for =0.05.

	AL1	AL5	AL8	AL32
pH	3.59 ^{a}	3.46 ^{b}	3.31 ^{c}	3.29 ^{c}
total butyric acid (g l^{-1})	1.39 ^{a}	1.16 ^{b}	0.95 ^{c}	0.82 ^{d}
undiss. butyric acid (g l^{-1})	1.31 ^{a}	1.11 ^{b}	0.92 ^{c}	0.80 ^{d}

Acetic and butyric acid were the main products (only minor amounts of lactic and propionic acid were detected) but no aliphatic alcohols were detected at all. The ratio of acetic-to-butyric acid remained constant for several days, but increased at the end of incubation. For all amounts of Al substitution this ratio was 0.83-0.9 (Table F.2). A ratio lower than 0.66 would indicate a disturbance of the oxidation of ferredoxin and, therefore restricted H_2 production and Fe reduction (*Jones* and *Woods*, 1986).

The fermentation products measured accounted for 40-60% of the glucose consumed (Table F.2). Although H_2 was not measured, the reduction equivalents can be calculated from the metabolism of *C. butyricum* (Saint-Amans, 2001). If either lactate or aliphatic alcohols are not produced, *C. butyricum* produces 4 [H] each butyrate or acetate. Though the production of reduction equivalents decreased with increasing Al substitution, the portion of produced electrons, which were transferred to Fe, decreased due to the excessive decrease of Fe reduction.

Al in the solid phase

Using DCB (*Mehra* and *Jackson*, 1960), chemical reductive dissolution of the goethite samples showed a congruent dissolution of Fe and Al (data not shown). This indicates that the Al was spread regularly over the goethite lattice. Contrastingly, by bacterial dissolution the dissolution of Al was significant lower than the dissolution of Fe. This means that the amount of Al (Al_s), which is the

difference between percentage of Fe and Al found in solution, must have been released from the lattice of goethite, but was adsorbed either to the surface of remaining goethite or to the cells of bacteria.

Table F.2: Metabolic parameters at the end of incubation (164 h). Different letters indicate significant differences according to Scheffé for $\alpha = 0.05$. Dissolved Al^{3+} (K_{so}) means activity of Al^{3+} according to the solubility product of gibbsite at the respective pH.

	AL1	AL5	AL8	AL32
acetic ac.-to-butyric ac. ratio	0.83 ^{a}	0.90 ^{a}	0.86 ^{a}	0.85 ^{a}
fermented portion of consumed glucose (%)	39.9 ^{a}	40.9 ^{a}	47.2 ^{a}	59.5 ^{a}
electrons produced (mmol)	17.18 ^{a}	14.83 ^{b}	8.69 ^{c}	7.20 ^{c}
portion of electrons transferred on Fe(III) (%)	3.2 ^{a}	1.7 ^{b}	1.2 ^{c}	0.6 ^{d}
pH	3.97 ^{a}	3.63 ^{b}	3.43 ^{c}	3.30 ^{d}
dissolved Al (µM)	10 ^{a}	45 ^{b}	43 ^{b}	23 ^{c}
dissolved Al^{3+} (K_{so}) (mM)	0.13 ^{a}	1.4 ^{b}	4.7 ^{c}	15 ^{d}

Figure 4 shows a transmission electron microscopy (TEM) image of sample Al8 at the end of incubation. One can detect a thin layer around each goethite crystal, which could be amorphous aluminum hydroxide. However, electron diffraction indicated only the presence of a crystalline goethite (data not shown). Perhaps the supposed amorphous layer was to thin to be detectable by this technique. Electron diffraction is a technique which shows similar to X-ray diffraction (XRD) the regularity of a lattice grid. Using electrons instead of X-ray this technique is often used in combination with electron microscopy.

Using EDX we determined a mean Al content of 9.4 mole% (ranging from 7.3 to 11.4 mole%) in Al8.

Table F.3 shows the amount of aluminum which was associated with the goethite surface (Al_g) and the bacterial (Al_b) cells determined by fractionating and analyzing the centrifugation pellet (see 2.3). In every sample Al_g was much greater than Al_b, i.e. 80.2-93.5% of the Al, which could not be attributed to the undissolved lattice of goethite was bound to goethite rather than to the bacteria. Al_s means the same fraction as Al_g + Al_b but was calculated from the concentrations in the solutions.

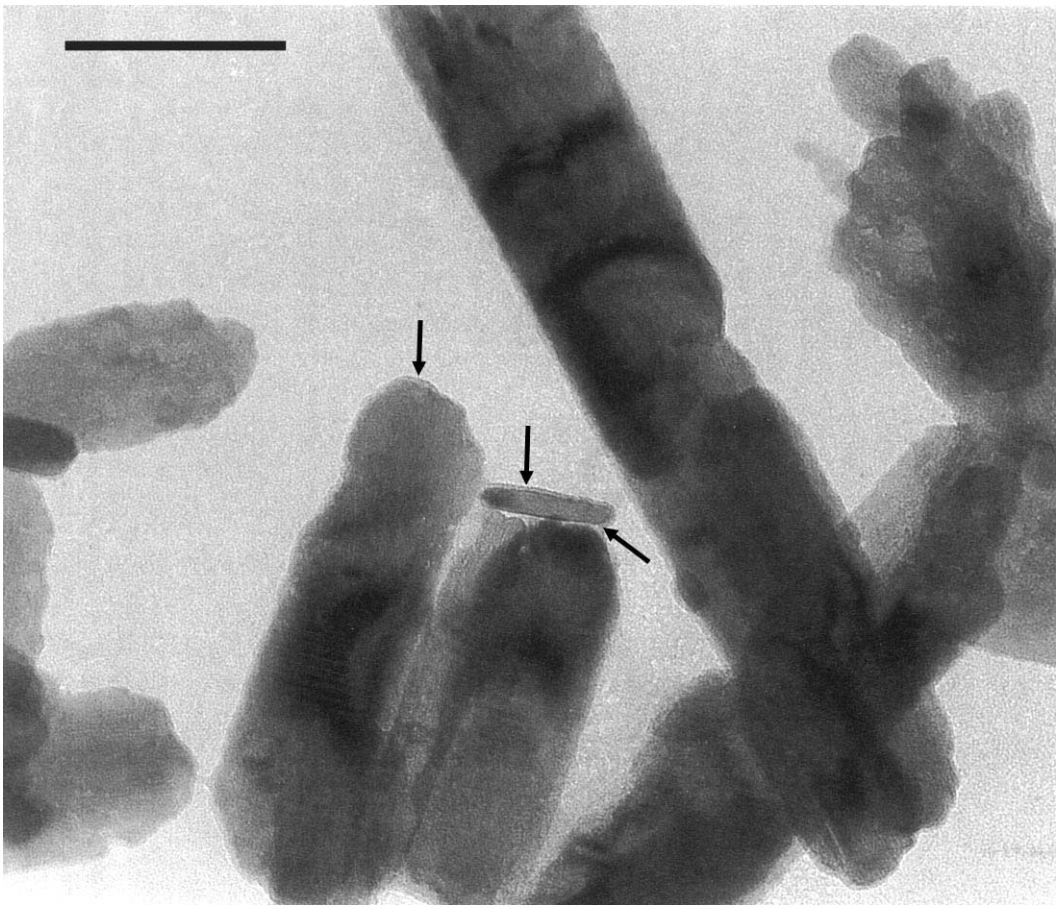

Figure F.4: TEM image of AL8 after 164 h of incubation with *C. butyricum*. Arrows show coatings on the surface. Bar = 0.1 µm.

If it is assumed, that the ratio of Al_g-to-Al_b was the same in both incubation experiments, the amount of Al_g was 1.2, 1.1 and 1.4 µmol m^{-2} initial surface of goethite at the end of the first incubation experiment for Al1, Al8 and Al32, respectively.

Table F.3: Analysis of the solid phase after bacterial incubation. Al_g: Al associated with goethites; Al_b: Al associated with bacteria; Al_s: fraction of Al_g+Al_b derived from the analysis of the solution; values are given as amount per experiment (mean ± standard deviation).

	AL1	AL8	AL32
Al_g (µmol)	2.08 ± 0.36	4.75 ± 1.09	19.56 ± 3.41
Al_b (µmol)	0.54 ± 0.28	0.90 ± 0.05	1.32 ± 0.40
Al_g+Al_b (µmol)	2.61 ± 0.56	5.64 ± 1.14	20.88 ± 3.27
Al_g (% of Al_g+Al_b)	80.2 ± 6.63	83.9 ± 2.05	93.5 ± 2.59
Al_s (µmol)	2.91 ± 0.97	4.52 ± 0.66	17.36 ± 1.23

Discussion

Dissolution kinetics

Initial rates of dissolution as well as the degrees of dissolution of Fe at the end of experiment decreased with increasing Al substitution of the employed goethites (Fig. F.1). Aluminum substitution does not only change the chemical composition, but also the size of the unit cell as well as the mean diameter of the crystal (*Schulze* and *Schwertmann*, 1984, 1987; *Schwertmann et al.,* 1989*; Gerth,* 1990; *Gasser et al.,* 1996). These crystal properties have a great influence on the chemical stability of Fe(III) oxides (*Schulze* and *Schwertmann,* 1984; *Schwertmann,* 1984; *Torrent et al.,* 1987*; Jeanroy et al*., 1991). Therefore the dissolution rates, i. e. the slope b of the curve in the exponential phase, can be discussed only in relation to the surface (s) of the sample. In this manner, *Torrent et al.* (1987*)* compared the chemical reductive dissolution rates in an extended study on Al substitution in goethites and hematites. Similar to their findings for the chemical reductive dissolution, we found a good linear correlation of the ratio b-to-s to the degree of Al substitution for bacterial dissolution. Only AL32, which was synthesized from a ferrous Fe system, whereas Al1, Al5, and Al8 were

synthesized from a ferric Fe system, did not fit within this linear relationship (Fig. F.2). Synthesis using ferrous Fe not only yields goethites with a higher specific surface but also decreased stability. As a consequence dissolution rate of goethites synthesized from the ferrous Fe system are much higher, even when normalized to specific surface, than samples from the ferric Fe system (*Dominik et al., 2000*). In contrast to our experiments, all goethites which were examined by *Torrent et al.* (1987) derived from the ferric Fe system and therefore showed an almost linear correlation of the ratio to the degree of Al substitution.

Our data do not prove, that the dissolution is really finished by the end of the experiment, because there might to be still a very low rate of dissolution (Fig. F.1). However, identical incubations over 500 h showed clearly that the entire process ceased after 200 h at decreasing degrees of dissolution (*Bousserine,* 1995).

The increasing stability of Al-substituted goethites can explain the lowered kinetics of Fe dissolution and glucose consumption only, but not their total inhibition. The question still remains: Why the dissolution of higher substituted goethites did not proceed slowly, until it is complete?

Metabolism

Lack of carbon substrate does not account for the inhibition of dissolution, because only in the case of Al1 was glucose consumed completely. However, it is surprising that the measured fermentation products only account for 40 % to 60 % of the consumed glucose (Table F.2). According to *Saint-Ama*ns *et al*. (2001*)* this value should be approximately 90 %. The available surface of goethite is not large enough to explain the missing fermentation products by adsorption phenomena. It is unlikely, that glucose was fermented to products in part, which were not be detected, because all known products of *C. butyricum* (*Saint-Amans et al.,* 2001) are detectable by the HPLC-method used.

Production of reduction equivalents (electrons) can be calculated form the production of organic acids and the metabolism of *C. butyricum* (*Saint-Amans,* 2001). The part of the electrons produced, which were used for Fe(III) reduction, decreased with increasing Al substitution (Table F.2). *Bousserrhine et al.* (1998)

found a higher value for a pure goethite and the same values for the 5 % and 32 % Al-substituted goethites as we did. As discussed for the dissolution kinetics, increasing Al substitution favors the stability of Fe(III) oxides. Our results indicate that increasing Al substitution seems to decrease accessibility for bacterial reduction, too. On the other hand, the increase in the portion of electrons produced and transferred on Fe, is too small to explain the great increase in glucose consumption with decreasing Al substitution. But a beneficial effect of Fe(III) on glucose consumption for Fe(III)-reducing, fermentative bacteria was reported by *Lovley* (1991), *Ehrlich* (1996*)* and *Bousserrhine et al.* (1999).

pH

Decreasing pH could have limited the reductive dissolution of Al-substituted goethites in our experiments. Depending on the pH of the incubation medium, the activity and effectiveness of reduction of the strain of *C. butyricum* used in our experiments has been tested (*Bousserrhine,* 1995*.*). In pH-stat assays the highest bacterial activity as well as the highest Fe(III) reduction activity were both at pH 5.2. In non pH-regulated assays, pH dropped below 3 and an inhibited bacterial activity . In our experiments the pH always exceeded 3, but inhibition by low pH can not be completely excluded. As discussed below, this is not necessarily due to proton activity directly, but also due to other chemical changes, affected by the decline in pH.

Organic acids

The formation of organic acids could have been another factor for the inhibition of bacterial activity. Their accumulation in the medium first stops bacterial growth and then provokes the transformation of the organic acids into acetone, ethanol and butanol (*Hartmanis et al.,* 1984). This process, called solventogenesis, requires further glucose for energy supply. Not the concentration of butyrate but the concentration of undissociated butyric acid (pKa=4,82) triggers the beginning of solvatogenesis. For batch cultures of *Clostridium acetobutylicum Long et al.,* (1984) and *Gottschal* and *Morris* (1981), reported a solvatogenesis threshold of

about 0,4 g l^{-1} of undissociated butyric acid, whereas *Monot et al.* (1984), found a threshold for start of solventogenesis of 1.6-1.9 g $l^{-1}$and a threshold for growth inhibition of 0.5 g l^{-1}. In assays with *C. butyricum* (*Vandak et al.,* 1997) solventogenesis began at similar concentrations of undissociated butyric acid. The concentrations at the end of our experiments are listed in Table F.1. Assuming a similar behaviour of our strain of *C. butyricum*, an inhibition of bacterial growth by an elevated concentration of butyric acid could have taken place in all cases, but no solvents were detected. On the other hand *Bousserrhine et al*. (1998), using the same strain, found slightly higher concentrations of undissociated butyric acid at the end of incubation. This indicates that the strain tolerates even higher values, but undissociated butyric acid could have been one of some factors, which acted in combination to halt the activity of *C. butyricum*.

Al toxicity

Another possible inhibiting factor in our experiments may have been Al-toxicity. Even if Al concentrations are low (17-30 µM in AL5, AL8 and AL32) it should be considered that under low pH conditions most of the Al is present as Al^{3+}, which is generally believed to be the toxic species (*Guida et al.,* 1991).

On the one hand *Illmer* and *Schinner* (1997) found for soil microorganims (*Pseudomonas sp.* and *Arthrobacter sp.*) that the toxic effects of acid Al salts must be attributed mainly to the decreased pH. On the other hand *Thampuran* and *Surendran* (1996) and *Guida et al*. (1991) found toxic effects of Al salts even in buffered media on *Bacillus sp.* and *E. coli,* respectively. Therefore, we calculated the concentration of Al^{3+} for their experiments [using pK_a values of the Al species from *Lindsay* (1977)]. Except for AL1, the final Al^{3+} concentration in all experiments exceeded the toxic levels of the studies of hand *Thampuran* and *Surendran* (1996) and *Guida et al*. (1991). Acids like malaic, oxalic, and citric are known to reduce Al toxicity (*Jones* and *Kochian,* 1996; *Jones et al.,* 1996), but we did not detect any di- or multicarboxylic acids, which should have appeared at the very beginning of the HPLC-chromatograms. Nevertheless, further experiments with our strain are needed to check if Al toxicity occured in our experiments.

Surface coatings

Our objective was to test the hypothesis of *Rajot* (1992), that adsorption of non-reducible elements on the surface of Fe(III) oxides can block the reactive sites and so inhibit further reduction (*Segal* and *Sellers*, 1984; *Borggaard,* 1990).

Congruent dissolution of all goethites in DCB showed clearly that Al is released proportional to Fe, when the goethites are dissolved in the presence of a complexant, which keeps Al in solution. This indicates, that Al was spread regularly over the lattice. As demonstrated by *Bousserrhine et al.* (1998), the bacterial dissolution of Al was non-congruent with the dissolution of Fe in our experiments. The question arises: Was the Al which must have been released from the lattice but not found in the solution bound to the goethites or the bacteria?

The initial composition of Al8 was of 8,14 ± 0,5 mole%Al (determined with ICP). If all Al released but not found in solution will be adsorbed to the goethites, the overall composition of Al8 would increase to 8.69 mole% Al. After the incubation a composition of 9,4 ±1,7 mole%Al was determined with EDX. These data indicate, that with these techniques it was not possible to prove the deposition of Al on the surface of goethite during incubation .

However, the analysis of the solid phase at the end of the second incubation experiment resulted in much higher values for Al_g than for Al_b (Table F.3). Hence, most of the Al released from the crystal lattice and not found in solution was associated with the mineral phase. When we use the solution data to calculate the amount of Al released but not found in the solution (Al_s) this value correspond quite well with the calculated amounts of Al bound to goethites and bacteria (Al_g+Al_b). This means, that besides all assumptions and possible errors during measurement the method proposed in 2.3 seems to work quite well.

Beveridge and *Murray* (1976) showed that no Al^{3+} was adsorbed to the cell walls of *Bacillus subtilis*. Because *B. subtilis* and *C. butyricum* are both Gram-positives with high G+C content, it can be assumed that the physico-chemical behaviour of their cellwalls is similar. If this is true, *C. butyricum* will adsorb little or essentially no Al^{3+}, which confirms our findings.

The thin layer on the surface on all goethite crystals (Fig. F.4) supports the idea of a blocking further reductive dissolution by coatings of Al. We assume, that the extent to which a goethite can be dissolved is determined by the surface available for adsorption of Al and by the level of Al substitution. The greater the amount of Al substitution the lower the extent of dissolution at which the available surface is covered with Al. Figure F.2 shows the relationship between degree of dissolution at the end of experiment and the ratio of mol% Al-Substitution-to-specific surface. The linear relationship would mean, that, for example, a goethite with 10.5 mole% Al-substitution and a specific surface of 50 m^2g^{-1} could not be dissolved to any extent. This would not meet our concept of dissolution until the surface is covered with Al. Additionally a pure goethite would be dissolved only to an extent of 67% in the linear relationship. *Bousserrhine et al*. (1998) demonstrated that under identical experimental conditions a pure goethite was dissolved almost completely (91%). This value fits very well to the exponential equation, which approaches asymptotically zero dissolution with increasing ratio of Al-substitution-to-specific surface. Therefore we believe that Fig. F.3 supports the hypothesis of *Rajot* (1992) that coatings of non-reducible Al inhibited further reduction of the goethites.

This hypothesis is also supported by an additional experiment, reported in *Bousserrhine et al.* (1999): These authors incubated *C. butyricum* with a goethite (5 mol% Al substitution) and yielded a final degree of dissolution of 30% (Fe). When they added this pre-incubated goethite sample to a fresh culture of *C. butyricum*, the degree of dissolution of the goethite was 38% as the sum of both experiments. However, when they had washed the pre-incubated sample with oxalate buffer according to *Tamm* (1922) before adding to a fresh culture, the final degree of dissolution was 60% as the sum of both experiments. Oxalate buffer is known to dissolve amorphous Fe hydroxides as well as crystalline Al hydroxides. This experiment clearly demonstrates, that factors of the solution (pH, dissolved Al, or butyric acid) have minor importance to the limitation of reductive dissolution of Al-substituted goethites by *C. butyricum*, than factors of the mineral surface!

The question remains: How Al was bound to the surface of goethites, e.g. whether it was precipitated as Al hydroxide or adsorbed as Al^{3+}? Solubility products indicate that all Al concentrations at the end of the experiment were significantly

below saturation (Table F.2) (*Lindsay,* 1977). As the Al originates from the crystal lattice, higher activities of Al may occur at the goethite solution interface than in the free solution. Therefore an accumulation of Al-hydroxide on the surface of goethites cannot be excluded.

Lövgren et al. (1990) reported for 200 µM dissolved Al at pH 4.0 an adsorption of 0.45 µmol Al m^{-2} and for 300 µM Al at pH 3.3 an adsorption of 0.11 µmol Al m^{-2} of goethite surface. Although the ionic strength was 3-fold higher in their experiments, it can be concluded, that our values of 1.1 – 1.4 µmol Al m^{-2} exceeded the adsorption capacity of goethite, because dissolved Al concentrations were from 10% to 2% less in our experiments.

Consequently, not all of the Al accumulation at the goethite surface can be explained by binary adsorption, with certainty. Ternary adsorption complexes with organic compounds , i. e. Al^{3+} is adsorbed to the goethite surface via a divalent organic acid bridge, mainly occur at low pH values. This has been shown by *Jones et al.* (1996) and *Ali* and *Dzombak* (1996) for Al^{3+} and other metal cations in interaction with different organic acids and goethite as well as other minerals.

Consequently, we believe that the accumulation of Al on the goethite surface in form of regular, thin amorphous coatings has to be explained by adsorption phenomena, partly due to binary, partly to ternary adsorption complexes.

Conclusions

- Increasing amounts of Al substitution in goethites leads to a reduced rate not only in chemical dissolution but also in bacterial reductive dissolution.
- It seems likely, that higher substituted goethites were dissolved to a lesser extent at the end of the experiment, than lower substituted ones, because of accumulation of non-reducible Al on the surfaces of goethite. However, other possible reasons could not be ruled out, completely.
- Further experiments are necessary to test whether toxicity of Al^{3+}, butyric acid, or H^{+} occured in our experiments.

Acknowledgements

We thank Emmanuel Jeanroy (CPB, CNRS, Nancy) for the preparation of the goethite samples. In addition, we thank Mrs. G Villemin (CPB, CNRS, Nancy) for supporting the TEM observations. This investigation was performed at the CPB, CNRS, Nancy and was supported by the C.P.B.-CNRS Geomicrobiology Programs.

G. Zusammenfassung der Ergebnisse und Schlussfolgerung.

Bestimmung der thermodynamischen Stabilität von FHO

$\Delta G_f°$ lässt sich selten direkt, und dann experimentell nur sehr aufwändig ermitteln. Als eine Möglichkeit einer thermodynamischen Größe, aus der $\Delta G_f°$ berechnet werden kann, bietet sich die Bestimmung des Standardpotentials $E_h°$ nach *Fischer* (1987) an, der berichtet, innerhalb von 24 h einen stabilen Messwert zu erhalten. Mir gelang es aber mit identischem Versuchsaufbau innerhalb von 10 Tagen nicht stabile Messwerte zu erhalten. Daher habe ich das Löslichkeitsprodukt $K_{SO} = \{Fe^{3+}\}\ \{OH^-\}^3$ der Oxide bestimmt, aus dem sich ebenfalls $\Delta G_f°$ berechnen lässt. Auch bei der Bestimmung von K_{SO} dauerte es ca. 5 Monate bis stabile Messwerte erhalten wurden, da es aber hierfür reicht, die Probe in Säure unter oxischen Bedingungen zu schütteln, war das der weniger aufwändige Weg (siehe **Abschnitt E**). Für die Probe Lepidokrokit wurde die o.g. $E_h°$-Bestimmung so lange durchgeführt, bis ein annähernd stabiler Wert erreicht war. Da dieser Wert, nach Umrechnung in den K_{SO}, identisch war mit dem für diese Probe gemessenen K_{SO}, kann davon ausgegangen werden, dass die so ermittelten K_{SO} Werte ausreichend präzise sind. Für die Bestimmung des K_{SO} ist es unerlässlich, nur die tatsächlich gelöste Konzentration an Fe(III) zu messen und nicht auch kolloidale FHO mitzubestimmen, denn durch die fortschreitende Auflösung entstanden immer kleinere, gut dispergierte Partikel, die teilweise nicht mehr abzutrennen waren. Mittels Atomabsorption wäre ein Teil der Partikel mitbestimmt worden. Daher wurde hier eine Methode entwickelt, um gelöstes Fe(III) photometrisch zu bestimmen (**Abschnitt B**). Die Methode beruht auf einer anerkannten Methode zur Bestimmung von gelöstem Fe^{2+} mittels Ferrozin, mit dem Unterschied, dass der Reaktionslösung Ascorbinsäure zugesetzt ist, so dass gelöstes Fe(III) zu Fe^{2+} reduziert wird, welches dann als $Fe(II)(Ferrozin)_3$-Komplex photometrisch gemessen werden kann. Diese Umsetzung erfolgt bei freiem Fe(II) schlagartig, während komplex gebundenes (**Abschnitt B**) oder kolloidales Fe(III) wesentlich langsamer (**Abschnitt C**) reagiert.

Auflösungskinetik von FHO

Beide genannten Methoden, um die thermodynamische Stabilität der FHO zu bestimmen, beschreiben die Stabilität des FHO nur beim jeweiligen Auflösungsgrad. Um einen Einblick in die komplette Auflösung zu erhalten und daraus ebenfalls einen Stabilitätsparameter zu erhalten, wurde auch die Auflösungskinetik der FHO bestimmt. Zum einen wurde die Auflösungskinetik in Oxalat-Puffer, pH 3,0 nach *Schwertmann* (1964) ermittelt. Andererseits erschien es, da die reduktive Auflösung durch Bakterien untersucht werden sollte, sinnvoll, auch eine reduktive Auflösungkinetik ohne den Einfluss von komplexierenden Substanzen oder niedrigem pH zu ermitteln. Solche Methoden haben aber den Nachteil, noch aufwändiger zu sein als andere Methoden zur Bestimmung einer Auflösunskinetik, die ebenfalls häufige Probenahme und Messung erfordern. Bei neutralem oder gar noch höherem pH-Wert wird das Reduktionsmittel durch Luftsauerstoff schnell oxidiert. Eine Endprodukthemmung muss aber unbedingt vermieden werden, um eine Auflösungskinetik zu ermitteln, deren Ratenänderung nur auf die Probe und nicht Veränderungen der Lösungszusammensetzung zurückzuführen ist. Daher müssen solche reduktiven Auflösungskinetiken unter Luftabschluss durchgeführt werden. Meistens wird hierzu die Suspension stetig mit N_2 gespült (*Larsen* und *Postma*, 2001; *Torrent et al.*, 1987). Hier bot sich daher eine Weiterentwicklung der o.g. Methode zur Bestimmung von gelöstem Fe(III) an. Ich habe eine Methode entwickelt, bei der eine sehr geringe Menge FHO in einem gasdicht verschlossenen Reagenzglas unter sauerstofffreien Bedingungen reduktiv durch Ascorbat aufgelöst wird. Das freigesetzte Fe^{2+} reagiert mit ungefärbtem Ferrozin zum violett gefärbten Komplex. Die Absorption des Komplexes, und damit das Ausmaß der Reaktion kann jederzeit gemessen werden, indem die Absorption des verschlossenen Reagenzglases (als Ersatz für eine Küvette) in einem Photometers mit einer speziellen Aufnahme für Reagenzgläser gemessen wird. Die eingebrachte Menge FHO ist so gering, dass sie eine kaum messbare Trübung verursacht. Mit dieser Methode lässt sich also die Auflösung von FHO durch Ascorbat sehr praktisch mit geringem Aufwand messen. Es konnten hier erstmals die mittels zwei verschiedenen Methoden (Oxalat und Ascorbat) gewonnenen Stabilitätsparameter (Ratenkonstante bzw.

„inital rate“) von mehreren FHO verglichen werden (**Abschnitt C**). Es zeigte sich, dass die Ergebnisse beider Methoden zwar gut miteinander korreliert sind, dass aber dennoch das Verhältnis der Stabilitätsparameter zweier beliebiger FHO sehr verschieden sein oder sich sogar umdrehen kann, je nachdem, welche Auflösungsmethode verwendet wird. Das ist ein neues und unerwartetes Ergebnis. Es zeigte sich weiterhin, dass die Oxalat-Methode reaktive FHO bevorzugt auflöst. Während sich reaktive FHO in Oxalat etwa 30 mal so schnell auflösten wie im reduktiven Ansatz, lösten sich stabile FHO in beiden Methoden beinahe gleich schnell auf. Dieser Befund bestätigt die besondere Eignung des Oxalat-Puffers zur nahezu selektiven Extraktion reaktiver FHO von Böden (*Schwertmann*, 1964). Die Ratenkonstanten beider Auflösungsmethoden korrelierten gut mit den anderen Stabilitätsparametern der FHO (spezifische Oberfläche, K_{SO} und damit auch mit $E_h°$).

Es bot sich nun an, die entwickelte Methode zur Messung einer reduktiven Auflösungskinetik so weiterzuentwickeln, dass damit die Auflösungskinetik der FHO einer Bodenprobe mit geringem Arbeitsaufwand bestimmt werden kann (**Abschnitt D**).

Zur Fraktionierung der FHO von Böden gibt es bisher nur die Möglichkeit, amorphe von kristallinen FHO durch o.g. Oxalat-Methode zu trennen. Die kristallinen FHO können nur weiter unterteilt werden, wenn es sich um verschiedene Minerale handelt. Dann kann durch die Kombination von Mössbauer-Spektroskopie und Röntgenbeugung jedem Mineral eine mittlere Kristallitgröße zugeschrieben werden, wenn der FHO Gehalt der Bodenprobe und/oder die Empfindlichkeit der Messung hoch genug ist.

Wenn es nun gelänge, die Auflösungskinetik der FHO eines Bodens in - über ihre Ratenkonstante definierte - Fraktionen zu unterteilen, dann könnte man die Stabilität der FHO besser beschreiben, und ihnen eventuell sogar eine spezifische Oberfläche und eine thermodynamische Stabilität zuordnen. Ein Vorversuch zeigte, dass es nötig ist, der Reaktionslösung noch 1 mM Citrat zuzusetzen, damit auch Aluminium-substituierte FHO (vergleiche **Abschnitt F**) vollständig aufgelöst werden können. Sowohl mittels eines neu entwickelten grafischen Verfahrens, als auch durch Anfitten einer Summenfunktion konnte die erhaltene Auflösungskinetik

in 3-4 Fraktionen zerlegt werden, die sich nach einer Kinetik pseudo-erster-Ordnung auflösen. Es ist noch nicht abschließend geklärt, ob den erhaltenen Fraktionen über die Ratenkonstanten physikochemische Parameter wie spezifische Oberfläche, K_{SO} und $E_h°$ zugeordnet werden können, da ein Kontrollversuch anzeigte, dass sich die Ratenkonstanten synthetischer FHO verändern, wenn sie in Gegenwart von Boden aufgelöst werden.

Über die o.g. Korrelation zur Auflösung in Oxalat konnte jedoch die Auflösung der einzelnen Bodenfraktionen nach 2 Stunden Oxalatextraktion abgeschätzt werden. Weil dies den tatsächlichen Fe_o-Anteil der Boden-FHO sehr gut vorhersagen konnte, ist zu hoffen, dass es sich bei o.g. Kontrollversuch um ein Artefakt handelt. Dann würde sich eine Methode ergeben, die es erlaubt, auch bei niedrigen Gehalten von FHO in der Bodenprobe und/oder fehlender apparativer Ausstattung eines Labors die FHO einer Bodenprobe nach Menge und physikochemischen Eigenschaften zu beschreiben und viele ökologisch bedeutende Funktionen der Bodenprobe vorherzusagen.

Test der Hypothesen: Begrenzung der bakteriellen FHO-Reduktion

1) thermodynamische Begrenzung der bakteriellen FHO-Reduktion.

Die hier durchgeführten Versuche mit *Geobacter metallireducens* (**Abschnitt E**) belegen eindeutig, dass unter den gewählten experimentellen Bedingungen die FHO-Reduktion nicht von der Thermodynamik der Reaktionsgleichungen 1 oder 2 (**Abschnitt A**) begrenzt wurde. Die Änderung der freien Reaktionsenthalpie ΔG_r war nach Abschluss der Reduktion zwischen allen FHO, und teilweise sogar zwischen den Acetat-Konzentrationen, signifikant verschieden. Eine Proportionalität des ungelösten Fe(II) mit der Oberfläche der FHO und eine, für alle Varianten ähnliche, Übersättigung des K_{SO} von Siderit zeigte dagegen an, dass die Reduktion durch Fe(II)-Präzipitate auf der Oberfläche der FHO begrenzt worden war. *Klüber* und *Conrad* (1998) sowie *Peters* und *Conrad* (1996) berichten Acetat Konzentrationen in überstauten Böden während der Methanbildung von 50 µM bis über 1 mM, *Lueders* und *Friedrich* (2002) nennen einen threshold für

acetoklastische Methanogene von 5 µM. Obwohl die Acetatkonzentrationen in den meisten Varianten meiner Versuchen über diesen Werten lagen, kann meinen Versuchen entnommen werden, dass *G. metallireducens* auch noch mit so niedrigen ΔG_r Werten wie –30 kJ je mol Acetat leben kann. Das bedeutet, dass selbst bei dem o.g. threshold der Methanogenen und pH 7 das stabilste in meiner Arbeit verwendete FHO noch bis zu einer Fe^{2+} Aktivität reduziert werden kann, bei der das K_{SO} des Siderits deutlich überschritten wird. Abschließend kann also aus den hier gewonnenen Ergebnissen, zusammen mit neueren Literaturdaten, geschlossen werden, dass auch an natürlichen Standorten die Reduzierbarkeit der FHO vermutlich durch Oberflächenpräzipitate begrenzt wird. Da in natürlichen Böden jedoch, gemessen an der Kristallitgröße, manchmal noch stabilere FHO auftreten (*Schwertmann*, 1988), als hier verwendet wurden, könnte es bei diesen vorkommen, dass die Reduktion für die respiratorischen Fe(III)-Reduzierer thermodynamisch begrenzt wird. Meine Ergebnisse zeigen jedoch weiterhin, dass die Begrenzung der Reduktion durch Oberflächenpräzipitate durch die Kinetik der Reduktion überlagert werden kann, denn in der Probe Lepidokrokit hatte sich je Oberfläche wesentlich mehr ungelöstes Fe(II)-Präzipitat gebildet als bei den anderen FHO. Das kann nur durch die wesentlich schnellere Kinetik der Reduktion des Lepidokrokits erklärt werden. Der gesamte Prozess der FHO-Reduktion kann also nur aus dem Zusammenspiel von spezifischer Oberfläche der FHO, sowie Thermodynamik und Kinetik der Reduktion verstanden werden.

Ein anderer Fall tritt ein, wenn das reduzierte Fe^{2+} aus dem System entfernt wird, wie *Roden et al.* (2000) in einem Modellversuch zeigen konnten. In einem durchströmten Reaktor konnte ein Goethit nahezu vollständig durch *Shewanella putrefaciens* aufgelöst werden, denn das Löslichkeitsprodukt von Siderit wurde nie überschritten. Dieser Prozess ist natürlich in Gleyen, Pseudo- und Stagnogleyen von großer Bedeutung.

2) Begrenzung der Reduktion durch Aluminium auf der Oberfläche von FHO.

In Zusammenarbeit mit dem Centre de Pédologie Biologique, CNRS in Nancy, Frankreich ergab sich die Möglichkeit, dort die Auswirkungen unterschiedlich

starker Aluminium-Substitution von Goethiten auf die bakterielle Reduktion zu untersuchen (**Abschnitt F**). In Nancy bestanden schon Erfahrungen aus Vorversuchen mit einem Stamm von *Clostridium butyricum* (*Bousserrhine*, 1995), in denen sich gezeigt hatte, dass der Auflösungsgrad der FHO am Ende der bakteriellen Inkubation mit zunehmender Aluminium-Substitution immer kleiner wurde. Da Aluminium im Gegensatz zu Fe(III) durch Bakterien nicht reduzierbar ist, stellte sich die Frage, ob das Ende der bakteriellen Auflösung auf die Blockierung der Oberfläche durch unlösliche Aluminium-Präzipitate zurückzuführen ist. Zwar konnte dies durch Aufnahmen und Röntgenfluoreszenz am Elektronenmikroskop nicht eindeutig nachgewiesen werden, aber eine von mir entwickelte physikalisch-mathematische Fraktionierung des ungelösten Aluminiums zeigte, dass dessen Konzentration auf der Oberfläche für alle Goethite gleich war. Zusammen mit Ergebnissen von *Bousserrhine et al.* (1999) konnte so gezeigt werden dass die durch steigende Substitution verursachte Hemmung der bakteriellen Reduktion zum größten Teil auf Aluminium-Beläge der Oberfläche der Goethite zurückzuführen ist. Aufgrund der Verwendung des fermentativen Bakteriums waren die pH-Werte bei Versuchsende mit 3,3 bis 4,0 sehr niedrig, während an natürlichen Standorten die pH-Werte durch die Reduktionsprozesse steigen (*Peters* und *Conrad*, 1996). Da aber die Löslichkeit von Aluminium mit steigendem pH abnimmt, kommt unseren Ergebnissen an natürlichen Standorten daher eher noch größere Bedeutung zu.

H. Kurzfassung

Dissimilatorisch-Fe(III)-reduzierende Bakterien (DIRB) konkurrieren mit methanogenen Archaeen (und Sulfat-reduzierenden Bakterien) um Elektronendonatoren, das sind Gärungsprodukte wie H_2 sowie niedermolekulare organische Säuren und Alkohole. Weil die Methanbildung den Organismen weniger Energie liefert als die Reduktion von Fe(III), können die Fe(III)-Reduzierer die Konzentration an Elektronendonator stärker erniedrigen (threshold) und so die Methanbildung vermindern. Der weitaus größte Teil des verfügbaren Fe(III) liegt jedoch als Fe(III)(Hydr)oxid (FHO) vor, dessen Löslichkeit gering ist. Allerdings weisen FHO eine große Spannbreite thermodynamischer Stabilität auf: So unterscheiden sich die Löslichkeitsprodukte von FHO in Böden um mindestens 3-4 Größenordnungen. Mit zunehmender Stabilität der FHO sinkt aber der Energiebetrag, den die Bakterien aus deren Reduktion nutzen können.

In Boden-FHO ist in Abhängigkeit vom Verwitterungsgrad der Böden ein gewisser Prozentsatz der Fe(III)-Atome durch Aluminium ersetzt (isomorphe Substitution). Da Aluminium im Gegensatz zu Fe(III) nicht reduziert werden kann, stellt sich die Frage, was mit dem schlecht löslichen Al(III) geschieht, wenn ein FHO reduziert wird.

Ziel dieser Arbeit war es daher (1) zu überprüfen, ob die Umsetzung unterschiedlich stabiler FHO durch DIRB von der thermodynamischen Stabilität der FHO begrenzt wird. Weiterhin sollte (2) die Hypothese geprüft werden, dass das Aluminium substituierter FHO bei deren bakterieller Reduktion auf der Oberfläche der FHO unlösliche Beläge bildet, die eine weitere Auflösung verhindern.

Es wurden FHO mit spezifischen Oberflächen von 89-280 $m^2\ g^{-1}$ synthetisiert und charakterisiert. Zur Messung des Löslichkeitsproduktes (lg K_{SO} von –39,1 bis -41,8) wurde eine neue photometrische Methode entwickelt, um ausschließlich echt gelöstes Fe(III), zu erfassen.

Zusätzlich zur thermodynamischen Stabilität wurde die FHO mittels Auflösungskinetiken charakterisiert. Eine neu entwickelte Methode ermöglichte es, die reduktive Auflösung durch Ascorbat bei pH 5,2 mit geringstem Aufwand zu messen. Die FHO werden in einem O_2-freien Reagenzglas aufgelöst und das Ausmaß der Reaktion kann jederzeit als Absorption des Fe(II)$(Ferrozin)_3$-

Komplexes in dem Reagenzglas ermittelt werden. Da auch die Auflösungskinetik in Oxalat-Puffer bestimmt wurde, konnten erstmals die Ergebnisse zweier Auflösungsmethoden an mehreren Proben verglichen werden. Zwar sind die Ratenkonstanten beider Methoden gut korreliert, aber Oxalat löst reaktive FHO gegenüber der reduktiven Methode bevorzugt auf. Der Vergleich der Stabilitäten zweier FHO kann mit beiden Methoden sehr unterschiedlich ausfallen. Die physikochemischen Eigenschaften der FHO (spezifische Oberfläche, K_{SO} (und damit E_h°) zeigen eine gute Korrelation zu den Ratenkonstanten.

Diese neu entwickelte Methode, wurde (leicht modifiziert damit auch Al-substituierte FHO aufgelöst werden) angewendet, um auch die Auflösungskinetik von Boden-FHO einfach zu bestimmen. Diese Auflösungskinetik setzte sich je nach Bodentyp aus 3-4 Fraktionen von FHO zusammen, deren pseudo-fist-order Ratenkonstanten sich im Durchschnitt um jeweils einen Faktor von 10 unterscheiden. Es besteht die Aussicht, dass es diese Methode erstmals erlaubt, die FHO von Böden in mehr als zwei Fraktionen zu unterteilen, und diesen Fraktionen sogar Eigenschaften wie spezifische Oberfläche oder K_{SO} zuzuordnen.

Die Umsetzung der FHO durch den DIRB *Geobacter metallireducens* mit Anfangskonzentrationen von 1, 10 und 100 mM des Elektronendonators Acetat zeigte, dass das Ende der Reduktion nicht durch die Thermodynamik der Reaktion bestimmt war, sondern dass die Oberfläche der FHO durch Fe(II)-Präzipitate blockiert wurde. Die Kombination der hier gewonnen Ergebnisse mit Literaturdaten zeigt, dass auch beim threshold der Methanogenen die hier verwendeten FHO soweit reduziert werden können, dass Siderit ausfällt. Lediglich noch stabilere FHO könnten nur bis zu niedrigeren Fe^{2+} Aktivitäten reduziert werden. Ein Abtransport des Fe^{2+} vom Ort der Reduktion, wie es für Gleye, Pseudogelye oder Stagnogelye typisch ist, erlaubt jedoch auch die vollständige Auflösung stabilster FHO.

Versuche mit dem DIRB *Clostridium butyricum* zeigten, dass auch bei pH-Werten von 3,3-4 nach Abschluss der Gärung, Oberflächenbeläge aus Aluminium die weitere reduktive Auflösung Aluminium-substituierter FHO behinderte. Es kann daher gefolgert werden, dass sich Aluminiumsubstitution bei höheren pH-Werten natürlicher Standorte noch stärker hemmend auf die Reduktion der FHO auswirkt.

Summary

Dissimilatory iron-reducing bacteria (DIRB) compete with methanogenic archaea and sulfate-reducing bacteria for common electron donors, like H_2 and low molecular acids. As formation of methane yields less energy than reduction of Fe(III) DIRB can reduce the concentration of the electron donors to a lower value (threshold). DIRB therefore can reduce formation of methane at anoxic sites. Most available Fe(III) exists as Fe(III) (hydr)oxides (FHOs) of low solubility. However, FHOs exhibit a broad range of thermodynamic stability. The range of the solubility product K_{SO} of soil FHOs is at least 3-4 orders of magnitude. Thus, the higher the stability of a FHO, the lower the Gibbs free energy of reaction (ΔG_r) which can be used by the bacteria.

In soil FHO Fe(III) is substituted by aluminum to a certain degree, depending on the degree of weathering of the soil. As Al(III) is non-reducible and of low solubility, the question arises whether aluminum remains as a coating on the surface of a FHO, which is reductively dissolved.

The objective of this work was (1) to test whether the reduction of FHOs is limited by their thermodynamic stability. In addition, (2) the hypothesis was to be tested whether aluminum forms non-dissolved precipitates on the surface of substituted FHOs, by which the reductive dissolution of the latter is restricted.

FHOs were synthesized and characterized, revealing specific surface areas of 89-280 $m^2\ g^{-1}$. For determination of the solubility product of FHOs (lg K_{SO} varied from –39.1 to –41.8) a new method for the determination of dissolved Fe was developed, which does not react with colloidal FHOs.

In addition, dissolution kinetics were determined to characterize the FHOs. A convenient method for determination of the entire reductive dissolution kinetics at near neutral pH was developed. A small quantity of FHO, which does not cause a visible turbidity is reduced by means of ascorbate at pH 5.2 in an anoxic glass tube. The Fe^{2+} formed, and thus the extent of the reaction, can be determined as the absorption of the colored Fe(II)(ferrozine)$_3$ complex at any time directly in the glass tube.

As the dissolution kinetics in oxalic acid buffer was also determined, it was possible to compare the results of two different methods for a set of FHOs, for the

first time. The dissolution rate constants of both methods were highly correlated. However, if the stability of two FHOs is compared, the result strongly depend on the dissolution method used. In addition, compared to the reductive method, oxalic acid buffer reveal a strong preferential dissolution of reactive FHOs. Physicochemical properties (specific surface area and K_{SO} together with standard redox potential $E_h°$) of FHOs show good correlation to the rate constants of both methods.

Adding 1 mM citrate, which complexes aluminum liberated from substituted FHOs, yielded a method for convenient determination of dissolution kinetics of soil FHOs. These sum dissolution kinetics could be reduced to 3-4 fractions that dissolve simultaneously according to pseudo-first-order kinetics, each fraction having a homogeneous rate constant. Thus, this method is the first one, which makes it possible to subdivide soil FHO into more than two fractions and gives reason to believe that approximated values of specific surface, K_{SO} and Eh° can be assigned to these fractions, via the above-mentioned correlations. This would enable the prediction of ecological important functioning of soil FHOs, like adsorption or redox phenomena.

Experiments with the DIRB *Geobacter metallireducens* in the presence of 1, 10, or 100 mM of the electron donor acetate revealed that surface precipitation of Fe(II) restricted the bacterial reduction of FHOs rather than thermodynamics of the reaction. Combination with literature data indicate that - at the threshold of methanogenic bacteria - all FHOs used herein can be reduced to an Fe^{2+} activity that allows precipitation of siderite. Thus, the extent of reduction will be limited by specific surface area of FHOs. Only the reduction of more stable FHOs could be limited by the thermodynamics of reaction. However, the dislocation of Fe^{2+} from the place of reduction, which is typical for soil types like gleysols and stagnosols even allows the complete dissolution of quite stable FHOs.

Experiments with the DIRB *Clostridium butyricum* indicated that even at low pH of 3.3-4 the reductive dissolution of Al-substituted goethites is limited by accumulation of aluminum on the surface of FHOs. As the solubility of Al(III) strongly decreases with increasing pH, it can be inferred from our data that aluminum coatings will be a significant limitation to the reduction of FHOs at natural sites.

Literatur

Achtnich, C., Bak, F. und Conrad, R. (1995) Competition for electron donors among nitrate reducers, ferric iron reducers, sulfate reducers, and methanogens in anoxic paddy soil. Biology and Fertility of Soils, 19: 65-72.

Ali, M.A., Dzombak, D.A. (1996) Effects of simple organic acids on sorption of Cu^{2+} and Ca^{2+} on goethite. Geochimica et Cosmochimica Acta, 60: 291-304.

Amonette, J. E., F. A. Khan, H. Gan, J. W. Stucki und A. D. Scott (1994) Quantitative Oxidation-State Analysis of Soils. In: J.E. Amonette und L.W. Zelazny (eds.) Quantitative Methods in Soil Mineralogy. SSSA Miscellaneous Publication, Madison, Wisconsin. p. 83-108.

Anonymous (1999) Lab tools. Merck, Darmstadt.

Balch, W. E., Fox, G. E., Magrum, L. J., Woese, C. R. und Wolfe, R. S. (1979) Methaongens; Reevaluation of a unique biological Group. Microbiological Reviews, 43: 260-296.

Berthelin, J. (1982) Processus microbiens intervenant dans les sols hydromorphes en regions temperees. Incidence sur la pedogenese. Pedologie, 32: 313-328.

Beveridge, T.J., Murray, R.G.E. (1976) Uptake and retention of metals by cell walls of Bacillus subtilis. Journal of Bacteriology, 127: 1502-1518.

Boer, J.K., De Linsen, B.G., Osinga, T.J. (1965) Studies on pore systems in catalysts. VI The universal t curve. Journal of Catalysis, 4: 643-648.

Borggaard, O.K. (1983) Effect of surface area and mineralogy of iron oxides on their surface charge and anion adsorption properties. Clays and Clay Minerals, 31: 230-232.

Borggaard, O.K. (1990) Kinetics and mechanisms of soil iron oxide dissolution in EDTA, oxalate and dithionite. Proceedings of the 9th International Clay Conference, Strasbourg, 1989. Farmer V.C., Tardy Y. (eds) Sciences Géologiques / éd. Institut de Géologie, Université Louis Pasteur et Centre de Sédimentologie et de Géochimie de la Surface, CNRS, Strasbourg. Mémoire, 85: 139-148.

Bousserrhine, N. (1995) Étude de Paramètres de la Réduction bactérienne du Fer et Application à la Déferrification de Minéraux industriels, Thesis, Université Henri-Poincaré, Nancy.

Bousserrhine, N., Gasser, U., Jeanroy, E., Berthelin, J. (1998) Effect of aluminium substitution on ferri-reducing bacterial activity and dissolution of goethites. Earth and Planetary Sciences, 326: 617-624.

Bousserrhine, N., Gasser, U. G., Jeanroy, E. und Berthelin, J. (1999) Bacterial and chemical reductive dissolution of Mn-, Co-, Cr-, and Al-substituted goehtites. Geomicrobiology Journal, 16: 245-258.

Bridge, T. A. M. und D. B. Johnson (1998) Reduction of soluble iron and reductive dissolution of ferric iron-containing minerals by moderately thermophilic iron-oxidizing bacteria. Appl.Environ.Microbiol., 64: 2181-2186.

Bromfield, S.M. (1954) Reduction of ferric compounds by soil bacteria. Journal of General Microbiology, 11: 1-6.

Brookins, D.G. (1988) Eh-pH Diagrams for Geochemistry. Springer-Verlag, Berlin.

Brunauer, S., Emmet, P.H., Teller, E. (1938) Adsorption of gases in multi-molecular layers. Journal of the American Chemical Society, 60: 309-319.

Christoffersen, J. und M. R. Christoffersen (1976) The kinetics of dissolution of calcium sulphate dihydrate in water. J. Crystal Growth., 35: 77-88.

Conrad, R. (1996) Soil microorganisms as controllers of atmospheric trace gases (H_2, CO, CH_4, OCS, N_2O and NO). Microbiological Reviews, 60: 609-640.

Cornell, R. M., Posner, A. M. und Quirk, J. P. (1974) The dissolution of synthetic goethites: the early stage. Soil Science Society of America Journal, 38: 377-378.

Cornell, R. M. und P. Schindler (1987) Photochemical dissolution of goethite in acid/oxalate solution. Clay and Clay Minerals: 35: 347-352.

Cornell, R. M. und Schwertmann, U. (1996) The iron oxides. VCH, Weinheim.

Cummings, D. E., F. Caccavo, S. Fendorf und R. F. Rosenzweig (1999) Arsenic mobilization by the dissimilatory Fe(III)-reducing bacterium Shewanella alga BrY. Environ.Sci.Technol., 33: 723-729.

Davies, C. W. (1962) Ion association. Butterworths, London.

Davies, M.B., Austin, J. und Partridge, D.A. (1991) Vitamin C: Its Chemistry and Biochemistry. Royal Society of Chemistry Paperbacks, Cambridge.

Deng, Y. (1997) Effect of pH on the reductive dissolution rates of iron(III) hydroxide by ascorbate. Langmuir, 13: 1835-1839.

Dominik, P. und Kaupenjohann, M. (2000) Simple spectrophotometric determination of Fe in oxalate and HCl soil-extracts. Talanta, 51: 701-707.

Dominik, P., Kaupenjohann, M., Peiffer, S. (2000) Direct photometric determination of reductive dissolution kinetics of Fe(III)(hydr)oxides. Mitteilungen der Deutschen Bodenkundlichen Gesellschaft, 92: 11-12.

Dominik, P., Pohl, H. N., Bousserrine, N., Berthelin, J. und Kaupenjohann, M. (2002) Limitations to the reductive dissolution of Al-substituted goethites by Clostridium butyricum. Soil Biology and Biochemistry, 34: 1147-1155.

Dominik, P., Peiffer, S. und Kaupenjohann, M. Simple on-line determination of reductive dissolution kinetics of Fe(III) (hydr)oxides versus dissolution in oxalate. Clay and Clay Minerals, submitted.

Dos Santos Afonso, M., Morando, P. J., Blesa, M. A., Banwart, S. und Stumm, W. (1990) The reductive dissolution of iron oxides by ascorbate. Journal of Colloid & Interface Science, 138: 74-82.

Ehrlich, H.L. (1996) Geomicrobiology. 2nd ed. Marcel Dekker, Inc. New York:

Fischer, W. R. (1973) Die Wirkung von zweiwertigem Eisen auf die Lösung und Umwandlung von Eisen(III)-hydroxiden. In: E. Schlichting und U. Schwertmann (eds.) Pseudogley & Gley. Verlag Chemie, Weinheim, p. 37-44.

Fischer, W. R. (1987) Standard potentials (Eh°) of iron(III) oxides under reducing conditions. Zeitschrift für Pflanzenernährung und Bodenkunde, 150: 286-289.

Fischer, W. R. und H. Fechter (1982) Analytische Bestimmung und Fraktionierung von Cu, Zn, Pb Cd, Ni und Co in Böden und Unterwasserböden. Z. Pflanzenernähr. Bodenk., 145: 151-160.

Francis, C. A., A. Y. Obraztsova und B. M. Tebo (2000) Dissimilatory metal reduction by the facultative anaerobe Pantoea agglomerans SP1. Applied & Environmental Microbiology, 66: 543-548.

Fredrickson, J. K., Zachara, J. M., Kennedy, D. W., Dong, H., Onstott, T. C., Hinman, N. W. und Shiu-Mei, L. (1998) Biogenic iron mineralization accompanying the dissimilatory reduction of hydrous ferric oxide by a groundwater bacterium. Geochimica et Cosmochimica Acta, 62: 3229-3257.

Frenzel, P., Bosse, U. und Janssen, P.H. (1999) Rice roots and methanogenesis in a paddy soil: ferric iron as an alternative electron acceptor in rooted soil. Soil Biology and Biochemistry, 31: 421-430.

Gasser, U.G., Jeanroy, E., Mustin, C., Barres, O., Nüesch, R., Berthelin, J., Herbillon, A. J. (1996) Properties of synthetic goethites with Co for Fe substitution. Clay Minerals, 31: 465-476.

Gerth, J. (1990) Unit-cell dimensions of pure and trace metal-associated goethites. Geochimica et Cosmochimica Acta, 54: 363-371.

Gottschal, J.C., Morris, J.G. 1981. The induction of acetone and butanol production of Clostridium acetobutylicum by elevated concentrations of acetate and butyrate. FEMS Microbiology Letters, 12: 385-389.

Greene, A. D., B. K. C. Patel und A. J. Sheehy (1997) Deferribacter thermophilus gen. nov., sp. nov., a novel thermophilic manganese- and iron-reducing bacterium isolated from a petroleum reservoir. Int.J.Syst.Bacteriol., 47: 505-509.

Griessbach, E. F. C. und R. G. Lehmann (1999) Degradation of polydimethylsiloxane fluids in the environment - A review. Chemosphere, 38: 1461-1468.

Guida, L., Saidi, Z., Hughes, M.N., Poole, R.K. (1991) Aluminium toxicity and binding to Escherichia coli. Archives of Microbiology, 156: 507-512.

Hartmanis, M.G.N., Klason, T., Gatenbeck, S. (1984) Uptake and activation of acetate and butyrate in Clostridium acetobutylicum. Applied Microbiology and Biotechnology, 20: 66-71.

Illmer, P., Schinner, F. (1997) Influence of aluminium on motility and swarming of Pseudomonas sp. and Arthrobacter sp.. FEMS Microbiology Letters, 155: 121-124.

Jeanroy, E., Rajot, J.L., Pillon, P., Herbillon, A.J. (1991) Differential dissolution of hematite and goethite in dithionite and its implication on soil yellowing. Geoderma, 50: 79-94.

Jones, D.L., Kochian, L. V. (1996) Aluminium-organic acid interactions in acid soils. I. Effect of root-derived organic acids on the kinetics of Al dissolution. Plant and Soil, 182: 221-228.

Jones, D.L., Prabowo, A. M., Kochian, L. V. (1996) Aluminium-organic acid interactions in acid soils. II. Influence of solid phase sorption on organic acid-Al complexation and Al rhizotoxicity. Plant and Soil, 182: 229-237.

Jones, D.T., Woods, D.R. (1986) Acetone-butanol fermentation revisited. Microbiological Reviews, 50: 484-524.

Jones, R. C. (1981) X-ray diffraction profile analysis vs. phosphorous sorption by 11 Puerto Rican soils. Soil Sci.Soc.Am.J., 45: 818-825.

Kashefi, K. und D. R. Lovley (2000) Reduction of Fe(III), Mn(IV), and toxic metals at 100°C by Pyrobaculum islandicum. Appl.Environ.Microbiol., 66: 1050-1056.

Kaupenjohann, M. (1989) Effects of acid rain on soil chemistry and nutrient availability in the soil. In: E.D. Schulze, O.L. Lange und R. Oren (eds.) Forest decline and air pollution. Ecological Studies. Springer-Verlag, Berlin, p. 297-340.

Kieft, T. L. et al. (1999) Dissimilatory reduction of Fe(III) and other electron acceptors by a Thermus isolate. Applied & Environmental Microbiology, 65: 1214-1221.

King, G. M. (1984) Utilization of hydrogen, acetate, and "noncompetitive" substrates by methanogenic bacteria in marine sediments. Geomicrobiology Journal, 3: 275-306.

Klüber, H. D. und R. Conrad (1998) Effects of nitrate, nitrite, NO and N_2O on methanogenesis ond other redox processes in anoxic rice field soil. FEMS Microbiol.Ecol., 25: 301-318.

Kostka, J. E. und Nealson, K. H. (1995) Dissolution and reduction of magnetite by bacteria. Environmental Science & Technology, 29: 2535-2540.

Küsel, K., T. Dorsch, G. Acker und E. Stackebrandt (1999) Microbial reduction of Fe(III) in acidic sediments: Isolation of Acidophilium cryptum JF-5 capable of coupling the reduction of Fe(III) to the oxidation of glucose. Appl.Environ.Microbiol., 65: 3633-3640.

Larsen, O. und Postma, D. (2001) Kinetics of reductive bulk dissolution of lepidocrcite, ferrihydrite, and goethite. Geochimica et Cosmochimica Acta, 65: 1367-1379.

Lindsay, W. L. (1979) Chemical equilibria in soils. John Wiley & Sons, New York.

Loeppert, R. H. (1988) Chemistry of iron in calcareous systems. In: J.W. Stucki, B.A. Goodman und U. Schwertmann (eds.) Iron in soils and clay minerals. D.Reidel Publishing Company, Dordrecht, NL, p. 689-714.

Long, S., Jones, D.T., Woods, D.R. (1984) Initiaion of solvent production, clostridial stage and endospore formation in Clostridium acetobutylicum P262. Applied Microbiology and Biotechnology, 20: 256-261.

Lövgren, L.; Sjöberg, S., Schindler, P.W. (1990) Acid/base reactions and Al(III) complexation at the surface of goethite. Geochimica et Cosmochimica Acta, 54: 1301-1306.

Lovley, D. R. (1991) Dissimilatory Fe(III) and Mn(IV) reduction. Microbiological Reviews, 55: 259-287.

Lovley, D.R., Baedecker, M.J., Lonergan, D.J., Cozzarelli, I.M., Phillips, E.J.P., Siegel, D.I. (1989) Oxidation of aromatic contaminants coupled to microbial iron reduction. Nature, 339: 297-300.

Lovley, D. R., Chapelle, F. H. und Woodward, J. C. (1994) Use of Dissolved H_2 Concentrations to Determine Distribution of Microbially Catalyzed Redox Reactions in Anoxic Groundwater. Environmental Science & Technology, 28: 1205-1210.

Lovley, D. R., Coates, J. D., Saffarini, D. und Lonergan, D. J. (1997) Dissimilatory iron reduction. In: Transition metals in microbial metabolism, G. Winkelmann und C. L. Canamo (eds). Harwood Academic Publishes, Netherlands, 187-215.

Lovley, D. R., Giovannoni, S. J., White, D. C., Champine, J. E., Phillips, E. J. P., Gorby, Y. A. und Goodwin, S. (1993) Geobacter metallireducens, new genus new species, a microorganism capable of coupling the complete oxidation of organic compounds to the reduction of iron and other metals. Archives of Microbiology, 159: 336-344.

Lovley, D. R. und Phillips, E. J. P. (1986a) Organic matter mineralisation with reduction of ferric iron in anaerobic sediments. Applied and Environmental Microbiology, 51: 683-689.

Lovley, D. R. und Phillips, E. J. P. (1986b) Availability of ferric iron for microbial reduction in bottom sediments of the freshwater tidal Potomac River. Applied and Environmental Microbiology, 52: 751-757.

Lovley, D.R. und Phillips, E.J.P. (1987) Competitive mechanisms for inhibition of sulfate reduction and methane production in the zone of ferric iron reduction in sediments. Applied and Environmental Microbiology, 53: 2636-2641.

Lovley, D.R. und Phillips, E.J.P. (1988) Novel mode of microbial energy metabolism: Organic Carbon Oxidation coupled to dissimilatory reduction of iron or manganese. Applied and Environmental Microbiology, 54: 1472-1480.

Lovley, D.R., Phillips, E.J.P. (1989) Requirement for a microbial consortium to completely oxidize glucose in Fe(III)-reducing sediments. Applied and Environmental Microbiology, 55: 3234-3236.

Lueders, T. und M. W. Friedrich (2002) Effects of amendment with ferrihydrite and gypsum on the structure and activity of methanogenic populations in rice field soil. Appl.Environ.Microbiol., 68: 2484-2494.

Mehra, O. P. und M. L. Jackson (1960) Iron oxide removal from soils and clays by a dithionite-citrate system buffered with sodium-bicarbonate. Clay and Clay Minerals, 7: 317-327.

Monot, F., Engasser, J.-M., Petitdemange, H. (1984) Influence of pH and undissociated butyric acid on the production of acetone and butanol in batch cultures of Clostridium acetobutylicum. Applied Microbiology and Biotechnology, 19: 422-426.

Motomura, S. und H. Yokoi (1969) Fractionation method of ferrous iron in paddy soil. Soil Sci.Plant Nutr., 15: 28-37.

Munch, J.C., Ottow, J.C.G. (1977) Modelluntersuchungen zum Mechanismus der bakteriellen Eisenreduktion in hydromorphen Böden. Zeitschrift für Pflanzenernährung und Bodenkunde, 140: 549-562.

Munch, J.C., Ottow, J.C.G. (1980) Preferential reduction of amorphous to crystalline iron oxides by bacterial activity. Soil Science, 129: 15-21.

Munch, J.C., Ottow, J.C.G. (1983) Reductive transformation mechanism of ferric oxides in hydromorphic soils. Environmental Biogeochemistry Ecology Bulletin, 35: 383-394.

Murad, E. (1990) Application of ^{57}Fe Mössbauer spectroscopy to problems in clay minerals and soils science: possibilities and limitations. Adv.Soil Sci., 12: 125-157.

Patrick, W.H. und Jugsujinda, A. (1992) Sequential Reduction and oxidation of inorganic nitrogen, manganese and iron in flooded soil. Soil Sci. Soc. Am. J., 56: 1071-1073.

Perez-Bendito, D. und M. Silva (1996) Recent advances in kinetometrics. Trac Trends in analytical chemistry, 15: 232-240.

Peters, V. und Conrad, R. (1996) Sequential reduction processes and initiation of CH_4 production upon flooding of oxic upland soils. Soil Biology and Biochemistry, 28: 371-283.

Petigara, B. R., N. V. Blough und A. C. Mignerey (2002) Mechanisms of hydrogen peroxide decomposition in soils. Environ.Sci.Technol., 36 639-645.

Phillips, E. J. P. und D. R. Lovley (1987) Determination of Fe(III) and Fe(II) in oxalate extracts of sediment. Soil Sci.Soc.Am.J., 51: 938-941.

Ponnamperuma, F. N., Tianco, E. M. und Loy, T. (1967) Redox equilibria in flodded soils. I. The iron hydroxide system. Soil Science, 103: 374-382.

Postma, D. (1993) The reactivity of iron oxides in sediments: A kinetic approach. Geochim.Cosmochim.Acta, 57: 5027-5034.

Quencer, B. M. und S. R. Crouch (1994) Multicomponent kinetic determination of lanthanides with stopped-flow, diode array spectrometry and the extended Kalman filter. Anal.Chem., 66: 458-463.

Rajot, J. L. (1992) Dissolution des oxydes de fer (hématite et goethite) d'un sol ferrallitique des Llanos de Colombie par des bactéries ferri-réductrices. Thesis, Universtié Henri-Poincaré, Nancy.

Rasmussen, H. und P. H. Nielsen (1996) Iron reduction in activated sludge measured with different extraktion techniques. Water Res., 30: 551-558.

Rilbe, H. (1996) pH and Buffer Theory - A new Approach. John Wiley & Sons, Chichester.

Roden, E. E. und Wetzel, R.G. (1996) Organic carbon oxidation and suppression fo methane production by microbial Fe(III) oxide reduction in vegetated and unvegetated freshwater sediments. Limnology and Oceanography, 41: 1733-1748.

Roden, E. E. und Zachara, J. M. (1996) Microbial reduction of crystalline iron(III) oxides: Influence of surface area and potential for cell growth. Environmental Science & Technology, 30: 1618-1628.

Roden, E. E. und Urrutia, M. M. (1999) Ferrous iron removal promotes microbial reduction of crystalline iron(III) oxides. Environmental Science & Technology, 33: 1847-1853.

Roden, E. E., Urrutia, M. M. und Mann, C. J. (2000) Bacterial reductive dissolution of crystalline Fe(III) oxide in continuous-flow column reactors. Applied and Environmental Microbiology, 66: 1062-1065.

Ruan, H.D. und Gilkes, R.J. (1995) Acid dissolution of synthetic aluminous goethite before and after transformation to hematite by heating. Clay Minerals, 30: 55-65.

Rueda, E. H., M. C. Ballesteros, R. L. Grassi und M. A. Blesa (1992) Dithionite as a dissolving reagent for goethite in the presence of EDTA and citrate. Application to soil analysis. Clay and Clay Minerals, 40: 575-585.

Saint-Amans, S., Gibral, L., Andrade, J. Ahrens, K., Soucaille, P. (2001) Regulation of carbon and electron flow in Clostridium butyricum VPI 3266 grown on glucose-glycerol mixtures. Journal of Bacteriology, 183: 1748-1754.

Scheffer, F. und Schachtschabel, P. (1998) Lehrbuch der Bodenkunde. Ferdinand Enke Verlag, Stuttgart.

Schnell, S., S. Ratering und K.-H. Jansen (1998) Simultaneous Determination of iron(III), iron(II), and Manganese(II) in environmental samples by ion chromatography. Environ.Sci.Technol., 32: 1530-1537.

Schulze, D.G., Schwertmann, U. (1984) The influence of aluminium on iron oxides: X. Properties of Al-substituted goethites. Clay Minerals, 19: 521-539.

Schulze, D.G., Schwertmann, U. (1987) The influence of aluminium on iron oxides: XIII. Properties of goethites synthesised in 0.3M KOH at 25°C. Clay Minerals, 22: 83-92.

Schwertmann, U. (1964) Differenzierung der Eisenoxide des Bodens durch Extraktion mit saurer Ammoniumoxalat-Lösung. Zeitschrift für Pflanzenernährung und Bodenkunde, 105: 194-202.

Schwertmann, U. (1984) The influence of aluminum on iron oxides. IX. Dissolution of Al-Goethites in 6 M HCl. Clay Minerals, 19: 9-19.

Schwertmann, U. (1988) Some properties of soil and synthetic iron oxides. In: J.W. Stucki, B.A. Goodman und U. Schwertmann (eds.) Iron in soils and clay minerals. D. Reidel Publishing Company, Dordrecht, NL, p. 203-250.

Schwertmann, U. (1991) Solubility and dissolution of iron oxides. Plant and Soil, 130: 1-25.

Schwertmann, U., Cambier, P. und Murad, E. (1985) Properties of goethites of varying cristallinity. Clay and Clay Minerals, 33: 369-378.

Schwertmann, U., Carlson, L. und Murad, E. (1987) Properties of iron oxides in two finnish lakes in relation to the environment of their formation. Clays and Clay Minerals, 32: 297-304.

Schwertmann, U. und R. M. Cornell (2000) Iron oxides in the laboratory - Preparation and characterization. 2nd edn. VCH, Weinheim.

Schwertmann, U. und Fischer, W.R. (1966) Zur Bildung von α-Fe_2O_3 aus amorphem Eisen(III)-hydroxid. III. Mitt. Zeitschrift für anorganische und allgemeine Chemie, 346: 137-142.

Schwertmann, U., W. R. Fischer und H. Fechter (1982a) Spurenelemente in Bodensequenzen I. Zwei Braunerde – Podsol - Sequenzen aus Tonschieferschutt. Z.Pflanzenernähr.Bodenk., 145: 161-180.

Schwertmann, U., W. R. Fischer und H. Fechter (1982b) Spurenelemente in Bodensequenzen II. Zwei Pararendzina - Pseudogley - Sequenzen aus Löss. Z.Pflanzenernähr.Bodenk. 145, 181-196.

Schwertmann, U., Gasser, U., Sticher, H. (1989) Chromium-for-iron substitution in synthetic goehites. Geochimica et Cosmochimica Acta, 53: 1293-1297.

Schwertmann, U., D. G. Schulze und E. Murad (1982) Identification of ferrihydrite in soils by dissolution kinetics, differential X-ray diffraction and Mössbauer spectroscopy. Soil Sci.Soc.Am.J., 46: 869-875.

Schwertmann, U. und R. M. Taylor (1989) Iron oxides. In: J.B. Dixon und S.B. Weed (eds.) Minerals in soil environment. Soil Science Society of America, Madison, p. 379-438.

Segal, R.G., Sellers, R.M. (1984) Redox reactions at solid-liquid interfaces. In: Sykes, A.G. (ed.).Advances in Inorganic and Bioinorganic Mechanisms, Vol. 3, Academic Press, London, pp 97-129.

Sigg, L. und Stumm, W. (1994) Aquatische Chemie. Verlag der Fachvereine, Zürich.

Slobodkin, A. I. und J. Wiegel (1997) Fe (III) as an elektron acceptor H_2 oxidation in thermophilic anaerobic enrichment cultures from geothermal areas. Extremophiles, 1: 106-109.

Slobodkin, A. I., T. P. Tourova, B. B. Kuznetsov, N. A. Kostrikina, N. A. Chernyh und E. A. Bonch-Osmolovskaya (1999) Thermoanaerobacter siderophilus sp. nov., a novel dissimilatory Fe(III)-reducing, anaerobic, thermophilic bacterium. Int.J.Syst.Bacteriol., 49: 1471-1478.

Stookey, L. L. (1970) Ferrozine - a new spectophotometric reagent for iron. Anal.Chem., 42: 779-781.

Stumm, W. und Morgan, J.J. (1981) Aquatic Chemistry. John Wiley & Sons, Inc., New York.

Sulzberger, B., Suter, C., Siffert, S., Banwart, S. und Stumm, W. (1989) Dissolution of Fe(III) (Hydr)oxides in natural waters; laboratory assessment on the kinetics controlled by the surface coordination. Marine Chemistry, 28: 127-144.

Süsser, P. und U. Schwertmann (1991) Proton buffering in mineral horizons of some acid forest soils. Geoderma, 49: 63-76.

Suter, D., Banwart, S. und Stumm, W. (1991) Dissolution of hydrous iron(III) oxides by reductive mechanisms. Langmuir, 7: 809-813.

Suter, D., C. Seiffert, B. Sulzberger und W. Stumm (1988) Catalytic dissolution of iron(III) (hydr)oxides by oxalic acid in the presence of Fe(II). Naturwissenschaften, 75: 571-573.

Szilagyi, M. (1971) Reduction of Fe^{3+} ion by humic acid preparations. Soil Sci., 111: 233-235.

Tamm, O. (1922) Om bestämning av de oorganiska komponenterna i markens gelkomplex. Meddelanden från Statens Skogsförsöksanstalt, 19: 385-404.

Thamdrup, B. (2000) Bacterial manganese and iron reduction in aquatic sediments. Advances in Microbial Ecology, 16: 41-84.

Thampuran, N., Surendran, P.K. (1996) Effect of chemical agents on swarming of Bacillus species. Journal of Applied Bacteriology, 80: 296-302.

Torrent, J., Schwertmann, U. und Barron, V. (1987) The reductive dissolution of synthetic goethite and haematite in dithionite. Clay Minerals, 22: 329-337.

Ueno, K.; Imamura, T. und Cheng, K.L. (1992) CRC Handbook of Organic Analytical Reagents. CRC- Press, Boca Raton.

Urrutia, M. M., Roden, E. E., Fredrickson, J. K. und Zachara, J. M. (1998) Microbial and surface chemistry controls on reduction of synthetic Fe(III) oxide minerals by the dissimilatory iron-reducing bacterium shewanella alga. Geomicrobiology Journal, 15: 269-291.

Van de Sand, M. (1997) Untersuchungen zur Versauerung von Waldböden. edn. Verlag D. Kovac, Hamburg.

Vandák, D., Zigová, J., Sturdík, E., Schlosser, S. (1997) Evaluation of solvent and pH for extractive fermentation of butyric acid. Process Biochemistry, 32: 245-251.

Ward, D. M. und M. R. Winfrey (1985) Interactions between methanogenic and sulfate reducing bacteria in sediments. Adv. Aquat. Microbiol., 3: 141-179.

Weast, R. C. (ed). (1985) Handbook of chemistry and physics. Boca Raton, Florida, CRC Press.

Widdel, F. und Bak, F. (1995) Gram-negative mesophilic sulfate-reducing bacteria. In: The Procaryotes, M. P. Starr, H. Stolp, H. G. Trüper, A. Balows and H. G. Schlegel (eds). Springer-Verlag, Berlin, Heidelberg, New York, 3352-3378.

Winfrey, M. R. und Zeikus, J. G. (1977) Effect of sulfate on carbon and electron flow during microbial methanogenesis in freshwater sediments. Applied and Environmental Microbiology, 33: 275-281.

Wolf, D. C., T. H. Dao, H. D. Scott und T. L. Lavy (1989) Influence of sterilisation methods on selected soil microbiological, physical, and chemical properties. J.Environ.Qual., 18 : 39-44.

Yao, H. und Conrad, R. (1999) Thermodynamics of methane production in different rice paddy soils from China, the Philippines and Italy. Soil Biology and Biochemistry, 31: 463-473.

Zehnder, A. J. B. (ed.) (1988) Biology of anaerobic microorganisms. John Wiley & Sons, Inc., New York.

Zeien, H. und Brümmer, G.W. (1989) Chemische Extraktionen zur Bestimmung von Schwermetallbindungsformen in Böden. Mitteilungen der Deutschen Bodenkundlichen Gesellschaft, 59: 505-510.

Zinder, B., Furrer, G. und Stumm, W. (1986) The coordination chemistry of weathering: II. Dissolution of iron oxides. Geochimica et Cosmochimica Acta, 50: 1861-189.